AD NUMBER

AD829650

LIMITATION CHANGES

TO:

Approved for public release; distribution is unlimited.

FROM:

**Distribution authorized to U.S. Gov't. agencies and their contractors;
Administrative/Operational Use; 1961. Other requests shall be referred to U.S. Naval Postgraduate School, Monterey, CA 93943.**

AUTHORITY

USNPS ltr, 27 Sep 1971

STEADY STATE RESPONSE OF A SECOND ORDER SERVOMECHANISM WITH BACKLASH AND RESILIENCE IN THE GEARS BETWEEN MOTOR AND LOAD

NORRIS O. ANDERSON, JR.
and
THOMAS W. LUCKETT

STEADY STATE RESPONSE
OF A
SECOND ORDER SERVOMECHANISM
WITH
BACKLASH AND RESILIENCE IN THE
GEARS BETWEEN MOTOR AND LOAD

* * * * *

Norris O. Anderson, Jr.

and

Thomas W. Luckett

STEADY STATE RESPONSE
OF A
SECOND ORDER SERVOMECHANISM
WITH
BACKLASH AND RESILIENCE IN THE
GEARS BETWEEN MOTOR AND LOAD

by

Norris O. Anderson, Jr.
Lieutenant, United States Navy

and

Thomas W. Luckett
Lieutenant, United States Navy

Submitted in partial fulfillment of
the requirements for the degree of

MASTER OF SCIENCE
IN
ELECTRICAL ENGINEERING

United States Naval Postgraduate School
Monterey, California

1961

STEADY STATE RESPONSE OF A SECOND ORDER SERVOMECHANISM WITH BACKLASH AND RESILIENCE IN THE GEARS BETWEEN MOTOR AND LOAD

by

Norris O. Anderson, Jr.

and

Thomas W. Luckett

This work is accepted as fulfilling
the thesis requirements for the degree of
MASTER OF SCIENCE
IN
ELECTRICAL ENGINEERING
from the
United States Naval Postgraduate School

ABSTRACT

This thesis is concerned with the steady state response to a step input of a non-linear servomechanism having viscous friction and a load position unity feedback loop. A gear train with backlash between resilient gear teeth was located between the motor and load.

The physical equations describing the system are presented and adapted to a form for the Control Data Corporation 1604 digital computer. The computer program used in this analysis is presented along with its flow diagram and description of its operation.

The results of this thesis are presented in several forms using the parameters of system damping coefficient, distribution of friction and inertia, backlash angle and coefficient of restitution. The results are applied to sample problems in illustration of their use for design and analysis.

The authors wish to express their appreciation to Dr. George J. Thaler of the Department of Electrical Engineering, and to Dr. William Wainwright and Mr. Edward N. Ward of the Department of Mathematics for their assistance and encouragement in completing this work.

TABLE OF CONTENTS

TABLE OF SYMBOLS

θ_R	(ONE)*	Angular step input (radians). Desired load displacement at steady state
θ_C	(THETAL)	Output displacement of load (radians).
$\dot{\theta}_C$	(THETADL)	Output velocity of load $\left(\frac{\text{radians}}{\text{sec}}\right)$
E		Error in radians. $E = \theta_R - \theta_C$
K	(KMOTCONST)	Constant of proportionality relating position error to torque developed by the motor.
T_m		Developed torque of motor.
T_L		Torque of load.
T_{Lm}		Torque of load referred to motor.
ρ	(RHO)	$\frac{\text{Number of teeth on gear 1}}{\text{Number of teeth on gear 2}}$
J_m	(MOINERT)	Inertia of motor measured at motor.
J_L	(JLOADVAL)	Inertia of load measured at load.
J		Total inertial measured at motor $J = Jm + \rho^2 J_L$
F_m	(FMOTOR)	Friction of motor measured at motor.
f_L	(FLOAD)	Friction of load measured at load.
Δ	(DELTA)	Backlash of gearbox measured in radians at the output.
N_S		Slope of phase trajectory (combined system). $N_S \triangleq \frac{d\dot{\theta}_c}{d\theta_c} = \frac{\ddot{\theta}_c}{\dot{\theta}_c}$
N_L		Slope of phase trajectory (load floating free). $N_L \triangleq \frac{d\dot{\theta}_c}{d\theta_c} = \frac{\ddot{\theta}_c}{\dot{\theta}_c}$
$\dot{\theta}_m', \dot{\theta}_c'$		Velocities of motor and load after impact.

*( ) Terms indicate computer mnemonics referred to in Sec. 3, Computer Program Development.

e	(RESTITUT)	Coefficient of restitution.
ζ	(ZETA)	System damping coefficient.
ω_n	(OMEGAN)	System natural frequency.
ω_n^2	(OMEGANSQ)	System natural frequency, squared.
$\frac{f_L}{F_T}$	(FLFTPRIN)	Load friction ratio with respect to friction of the system.
$\frac{J_m}{J_L}$	(INERTRAT)	Inertia ratio.
θ_m	(THETAM)	Displacement of motor (radians).
$\dot{\theta}_m$	(THETADM)	Velocity of motor $\left(\frac{\text{radians}}{\text{sec}}\right)$

1. Introduction and Background

The problem under investigation was the response to a unit step input of a nonlinear servomechanism having viscous friction and load-position unity feedback loop. A gear train with backlash between the resilient gear teeth was located between the motor and load. A determination of the possible existence of a limit cycle with variation of several parameters was made. The variable parameters considered were motor, load, and system time constants, backlash and the coefficient of restitution of the gear teeth. If a limit cycle existed, a further investigation was made into the change of the size of the limit cycle with variation of the above parameters.

If a gear train is required between the motor and load in a servomechanism, the gear train may be treated as ideal with perfect meshing of the gears. In this case the components of the system are joined at all times and the system may be described by a single linear differential equation. The classical linear solution in either the frequency or time domain is the result.

Present production methods cannot meet the requirements of an ideal gear train, having perfect engagement of the teeth, nor is the ideal gear train desirable from the standpoint of wear on the gear faces. The result is that the practical gear train has separation of the gear teeth when the velocities of the motor and load are different. The response of a servomechanism with backlash is in effect discontinuous or nonlinear. The net system acts as three individual but dependent systems with the boundary conditions of each being specified by certain physical laws.

Two accepted methods of analysis are available for solution of the

problem. The first is the solution by describing function methods while the second is by analytical methods. Describing function methods are primarily frequency response techniques and depend upon the assumption that the nonlinear element may be considered as linear over the range of consideration. A further assumption is made that the input to the nonlinear element is a pure sinusoid with no harmonic frequencies. The describing function method is primarily concerned with steady state results.

The analytical solution, which is the second method of considering the problem is primarily a transient response technique concerned with solution in the time domain. This approach also requires certain assumptions concerning the behavior of the system. The assumptions used in several investigations are pointed out in the following paragraphs, while the assumptions of this investigation are outlined in Section 3, Development of Equations. The validity of the analysis by any method depends on the accuracy with which the real system has been defined.

Chestnut and Mayer, Ref. a, have considered the backlash problem using describing functions and supported the findings by analog computer studies. The main difference between this cited work and previous describing function analyses was the simulation of backlash by a dead zone between the motor and load and springiness in the interconnecting shaft.

Various analytical approaches have been made to the problem of backlash, Lutkenhouse, Ref. b, used graphical methods in the phase plane to solve several cases of plastic impact between the gear teeth of a second order servomechanism. Pastel and Thaler, Ref. c, developed

analytical equations for the existence of limit cycles using phase plane equations for the case of plastic impact and no load inertia. Knoll and Narud, Ref. d, investigated limit cycles in the phase plane using an analog computer. The investigation of Knoll and Narud covered a wide range of parameters for the case of plastic contact between the gear teeth.

To analytically describe the total system response of a second order servo with backlash, three differential equations and one or more algebraic equations are required. The system as a whole may be treated as being piece wise linear. One differential equation is used to describe the entire system when the gear teeth are in contact and the motor is driving or braking. When the gear teeth are not in contact, two more differential equations are required, one for the motor alone and one for the load alone. The boundary conditions of the differential equations are determined from the solution of one or more algebraic equations, expressing the laws of conservation of momentum and energy. For plastic impact with no bounce of the gear teeth, the law of conservation of momentum must be satisfied. For perfect elastic contact between the gear teeth the law of conservation of momentum and the law of conservation of energy must be satisfied simultaniously. Intermediate cases between perfect elastic and perfect plastic contact can fulfill only the law of conservation of momentum. However, total energy accounting may be made in the intermediate and perfect plastic impact cases.

New, Ref. e, adapted the differential equations of system motion and the law of conservation of momentum (plastic contact) to a digital computer analysis of a second order servomechanism with backlash. The

digital computer was chosen as the method of solution for this investigation primarily because of the flexibility of data presentation and the ease with which cyclic parameter variation could be obtained.

In later sections of this thesis, the differential equations for the system and the algebraic equations for the impact boundary conditions are developed. The computer program and its flow diagram and modes of operation are pointed out. The results of the solutions of problems are presented in several forms and observations are made in Section 5, Results and Discussion. Sample applications of the results to mechanical systems are presented in Section 6, Application of Results.

At this writing, associated work in the area of transient response, primarily peak overshoot and settling time, of a second order servomechanism with backlash and plastic and elastic impact is being prepared as a thesis by C. E. Andrews and R. A. Kelley at the U. S. Naval Postgraduate School.

2. Development of Equations

The equations developed were those of a phase plane analysis. Prior to defining the net system equations, the assumptions under which the analysis was made will be stated. When necessary these assumptions will be amplified and referred to later in this work.

It was assumed that:

1. The gear teeth were initially in contact and the initial conditions of the system were all equal to zero. This was later proved to be an unnecessary limitation for the study of steady state response.
2. Plastic deformation of the gear teeth during steady contact and impact and any torsional deformations of driving shafts are negligible.
3. The inertias of the gears and drive shafts are considered as part of the load or motor inertia depending on their attachment in the system.
4. The law of conservation of energy was completely satisfied in only the perfect elastic case by maintaining the total mechanical rotational energy of the system constant at the instant prior to and after impact. The law of conservation of momentum is satisfied in plastic, elastic, and intermediate cases. When the law of conservation of momentum is the only equation required to be satisfied, the energy lost from the system is dissipated in the heat of infinitesimal deformations of the gear teeth.
5. The gear teeth are in contact only instantaneously during impact for the elastic and intermediate cases (excluding

plastic) and that the impulse torques of drive, friction and bearing supports, etc., are zero during impact, e.g.

$$\int_{dt \to 0} T_m \, dt = 0 \qquad \text{and} \qquad \theta = \theta'$$

6. The coefficient of restitution of the two opposing gear teeth is the same or is described by an equivalent coefficient if the two gear teeth are of unequal coefficients.
7. Backlash is assumed to be equal at all points on the gear circumference. Backlash is measured at the output shaft.

A block diagram of the system considered is presented below.

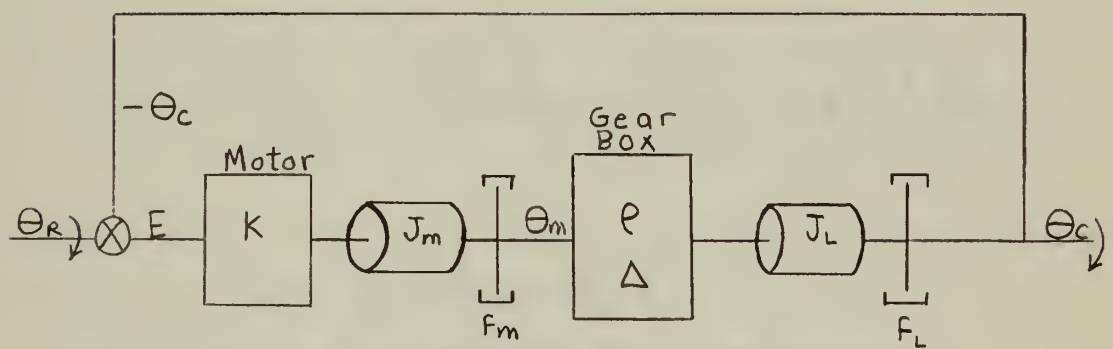

The equations for the motor and load in contact are:

$$E = \theta_R - \theta_c$$

$$T_m = KE = K(\theta_R - \theta_c)$$

$$T_L = J_L \ddot{\theta}_c + f_L \dot{\theta}_c$$

$$T_{Lm} = \rho T_L = \rho(J_L \ddot{\theta}_c + f_L \dot{\theta}_c)$$

$\theta_c = \rho \theta_m$ forward drive $\qquad \theta_c = \rho \theta_m + \Delta$ backward drive

$\dot{\theta}_c = \rho \dot{\theta}_m$ forward and backward drive

hence $T_{Lm} = \rho(J_L \rho \ddot{\theta}_m + f_L \rho \dot{\theta}_m)$

$= \rho^2 (J_L \ddot{\theta}_m + f_L \dot{\theta}_m)$

$T_m = J_m \ddot{\theta}_m + f_m \dot{\theta}_m + T_{Lm}$

$= J_m \frac{\ddot{\theta}_c}{\rho} + f_m \frac{\dot{\theta}_c}{\rho} + \rho^2 \left(J_L \frac{\ddot{\theta}_c}{\rho} + f_L \frac{\dot{\theta}_c}{\rho} \right)$

$= \left(\frac{J_m}{\rho} + \rho J_L \right) \ddot{\theta}_c + \left(\frac{f_m}{\rho} + \rho f_L \right) \dot{\theta}_c$

$T_m = K (\theta_R - \theta_c)$

$K \theta_R = \left(\frac{J_m}{\rho} + \rho J_L \right) \ddot{\theta}_c + \left(\frac{f_m}{\rho} + \rho f_L \right) \dot{\theta}_c + K \theta_c$

$$\ddot{\theta}_c + \frac{\left(\frac{f_m}{\rho} + \rho f_L \right) \dot{\theta}_c}{\left(\frac{J_m}{\rho} + \rho J_L \right)} + \frac{K \theta_c}{\left(\frac{J_m}{\rho} + \rho J_L \right)} = \frac{K \theta_R}{\left(\frac{J_m}{\rho} + \rho J_L \right)}$$

$$\rho\dot{\theta}_m - \dot{\theta}_c = -\rho\dot{\theta}'_m + \dot{\theta}'_c$$

$$\rho(\dot{\theta}_m + \dot{\theta}'_m) = \dot{\theta}'_c + \dot{\theta}_c$$

For conservation of energy

$$\frac{1}{2}\left(J_m\dot{\theta}_m^2 + J_L\dot{\theta}_c^2\right) = \frac{1}{2}\left(J_m\dot{\theta}_m'^2 + J_L\dot{\theta}_c'^2\right)$$

or $$\frac{J_m}{J_L}\left(\dot{\theta}_m^2 - \dot{\theta}_m'^2\right) = \left(\dot{\theta}_c'^2 - \dot{\theta}_c^2\right)$$

and factoring

$$\frac{J_m}{J_L}\left(\dot{\theta}_m + \dot{\theta}'_m\right)\left(\dot{\theta}_m - \dot{\theta}'_m\right) = \left(\dot{\theta}'_c + \dot{\theta}_c\right)\left(\dot{\theta}'_c - \dot{\theta}_c\right)$$

The momentum equation which is independent of e is:

$$\frac{J_m}{\rho J_L}\left(\dot{\theta}'_m - \dot{\theta}_m\right) = \left(\dot{\theta}_c - \dot{\theta}'_c\right)$$

or rearranging $$\frac{J_m}{\rho J_L}\left(\dot{\theta}_m - \dot{\theta}'_m\right) = \left(\dot{\theta}'_c - \dot{\theta}_c\right)$$

The factored energy equation is now divided by the momentum equation to yield $$\rho\left(\dot{\theta}_m + \dot{\theta}'_m\right) = \left(\dot{\theta}'_c + \dot{\theta}_c\right)$$

which checks with the definition of the coefficient of restitution for e=1.

The momentum equation implied from the impulse approach that $dt \to 0$ hence $\theta_c = \theta'_c$ and $\theta_m = \theta'_m$. The definition of the coefficient of restitution is independent of position. It may be noted that the equations for energy and momentum depend only on the inertia distribution, gear ratio and angular velocities.

In manipulation of these equations it is seen that load inertia may be transferred to the θ_1, shaft by multiplication ρ^2, the same transfer may be accomplished with load friction. Since θ_1, and $\dot{\theta}_1$, are related to θ_L and $\dot{\theta}_L$ it may be reasoned that the results

for $\rho = 1$ may be extrapolated to physical systems where $\rho \neq 1$.

Since a total energy accounting may be made for the system with the equations used, the rotational energy lost is attributed to the heat of deformation of the gear teeth. This transfer of energy could in fact be determined from the equations used. Thus the conservation of rotational energy e=1 is a special case of a broad interpretation of the law of conservation of energy.

$$\ddot{\theta}_c + 2\zeta\omega_n\dot{\theta}_c + \omega_n^2\theta_c = \omega_n^2\theta_R$$

where $$\omega_n^2 = \frac{\rho K}{J_m + \rho^2 J_L}$$

$$2\zeta\omega_n = \frac{f_m + \rho^2 f_L}{J_m + \rho^2 J_L}$$

The equation for load alone with gears not in contact is:

$$J_L\ddot{\theta}_c + f_L\dot{\theta}_c = 0$$

or $$\ddot{\theta}_c + \frac{f_L}{J_L}\dot{\theta}_c = 0$$

The equation for the motor alone with the gears not in contact is.

$$J_m\ddot{\theta}_m + f_m\dot{\theta}_m = K(\theta_R - \theta_c)$$

The method of analysis used by New, Ref. e, is used in order to be able to examine the system independently of its ω_n

Defining first $\omega_n t \triangleq t^*$

and differentiating $\omega_n dt = dt^*$

$$\omega_n = \frac{dt^*}{dt} \quad \text{and} \quad \omega_n^2 = \left(\frac{dt^*}{dt}\right)^2$$

$$\dot{\theta}_c = \frac{d\theta_c}{dt} = \frac{d\theta_c}{dt^*}\frac{dt^*}{dt}, \quad \frac{d\theta_c}{dt^*} = \dot{\theta}_c^*$$

hence $$\dot{\theta}_c = \dot{\theta}_c^*\omega_n$$

similarly

$$\ddot{\theta}_c = \frac{d^2\theta_c}{dt^2} = \frac{d^2\theta_c}{(dt^*)^2}\left(\frac{dt^*}{dt}\right)^2 = \frac{d^2\theta_c}{(dt^*)^2}\,\omega_n^2$$

$$\frac{d^2\theta_c}{(dt^*)^2} = \ddot{\theta}_c^* \quad \text{and} \quad \ddot{\theta}_c = \ddot{\theta}_c^*\,\omega_n^2$$

$$\text{finally} \quad \dot{\theta}_c = \dot{\theta}_c^*\,\omega_n = \dot{\theta}_c^*\,\frac{dt^*}{dt}$$

$$\int \dot{\theta}_c\,dt = \int \dot{\theta}_c^*\,dt^* \quad \text{or} \quad \theta_c = \theta_c^*$$

Using the equations of the combined system and the load alone,

$$\ddot{\theta}_c + 2\zeta\omega_n\dot{\theta}_c + \omega_n^2\theta_c = \omega_n^2\theta_r \quad \text{combined system}$$

$$\ddot{\theta}_c + \frac{f_L}{J_L}\dot{\theta}_c = 0 \quad \text{load alone}$$

and making the indicated substitution to a transformed (*) coordinate system for the system equation

$$\omega_n^2\ddot{\theta}_c^* + 2\zeta\omega_n^2\dot{\theta}_c^* + \omega_n^2\theta_c^* = \omega_n^2\theta_R$$

$$\ddot{\theta}_c^* + 2\zeta\dot{\theta}_c^* + \theta_c^* = \theta_R$$

and introducting the slope equations of the phase plane

$$N_S\dot{\theta}_c^* + 2\zeta\dot{\theta}_c^* + \theta_c^* = \theta_R \quad \text{results.}$$

If the load equation is first put in the form for the phase plane

$$N_L\dot{\theta}_c + \frac{f_L}{J_L}\dot{\theta}_c = 0$$

and then transformed to the (*) coordinate system where $\dot{\theta}_c^* \neq 0$

$$N_L\dot{\theta}_c^* + \frac{f_L}{J_L}\dot{\theta}_c^* = 0 \quad \text{results.}$$

The same result may be obtained by setting $\omega_n = 1$. The results of such a transformation require inverse scaling for practical application, examples of which given in Section 6. It is noted that the slope of the load-free equation is mathematically the same whether in the phase plane or in the transformed phase plane. It is pointed out at this time that the equations later developed to satisfay the laws of conservation of momentum and energy are independent of the system natural frequency.

To establish equations for the law of the conservation of momentum and a relationship satisfying the law of the conservation of energy, the following schematic is used.

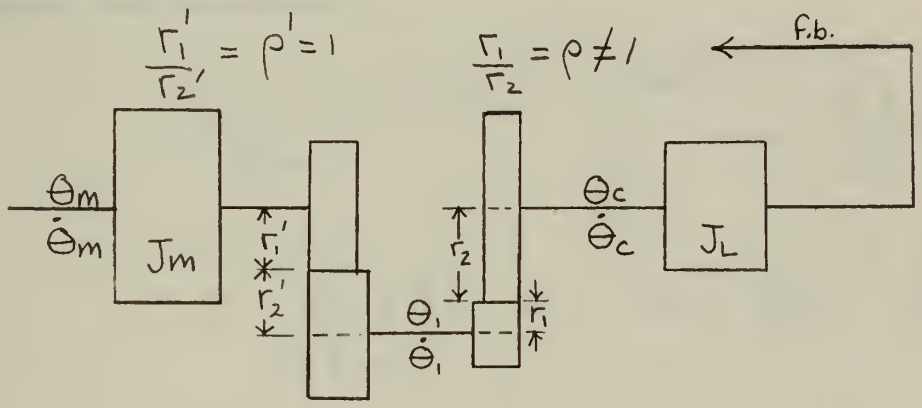

It is seen that $\theta_c = -\rho\,\theta_1$, $\dot{\theta}_c = -\rho\,\dot{\theta}_1$

and since $\rho' = 1$ an equivalent schematic results

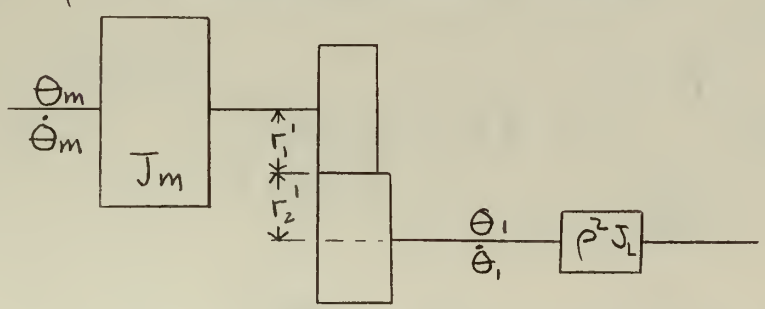

By representing the inertia of the load and motor as inertia of the gears the following figure is obtained at the instant of impact.

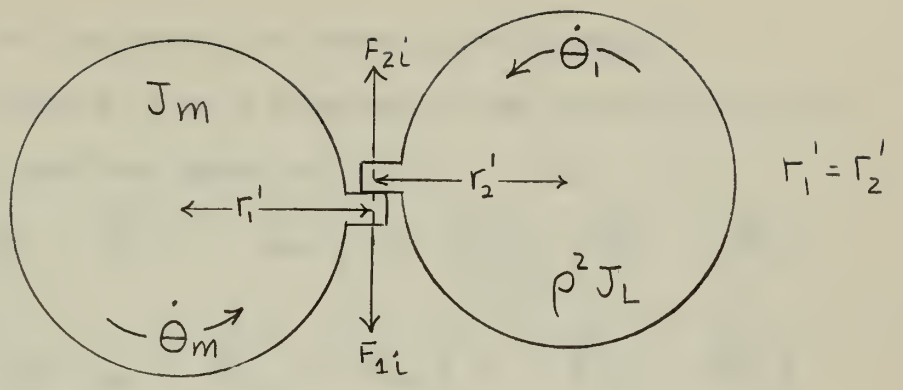

The torque equation may be expressed $T = J\ddot{\theta} = J\frac{d\dot{\theta}}{dt}$

Impulse is equal to the time rate of change of momentum. The expressions for the rates of change of momentum of the gears treated separately may be written:

$$-\int_{dt\to 0} |F_{1i}|\, r_1'\, dt = \int_{\dot{\theta}_m}^{\dot{\theta}_m'} J_m \frac{d\dot{\theta}_m}{dt}\, dt$$

$$-r_1' \int_{dt\to 0} |F_{1i}|\, dt = J_m(\dot{\theta}_m' - \dot{\theta}_m)$$

$$-\int_{dt\to 0} |F_{1i}|\, dt = \frac{J_m}{r_1'}(\dot{\theta}_m' - \dot{\theta}_m)$$

for the motor

and

$$\int_{dt\to 0} |F_{2i}|\, r_2'\, dt = \int_{\dot{\theta}_1}^{\dot{\theta}_1'} \rho^2 J_L \frac{d\dot{\theta}_1}{dt}\, dt$$

$$\int_{dt\to 0} |F_{2i}|\, dt = \rho^2 \frac{J_L}{r_2'}(\dot{\theta}_1' - \dot{\theta}_1)$$

where the primed velocities are those following impact.

If the momentum is to be conserved in the system the impulse functions are equal and opposite.

$$\frac{J_m}{r_1'}\left(\dot\theta_m' - \dot\theta_m\right) = \rho^2\frac{J_L}{r_2'}\left(\dot\theta_1' - \dot\theta_1\right)$$

and

$$\frac{J_m}{J_L}\frac{1}{\rho}\left(\dot\theta_m' - \dot\theta_m\right) = \left(\dot\theta_c - \dot\theta_c'\right)$$

from substitution of the equations

$$r_1' = r_2' \quad , \qquad \dot\theta_c = -\rho\,\dot\theta_1$$

The assumption that all other impulse functions are zero at the instant of impact is restated at this point.

A definition of the coefficient of restitution will be made for purposes of this work:

$$e \triangleq -\frac{\left(\dot\theta_m' + \dot\theta_1'\right)}{\left(\dot\theta_m + \dot\theta_1\right)} = -\frac{\left(\rho\,\dot\theta_m' - \dot\theta_c'\right)}{\left(\rho\,\dot\theta_m - \dot\theta_c\right)}$$

It will be shown that this definition of e will satisfy the law of conservation of energy. Consider the case of e=0,

$$0 = -\left(\rho\,\dot\theta_m' - \dot\theta_c'\right), \qquad \rho\,\dot\theta' = \dot\theta_c$$

in which case for plastic impact (e=0) the gears are moving at the same velocity following impact.

The expression for the coefficient of restitution is examined for the case of perfect elastic contact, e=1, for which the law of conservation of energy is satisfied.

Solution of the restitution equation for e=1 yields

3. Computer Program Development

The physical equations of the net systems were programmed for solution using the Control Data Corporation 1604 high speed digital computer utilizing paper tape program input and magnetic tape output. An IBM 717 line printer was used to extract data from the magnetic tape. The Control Data Corporation machine library and the U. S. Naval Postgraduate School computer subroutine library were used for assembly, Runge-Kutta-Gill numerical integration, and decimal output.

Several changes were made in the forms of the physical equations of the net system in order to eliminate duplicate computing operations and to fit the equations to a form suited to the variable parameters. In the table of symbols, computer mnemonic (m) terms which are used in the assembly subroutine have been indicated by parenthises and will be defined when encountered.

The equation of the system with motor and load combined

$$\ddot{\theta}_c = \omega_n^2 \theta_R - \omega_n^2 \theta_c - 2\zeta\omega_n \dot{\theta}_c$$

was put in the form

$$\ddot{\theta}_c = \omega_n^2 \theta_R - \omega_n^2 \theta_c - \underline{A}\,\dot{\theta}_c \quad \text{where}$$

$$\underline{A} = 2\zeta\omega_n \quad \text{and}$$

$\underline{\text{THETAL}} = \theta_c$ $\qquad$ $\underline{\text{ONE}} = \theta_R$

$\underline{\text{THETALD}} = \underline{U} = \dot{\theta}_c$ $\qquad$ $\underline{\text{ZETA}} = \zeta$

$\underline{\text{UDOT}} = \ddot{\theta}_c$ $\qquad$ $\underline{\text{OMEGANSQ}} = \omega_n^2$

were the computer m terms used. Underlining will be used in this section to denote the transition to the m terms of the computer equations.

The differential equations were solved using the Runge-Kutta-Gill,

(RUNGE), numerical integration method. The RUNGE subroutine required the definition of synonymous terms for the four iterative cycles used to produce one extrapolated set of variables. The increment of the independent time variable chosen was 0.01 sec. for all $\zeta > 0.1$ and 0.004 sec. for all $\zeta \leq 0.1$.

The load free equation

$$\ddot{\theta}_c + \frac{f_L}{J_L}\dot{\theta}_c = 0$$

was put in the form

$$\ddot{\theta}_c + \underline{B}\,\dot{\theta}_c = 0$$

for the computer.

A separate set of RUNGE synonyms was used for the load free equation in order not to destroy the previous computations before they were determined of no further value in computing and also in the making of program decisions.

$\dot{\theta}_c$ was designated V and $\ddot{\theta}_c$ was designated VDOT for the computer program.

The equation for the motor alone

$$\ddot{\theta}_m + \frac{f_m}{J_m}\dot{\theta}_m + \frac{k}{J_m}\theta_c = \frac{k}{J_m}\theta_R$$

was put in the form

$$\ddot{\theta}_m = -\frac{f_m}{J_m}\dot{\theta}_m + \frac{k}{J_m}(\theta_R - \theta_c)$$

$$\ddot{\theta}_m = -\underline{D}\,\dot{\theta}_m + \underline{C}\,(\theta_R - \theta_c)$$

and for RUNGE, the terms

θ_m = THETAM $\qquad \dot{\theta}_m$ = THETADM = W

and $\ddot{\theta}_m$ = WDOT were used.

The equation representing the law of conservation of momentum and the definition of coefficient of restitution were combined to the forms

$$\dot{\theta}_c' = \frac{J_m}{J_m + \rho^2 J_L}\left[\rho\,\dot{\theta}_m(1+e) + \dot{\theta}_c\left(\rho^2\frac{J_L}{J_m} - e\right)\right]$$

$$\dot{\theta}_m' = \frac{\dot{\theta}_c' - e\rho\dot{\theta}_m + e\,\dot{\theta}_c}{\rho}$$

for the computer program. No provision for additional m terms was made to denote the primed values. The additional terms:

e = RESTITUT ρ = RHO and ρ^2 = RHOSQ

were used.

Two equations were used to define the boundaries of operation of the load and motor when they were acting separately,

$$\theta_c = \rho\,\theta_m \quad \text{and} \quad \theta_c = \rho\,\theta_m + \Delta$$

Two major decisions of the computing cycle were the determination of the point where the motor and load would float free, FLOATEST, and the response of the system to impact of the load and motor gears when the boundary conditions on position were met, COMBTEST.

The first decision, the point of float free, is made on the equality or inequality of slopes in the phase plane, i.e., at separation $N_L = N_S$. Equating the slopes:

$$\frac{\omega_n^2}{\dot{\theta}_c}(\theta_R - \theta_c) - A + B = 0$$

The above equation is solved after computing each point in the combined phase trajectory. If $N_S + N_L > 0$ the system remains combined. If $N_S + N_L \leq 0$ the system separates, having the response motor alone and load alone immediately thereafter.

The second major decision, that of whether after impact the

response should be that of the combined system or the response of the load and motor acting separately, is made on the basis of the resultant velocities after impact and upon which side of the backlash the motor and load positions are found.

The computer program, its flow diagram, a description of the program operation, and an explanation of the readout of information with examples are presented in the Appendix.

4. Methods and Scope of Examination

Two modes of operation of the computer program were used. The first mode considered was the phase trajectory. This mode was used to check the operation of the computing cycle. Time, velocity and position of the load were printed when the system was combined. When the system was separated, the values of motor velocity and motor position were also printed. Although the time increment used for computations was either 0.01 sec. or 0.004 sec., printed outputs for the first mode were taken only every 0.1 sec. Additional printed outputs were taken at the time of contact of the gears just prior to and immediately following the solution of the momentum and restitution equations. A typical printout of the phase trajectory mode of operation is shown in Appendix C.

The second mode of operation was used for printing only the maximum computed positive load overshoot position for each cycle, the associated load velocity and the exact problem time of the computation. A sufficient number of print-outs for each problem was obtained to prove limit cycle existence and average size. Since this investigation was concerned primarily with the steady state response, the second mode of operation was the one utilized to obtain the majority of the data. This read-out method markedly decreased the data reduction time for the problem analysis, as opposed to the analysis of steady state conditions provided by a full phase trajectory print-out. Since the time required for computer read-out was several magnitudes greater than the computing time, valuable computer time was saved by this mode of operation. An example of the printed output obtained when only maximum load position overshoot was of interest is given in Appendix D. Approximately 1400

phase trajectories were solved using this mode of operation. Each solution required an average of three minutes of computer time.

For the purpose of general examination of the problem it was assumed that $\rho = 1$, $K = 1$, $\omega_n = 1$, $J_m + \rho^2 J_L = 1$. Specific solutions were made with $\rho \neq 1$, $\omega_n \neq 1$ to determine scaling effects. The results of these solutions are presented in Section 6, Application of Results.

The program can also be made to solve linear systems by setting $\Delta = 0$.

The major variable parameters used in this investigation were:

$\zeta = 0.1, 0.2, 0.3, 0.4, 0.5, 0.6, 0.8, 1.0$

$\frac{\rho^2 f_L}{F_T} = 0\ , 0.2, 0.4, 0.6, 0.8, 1.0$

$\frac{\rho^2 J_L}{J_m} = \frac{0.1}{0.9}, \frac{0.2}{0.8}, \frac{0.5}{0.5}, \frac{0.8}{0.2}, \frac{0.9}{0.1}$

$\Delta = 0.3$ radians

$e = 0, 0.6, 0.8, 1.0$

Additional parameters of

$\frac{\rho^2 f_L}{F_T} = 0.04, 0.1, 0.9$; and $\Delta = 0.01, 0.03, 0.01, 0.15$ radians

were used in certain instances to examine particular characteristics of the response.

The program was limited somewhat in that the value of $\frac{\rho^2 J_L}{J_m} = \infty$ and zero were exluded due to generation of undefined mathematical quantities.

The value of backlash was made abnormally large, $\Delta = 0.3$ radians, to allow an easier interpretation of the non-linear response. Since the influence of Δ was linear, this caused no inaccuracies. All

graphs for limit cycle size were plotted with Δ = 0.3 radians. The effect of values for Δ other than 0.3 is also shown in graphical form.

5. Results and Discussion

Two types of system response were observed. The first type was a convergence to zero error, which was a case of static and dynamic equilibrium of the system. This is a characteristic of a linear second order servomechanism. The second type of system response observed was the divergence or convergence to a state of dynamic equilibrium. This second type of response is termed a limit cycle and is characterized by cyclic travel of the load through the same points of the phase trajectory. When the second mode of computer operation was used, both the maximum load position per cycle and the period of the recorded position were analyzed to determine if the characteristic response was a limit cycle. Exact repetition of cyclic values was impossible due to the numerical methods used and the computer round-off error for the output routine. Typical examples of the limit cycle and no limit cycle response are given in Appendices D 1 and D 2.

No case of dynamic instability or divergence of the system without bound was observed in the investigation. Intuition might lead to this same conclusion when the following unique characteristics of this system are pointed out: (a) As a maximum limit, energy was conserved at the instant of impact. (b) Energy was supplied to the system only in finite amounts and at a finite rate by the error detector. (c) Energy sinks were present in the system frictional elements while energy storage units were present in both the motor and load. (d) No undefined limits appeared in the applied physical equations,

$\rho^2 \frac{J_L}{J_m} = 0$ and ∞ excluded.

The results of the investigation are offered in the form of charts for parameter areas of limit cycle existence and nonexistence in Fig. 1 for e = 0., 0.6, 0.8 and Fig. 2 for e = 1.0. The parameters $\rho^2 \frac{f_L}{F_T}$ and $\rho^2 \frac{J_L}{J_m}$ are designated abscissa and ordinate respectively. The parameter points of examination for which solutions were obtained are circled. The zone enclosed by a particular ζ line is largely an interpretation by the authors of the results of the investigation, and shows the area in which no limit cycle existed. Due to the large change of the variable parameter values between solutions, the charts are <u>not exact</u>. All circled intersections interior to the ζ line indicate parameters which resulted in no limit cycles, e.g., Fig. 1 for e = 0, 0.6, 0.8 at a ζ = 0.4, the values of $\rho^2 \frac{f_L}{F_T}$ = 0.6, 0.8 at a $\rho^2 \frac{J_L}{J_m}$ = 9.0 and the value of $\rho^2 \frac{f_L}{F_T}$ = 0.6 at a $\rho^2 \frac{J_L}{J_m}$ = 4.0 resulted in no limit cycle. Similarly, for ζ = 0.5, the values of $\rho^2 \frac{f_L}{F_T}$ = 0.4, 0.6, and a $\rho^2 \frac{J_L}{J_m}$ = 1.0 as well as all other parameter intersections interior to the ζ = 0.5 curves, resulted in no limit cycles.

All circled parameter intersections exterior to particular ζ lines define paramters which were examined and resulted in a steady state limit cycle. The area to the right of the single ζ = 1.0 line designates the parameters for which no limit cycles were observed. Limit cycles were observed for all $\zeta \leq$ 0.3 for the parameters examined.

The investigation was made with Δ = 0.3 radians; however, results of the investigation of variation of limit cycle size indicate

that existence of the limit cycle is independent of the size of backlash in a nonlinear system for a Δ greater than zero. Variation of Δ had the effect of a linear variation of limit cycle size only.

The zones depicted on the existence charts are approximately represented by straight lines; however there is reason to believe that a complete examination would show a curvature in the lines. This observation will be elaborated upon later when the relationship between the existence charts and the figures of limit cycle size is discussed.

From Fig. 1 it is seen that there is only a very small difference in the limit cycle existence zones for plastic impact (e = 0) and the intermediate values of the coefficient of restitution, e = 0.6 and 0.8. When comparing the elastic impact (e = 1) in Fig. 2 to the plastic and intermediate cases in Fig. 1, the most obvious point of comparison is the drastic reduction of the areas in which limit cycles did not result for e = 1.0. However, it may be generally observed that with any e held constant, the area in which a limit cycle could not be obtained increased with the increase of system ρ .

For all values of e, there is an apparent common enclosed zone centroid which is described by the system parameters $\rho^2 f_L/F_T = 0.5$ and $\rho^2 J_L/J_m = 1.0$. These parameters result in the system time constants $f_L/J_L = f_m/Jm$, since $\omega_n = 1$ and $\rho = 1$ were chosen for the investigation. There is also an apparent symmetry about the centroid of opposite quadrants which can be related to the fact that since $\omega_n = 1$ and $\rho = 1$, the points diametrically opposite across the centroid of the figure (using the decimal values of the parameter intersection) represent an exact exchange of component time constants. (See Fig. 2 for example). Two diametrically opposite points may have

exactly the same motor and load time constants; however, they are descriptive of two different systems since the friction and inertia distributions are different for the two points.

Figs. 3 through 26 present the maximum positive error in radians of the limit cycle for a unit step input and with backlash equal to 0.3 radians. The use of the charts is explained in Section 6, Application of Results. Each figure is presented with $\rho^2 f_L/F_T$ and e constant. The independent parameter $\rho^2 J_L/J_m$ is indicated as abscissa and curves of constant ζ are plotted with limit cycle error as the ordinate. The results were presented on a log log plot since the observed limit cycle errors encompassed a range from 0.01 to 1.0 radians, and the appearance and disappearance of limit cycles and the change of limit cycle error was more readily apparent on the log log form.

In general as e increases, the size of limit cycle decreases, all other parameters remaining constant. However this is not without a few exceptions; the generalization is most accurate for large size limit cycles. It may be noted that when viewing the individual charts, if a limit cycle exists at very low $\rho^2 J_L/J_M$ ratio there is a tendency for the same system to have a smaller limit cycle for higher $\rho^2 J_L/J_m$ ratio. In addition, for these same conditions, if limit cycles exist for several values of ζ, there is a convergence toward the same size of limit cycles for each ζ as $\rho^2 J_L/J_m$ increases. At the value $\rho^2 f_L/F_T = 0$, a limit cycle will always occur for any value of e or ζ.

Viewing the charts in sequence, with either e constant or $\rho^2 f_L/F_T$ constant, it is noted that there is continuity of pattern flow between

adjacent charts. This continuity between charts appears to form a symmetrical pattern of constant ζ lines which can be interpolated for intermediate values. When the figures for $\rho^2 f_L/F_T = 0.4$ and 0.6 are analyzed, this symmetrical pattern is observed in each chart about $\rho^2 J_L/J_m = 1$. The limit cycle decreases and disappears at the opposite extremes of $\rho^2 J_L/J_m$. The charts of $\rho^2 f_L/F_T = 0.4$ and 0.6 are symmetrical to each other, while $\rho^2 f_L/F_T = 0.2$ and 0.8 are similar. At the extreme values of $\rho^2 f_L/F_T = 0$ and 1.0, no symmetrical comparison can be made. An additional point of symmetry about $\rho^2 f_L/F_T = 0.5$ can be visualized for all values of e. These parameters for symmetry are noted in the discussion of the existence charts. The irregularities in the curves of medium values of ζ can not be explained by the authors; however, it may be mentioned again that the points of symmetry are characterized by exact exchange of component time constants.

The noted symmetry of the limit cycle size charts shows a direct relationship to the symmetry found in the existence charts. Since the existence charts show contours of constant ζ for a surface of zero limit cycle size, one is led to the possibility of a three dimensional presentation to show a variation of limit cycle size for the same parameters used in the existence charts. Such a three dimensional figure for constant e using $\rho^2 f_L/F_T$, $\rho^2 J_L/J_m$ and ζ as the axes is shown in Fig. 27. Other surfaces could be added above this zero limit cycle "floor" to show the variation of a given limit cycle size by contours of ζ. The ultimate result of this line of investigation would be the evaluation of the poles and zeros for a conformal mapping presentation. Unfortunately, time did not permit the authors to investigate

this avenue further.

The results of the investigation of the dependence of limit cycle size on the amount of backlash are presented in Figs. 28 and 29 using coefficients of restitution of 0 and 1.0 at a ζ = 0.6. A thorough investigation was made at this ζ since it is an average system parameter often used in design work. The limit cycle size was found to vary directly with backlash size without exception between the values of 0.3 and 0.01 radians. When limit cycles existed at Δ = 0.3, there was no disappearance of limit cycle with decreasing magnitude of Δ . Where no limit cycle existed, at Δ = 0.3, limit cycles continued to be non-existent throughout the range of Δ examined. Several solutions of problems with ζ = 0.6 and e = 0.6 &0.8 and ζ = 0.1 & e = 1.0 & 0 with various Δ values, proved the linear variation of limit cycle size with backlash size for all values of e.

When a servomechanism under steady state conditions is disturbed by a small perturbation, it will return to the original steady state conditions. However, the transient response due to the perturbation may be quite different from the transient response which occured due to the original signal input. The concepts of energy and static and dynamic equilibrium mentioned in Section 1 may be better understood as a result of the perturbation technique if the usual initial conditions of $\dot{\theta}_c(0) = \theta_c(0) = 0$ are considered as a disturbance from the stability conditions predetermined by selection of system parameters and signal input.

This same small perturbation technique was simulated mathematically using the digital computer to obtain several solutions. The cases examined and their initial conditions were:

a) $\zeta = 0.6$, $\rho^2 J_L/J_m = 0.8/0.2$, $\rho^2 f_L/F_T = 0$, $e = 0$, $\Delta = 0.3$

$\dot{\theta}_c(0) = 0$, $\theta_c(0) = 1.2$

$\dot{\theta}_m(0) = 0$, $\theta_m(0) = 1.0$

system separated.

b) $\zeta = 0.6$, $\rho^2 J_L/J_m = 0.1/0.9$, $\rho^2 f_L/F_T = 1.0$, $e = 1.0$, $\Delta = 0.3$

$\dot{\theta}_c(0) = 1.0$, $\theta_c(0) = 1.0$

$\dot{\theta}_m(0) = 1.0$, $\theta_m(0) = 1.0$

system combined

c) $\zeta = 0.4$, $\rho^2 J_L/J_m = 0.5/0.5$, $\rho^2 f_L/F_T = 0.4$, $e = 0.6$, $\Delta = 0.3$

$\dot{\theta}_c(0) = 0$, $\theta_c(0) = 1.005$

$\dot{\theta}_m(0) = 0$, $\theta_m = 1.00$

system separated

In the three cases examined, the same limit cycle was obtained, both in size and period, as that resulting from the normally used initial conditions, $\dot{\theta}_c(0) = \theta_c(0) = 0$. The maximum difference between the perturbation response and the original limit cycle size for the three cases was 18×10^{-5} radians. Two types of transient response were observed. These were convergence to limit cycle in the first two cases and divergence to limit cycle in the last case.

The results obtained by the small perturbation technique supported the validity of the analysis of the problem by digital methods. This result also concurs with the findings for the case of $e = 0$ by Knoll and Narud, Ref. d, in that the steady state limit cycle size is completely specified by the choice of system parameters and independent of system initial conditions.

Mention is made here that the computer program could not be run normally for the perturbation method. The computer was stopped after

the print out of system constants, then the initial conditions of the servo system were inserted manually. The program was then restarted at the desired point for computing, either as a combined system or with the motor and load separated. The program was then allowed to operate to the normal completion of the solution.

The work of Ref. d reported that the system transient response for the case e = 0 arrived at a steady state limit cycle by two possible phase trajectories. One of these phase trajectories was smooth convergence to the limit cycle, while the second was a converging overshoot toward the inside of the limit cycle followed by a divergence to the limit cycle. From the results of this investigation for the cases e = 0, 0.6, 0.8 and 1.0, similar transient indications were obtained.

Several computer solutions were accomplished for the cases Δ = 0.3 radians, e = 0, 1.0, ρ = 1.0, ω n = 1.0, K = J $\neq$ 1.0. In addition various combinations of $\rho \neq 1.0$ and $\omega n \neq 1.0$ were obtained. The purpose of these solutions were:

1. To determine the general applicability of the computer program.
2. To verify the scaling developed in Section 2, Development of Equations.
3. To determine the applicability of the results of this thesis.

The following results were determined:

A. Two solutions were obtained (e = 0 & 1.0) for the case $\zeta = 0.4$, $\rho = 1.0$ ω n = 1.0, J = 2.0, K = 2.0, $\rho^2 \frac{f_L}{F_T} = 0.4$, $\rho^2 \frac{J_L}{J_m} = 4.0$. The results of these solutions were the same (time, load velocity, load position, and limit cycle size) as the solutions obtained for $\rho^2 \frac{f_L}{F_T} = 0.4$, $\rho^2 \frac{J_L}{J_m} = 4.0$, $\zeta = 0.4$ using the nondimensional parameters ω n = 1.0, ρ = 1.0, J = 1.0, K = 1.0.

B. Solutions were obtained for e = 0 & 1.0 for the case $\zeta = 0.4$, $\rho = 1.0$, $\omega_n = 2.0$, J = 1.0, K = 4.0, $\rho^2 \frac{f_L}{F_T} = 0.4$, $\rho^2 \frac{J_L}{J_m} = 4.0$. The results of these solutions yielded the same size maximum overshoots and limit cycle size as the nondimensional solutions for $\zeta = 0.4$, $\rho^2 \frac{f_L}{F_T} = 0.4$, $\rho^2 \frac{J_L}{J_m} = 4.0$. The times of maximum overshoots in this case were one-half the times of occurence of the same overshoots for the nondimensional solution. The velocity at a maximum overshoot was twice the value of velocity obtained for the same overshoot in the nondimensional solution. This same comparison can be made for Cases A and B. The results of these and other solutions prove the validity formulae used in Section 2, Development of Equations, concerning the transformation to the coordinate system. (*)

C. Solutions were obtained for the case e = 0 & 1.0, $\zeta = 0.4$, $\rho = 0.5$, $\omega_n = 1.0$, $\frac{f_L}{F_T} = 0.8$, $\frac{J_L}{J_m} = 4.0$, $\rho^2 \frac{f_L}{F_T} = 0.2$, $\rho^2 \frac{J_L}{J_m} = 1.0$. The results of these solutions were the same (time, load velocity, maximum overshoots and limit cycle size) as for the nondimensional solutions $\zeta = 0.4$, $\rho = 1.0$, $\omega_n = 1.0$, $\rho^2 \frac{f_L}{F_T} = 0.2$, $\rho^2 \frac{J_L}{J_m} = 1.0$.

D. Solutions were obtained for the case e = 0 & 1.0, $\zeta = 0.4$, $\rho = 0.5$, $\omega_n = 2.0$, $\frac{f_L}{F_T} = 0.8$, $\frac{J_L}{J_m} = 4.0$, $\rho^2 \frac{f_L}{F_T} = 0.2$, $\rho^2 \frac{J_L}{J_m} = 1.0$. The results of these solutions yielded the same size maximum overshoots and limit cycle size as the nondimensional solutions for $\zeta = 0.4$, $\rho^2 \frac{f_L}{F_T} = 0.2$, $\rho^2 \frac{J_L}{J_m} = 1.0$. The times and velocities in this case were scaled by ω_n as in Case B.

Several phase trajectories using e = 0 were compared with those obtained by New, Ref. e. Generally good correlation was obtained on the value of limit cycle error and in the transient response. Small disagreements were expected, resulting primarily from differences in the

programming procedures and analysis of results by read-out methods.

Sample phase trajectories for the cases of e = 0 & 1.0 are presented in Figs. 30 and 31. Although the transient analysis of the system is beyond the scope of this work, these figures may aid in understanding the physical problem.

Of academic interest was the accidental operation of the computer program for several solutions using $\zeta = 0$. Several responses were observed. One was a nearly pure oscillatory system from the first overshoot and thereafter another was a very slow convergence or slow divergence of the oscillations after the first overshoot. The convergence or divergence probably resulted from errors generated in numerical iterations and approximations.

6. Application of Results

In this section, the results of this thesis will be applied to hypothetical physical systems. Methods will be indicated by which physical systems may be analyzed or designed. Attention is called to the assumptions stated in Section 2 under which this study was made.

It is desirable to find an equation relating certain system variables, therefore the equations:

$$(1) \qquad \omega_n^2 = \frac{\rho k}{J_m + \rho^2 J_L} = \frac{\rho k}{J_m}\left[\frac{1}{1+\rho^2\frac{J_L}{J_m}}\right]$$

and

$$(2) \qquad 2\zeta\omega_n = \frac{f_m + \rho^2 f_L}{J_m + \rho^2 J_L} = \frac{\rho^2 f_L\left[\frac{f_m}{\rho^2 f_L} + 1\right]}{J_m\left[1 + \rho^2\frac{J_L}{J_m}\right]}$$

will be manipulated to the form

$$(3) \qquad \zeta = \frac{1}{2}\rho^2\frac{f_L}{J_m}\frac{\left[\frac{f_m}{\rho^2 f_L} + 1\right]}{\left[1+\rho^2\frac{J_L}{J_m}\right]}\frac{\sqrt{J_m}}{\sqrt{\rho}\sqrt{K}}\sqrt{1+\rho^2\frac{J_L}{J_m}}$$

or

$$(4) \qquad \zeta = \frac{1}{2} f_L\left[\frac{f_m}{\rho^2 f_L} + 1\right]\left[\frac{\rho^3}{J_m K\left(1+\rho^2\frac{J_L}{J_m}\right)}\right]^{1/2}$$

In view of the form of Equation (4) for ζ and recalling that the variable parameters used on the figures were $\rho^2\frac{J_L}{J_m}$ and $\rho^2\frac{f_L}{f_T} = \frac{\rho^2 f_L}{f_m + \rho^2 f_L} = \frac{1}{\frac{f_m}{\rho^2 f_L} + 1}$ it is seen that the expression for ζ in fact includes the other two variable parameters.

From discussion concerning the effects system natural frequency, it will be recalled that the value of overshoot and hence limit cycle are not affected by ω n; however, the time and velocity are scaled for ω n $\neq$ 1.0. Thus the transient response characteristics may be related to the same parameters used in these applications.

If a motor and load are selected for a system and the limitation is imposed that system operation shall not result in a limit cycle, Equation (4) and the limit cycle existence charts may be used to determine the unspecified system parameters ζ, K and ρ. The coefficient of restitution for the proposed gear train material may be determined by the use of the equation in Section 2.

To proceed, select a value of K and ρ, then determine the value of ζ from Equation (4). Enter the limit cycle existence chart for the value of e, system ζ and the parameters $\rho^2 \frac{J_L}{J_m}$ and $\frac{1}{\frac{f_m}{\rho^2 f_L} + 1}$. Determine if the selected parameters describe a point of no limit cycle. Since limit cycle existence is independent of backlash ($\Delta \neq 0$ excluded), backlash is not a variable parameter. Successive trial values of the unspecified parameters may be required to meet the limitation of no limit cycle. If it is also required that certain transient response characteristics be met, these conditions could be examined by a similar method.

In the event that no acceptable parameters are found to satisfy the system requirements for no limit cycle, the figures for limit cycle size may be examined to obtain a minimum size limit cycle. The method of solution is similar to that previously described.

Example: The material intended for use in the gears has an e = 0.6.

The motor and load have the parameters fm = 0.64, Jm = 0.25, f_L = 0.64, J_L = 1.0 and it desired that the system operate with no limit cycle. If the values are selected K = 4.0, ρ = 0.5, the values $\rho^2 \frac{J_L}{Jm} = 1.0$ and $\frac{fm}{\rho^2 f_L} = 4.0$, $\frac{1}{\frac{fm}{\rho^2 f_L} + 1} = 0.2$ result.

Solve Equation (4) for $\zeta = .5(.64)(5+1) \frac{.5^{3/2}}{[.25(4)(1+1)]^{1/2}}$, thus $\zeta = 0.4$. Enter the chart for limit cycle existence, Fig. 1, e = 0.6, ζ = 0.4, $\frac{1}{\frac{fm}{\rho^2 f_L} + 1} = 0.2$, $\rho^2 \frac{J_L}{Jm} = 1.0$

It can be seen that limit cycle will exist for these parameters.

Since K is most easily varied in equation (4), a new K is selected at 1.0 in an effort to find parameters for no limit cycle. It is seen that

$$\zeta_{K=1.0} = \zeta_{K=4.0} \sqrt{\frac{4}{1}} = 0.4(2)$$

with all other parameters constant, thus ζ = 0.8 Enter Fig. 1 with e = 0.6 , $\zeta = 0.8$ $\rho^2 \frac{J_L}{Jm} = 1.0$, $\frac{1}{\frac{fm}{\rho^2 f_L} + 1} = 0.2$

These parameters describe system operation with no limit cycle and are well within the area limits. The transient response of this system may be undesirable and various combinations of ρ and K would have to be tested to satisfy the additional requirements of the problem. It will be restated that the existence areas of Figs. 1 and 2 are not exact.

The figures of limit cycle size may be used in the same manner as the existence charts. The same parameters of the first case are assumed: K = 4.0, ρ = 0.5, $\rho^2 \frac{J_L}{Jm} = 1.0$, $\frac{1}{\frac{fm}{\rho^2 f_L} + 1} = 0.2$ $\zeta = 0.4$

e = 0.6, Δ = 0.1 radians. Enter Fig. 10 with the parameters given. The ordinate, Limit Cycle Error $\left(\frac{0.3}{\Delta}\right)$ = 0.13 radians, is obtained. The maximum positive error in the limit cycle = $0.13 \frac{(0.1)}{(0.3)}$ = 0.0434 radians. Enter the same figure for e = 0.6, ζ = 0.8, $\rho^2 \frac{J_L}{J_m}$ = 1.0, $\frac{1}{\frac{f_m}{\rho^2 f_L}+1}$ = 0.2, Δ = 0.5 radians; this is the second case of examination for existence. No ζ = 0.8 curve exists; hence no limit cycle exists for this choice of parameters for any nominal value of backlash.

7. Conclusions

Within the limitations of the assumptions made and the scope of this thesis, it is concluded that:

A. Two types of system steady state response result. The type of response is independent of backlash size, system natural frequency and initial conditions. The types of response are convergence to signaled input position and convergence to a limit cycle.

B. If a limit cycle exists in the steady state response of a system, the size of the limit cycle varies directly with the size of backlash, all other parameters constant.

C. The greatest change in system steady state response occurred for the case when system rotational energy is conserved ($e = 1.0$).

D. A point of symmetry for the type of system steady state response exists with equal motor and load time constants. For medium to high values of system damping coefficient, symmetry with respect to limit cycle size exists for an exchange of motor and load time constants.

E. The results of this thesis are presented in a form which may aid in system design or analysis.

8. Recommendations

From the results of this thesis it can be seen that there remain many fertile areas for further investigation. For studies of this type it is strongly recommended that the digital computer be used because of its speed and versatility. The limits of investigation depend to a great extent on the ingenuity of the programmer. Some recommended areas of future investigation are:

a) More precise definition of the limit cycle existence zones and a more thorough coverage of the limit cycle size of similar systems having the same type of parameters. A three-dimensional presentation as mentioned in the discussion could be obtained.

b) Include torsion and other deformations of the mechanical system in the physical equations of the system to determine their affect on the system response.

c) An analysis of the limit cycle existence zone and transient response of a system to determine if there is a relationship between the two. An analytical expression for the possibility of limit cycle existence might be developed in terms of system parameters.

d) Examine the transient and frequency response of the system due to various Θ_R input functions. This would require minor modifications to the computation section of the existing computer program.

e) Since the physically realizable quantities of position, velocity and acceleration of both the motor and load are available as computed quantities, the study of the compensation problem and its optimization are obvious areas for further consideration.

f) The general study of other higher order nonlinear systems is suitable for digital computer programming since most numerical inte-

gration methods will handle systems having equations of any order.

9. REFERENCES

a. Chestnut, H. and Mayer, R.W., Servomechanisms and Regulating System Design, John Wiley & Sons, Inc., New York, N. Y., 1955.

b. Lutkenhouse, W.J., "Dividing Lines for Backlash in the Phaseplane", Unpublished Master's Thesis, United States Naval Postgraduate School, 1959.

c. Pastel, M.P. and Thaler, G.J., "Instrument Servomechanisms with Backlash, Couloumb Friction, and Stiction", Trans. A.I.E.E. (Applications and Industry) July 1960.

d. Knoll, A.L. and Narud, J.A., "Phase Plane Investigation of a Servomechanism with Backlash between Motor and Load", Technical Report 309 for Office of Naval Research, NR-375-017, Cruft Laboratory, Harvard University, Cambridge, Massachusetts, July 30, 1959.

e. New, N.C., "Effects of Backlash in the Second Order Servo", Unpublished Master's Thesis, United States Naval Postgraduate School, 1960.

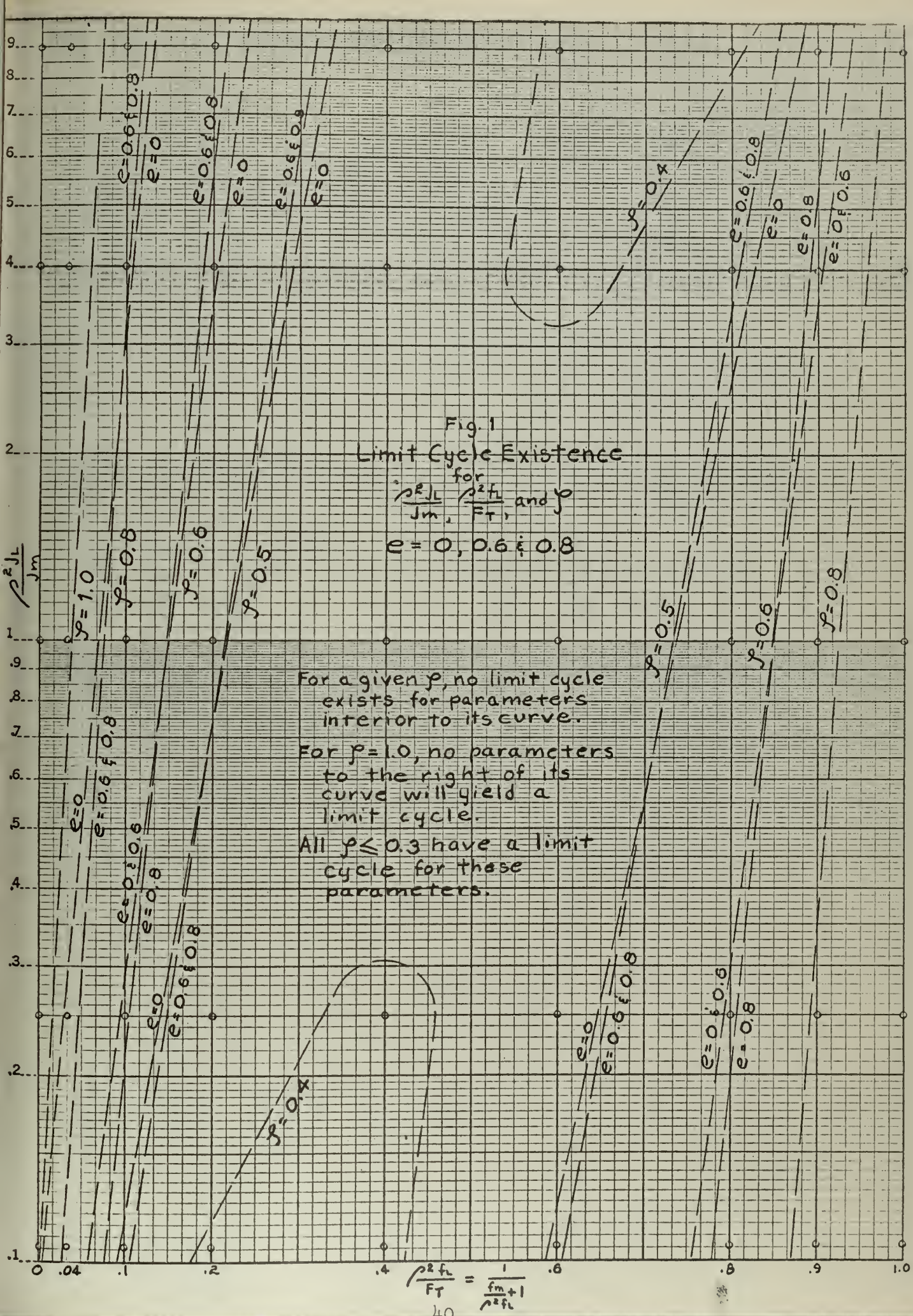

Fig. 1
Limit Cycle Existence
for
$\frac{\rho^2 J_L}{J_m}$, $\frac{\rho^2 f_L}{F_T}$, and ρ
$e = 0, 0.6$ & 0.8

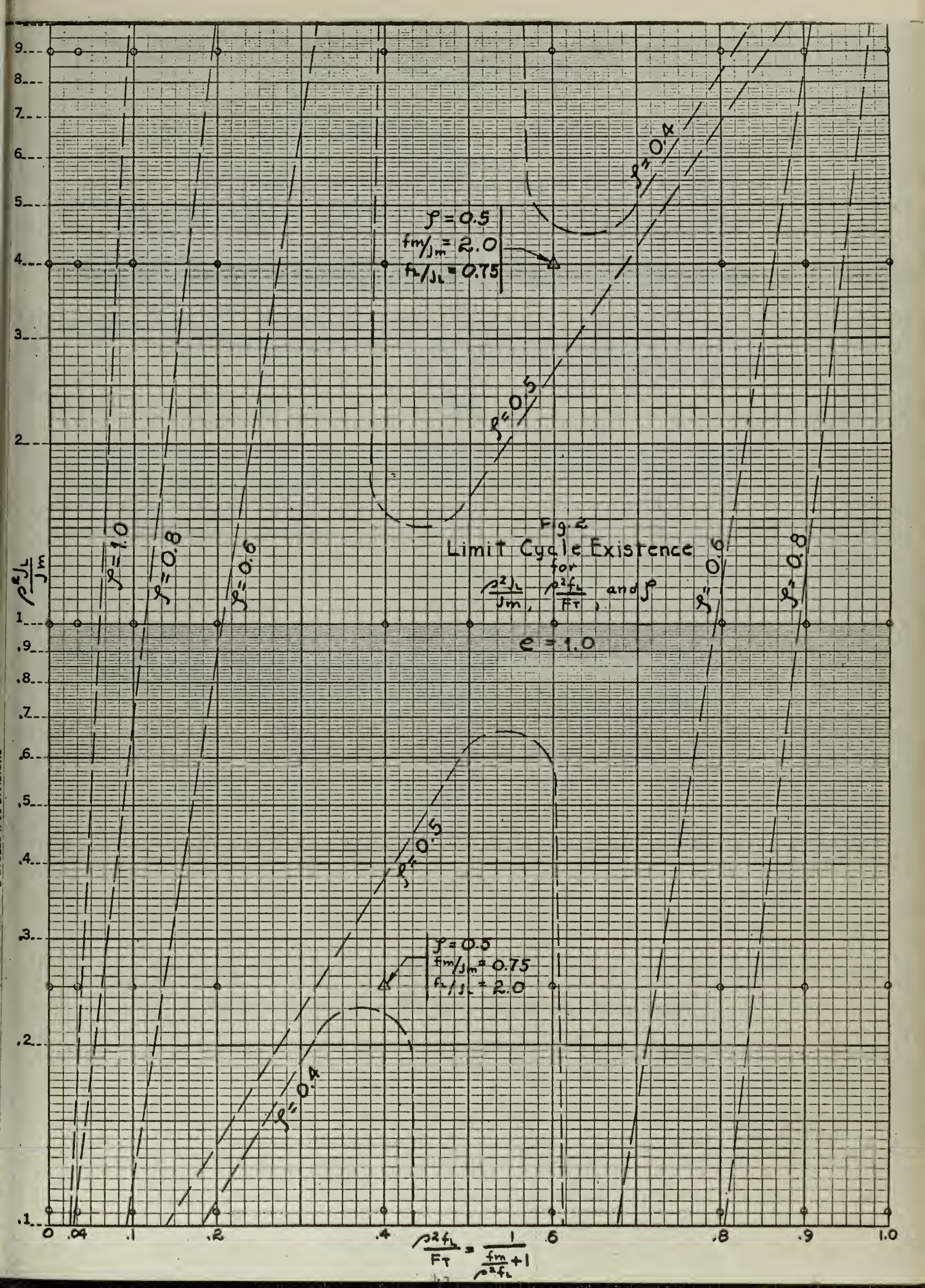

Fig. 2

Limit Cycle Existence for $\frac{\rho^2 J_L}{J_m}$, $\frac{\rho^2 f_L}{F_T}$, and ζ

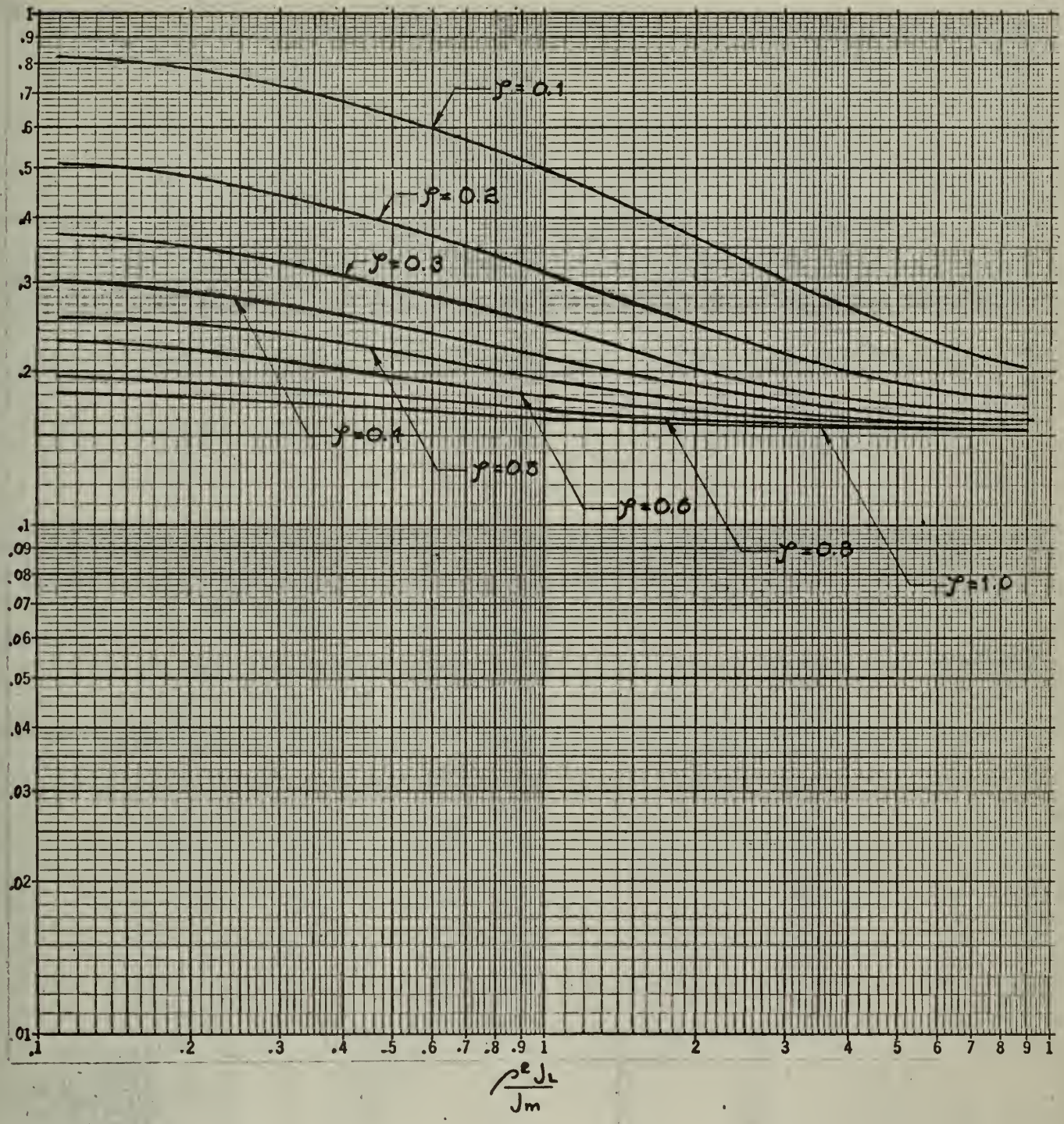

Fig. 3

Maximum Error of Limit Cycle from Unit Step Input

Limit Cycle Error (Radians) $\left(\frac{0.3}{\Delta}\right)$ for $\frac{\rho^2 J_L}{J_m}$ Variable

$$\frac{\rho^2 f_L}{F_T} = \frac{1}{\frac{f_m}{\rho^2 f_L} + 1} = 0$$

$$e = 0$$

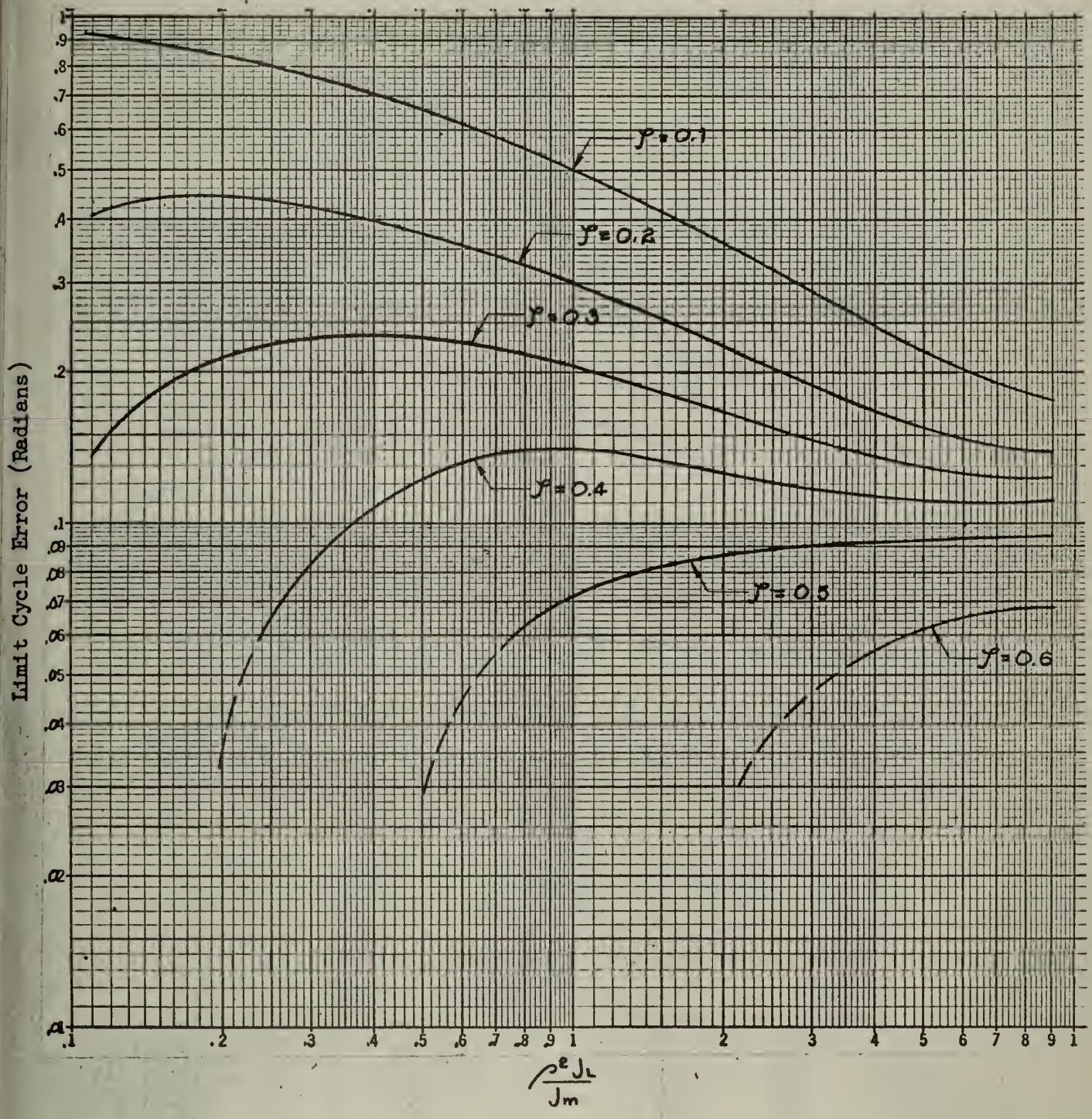

Fig. 4

Maximum Error of Limit Cycle from Unit Step Input

Limit Cycle Error (Radians) $\left(\frac{0.3}{\Delta}\right)$ for $\frac{\rho^2 J_L}{Jm}$ Variable

$$\frac{\rho^2 f_L}{F_T} = \frac{1}{\frac{f_m}{\rho^2 f_L} + 1} = 0.2$$

$$e = 0$$

No limit cycle exists for $\zeta \geq 0.8$

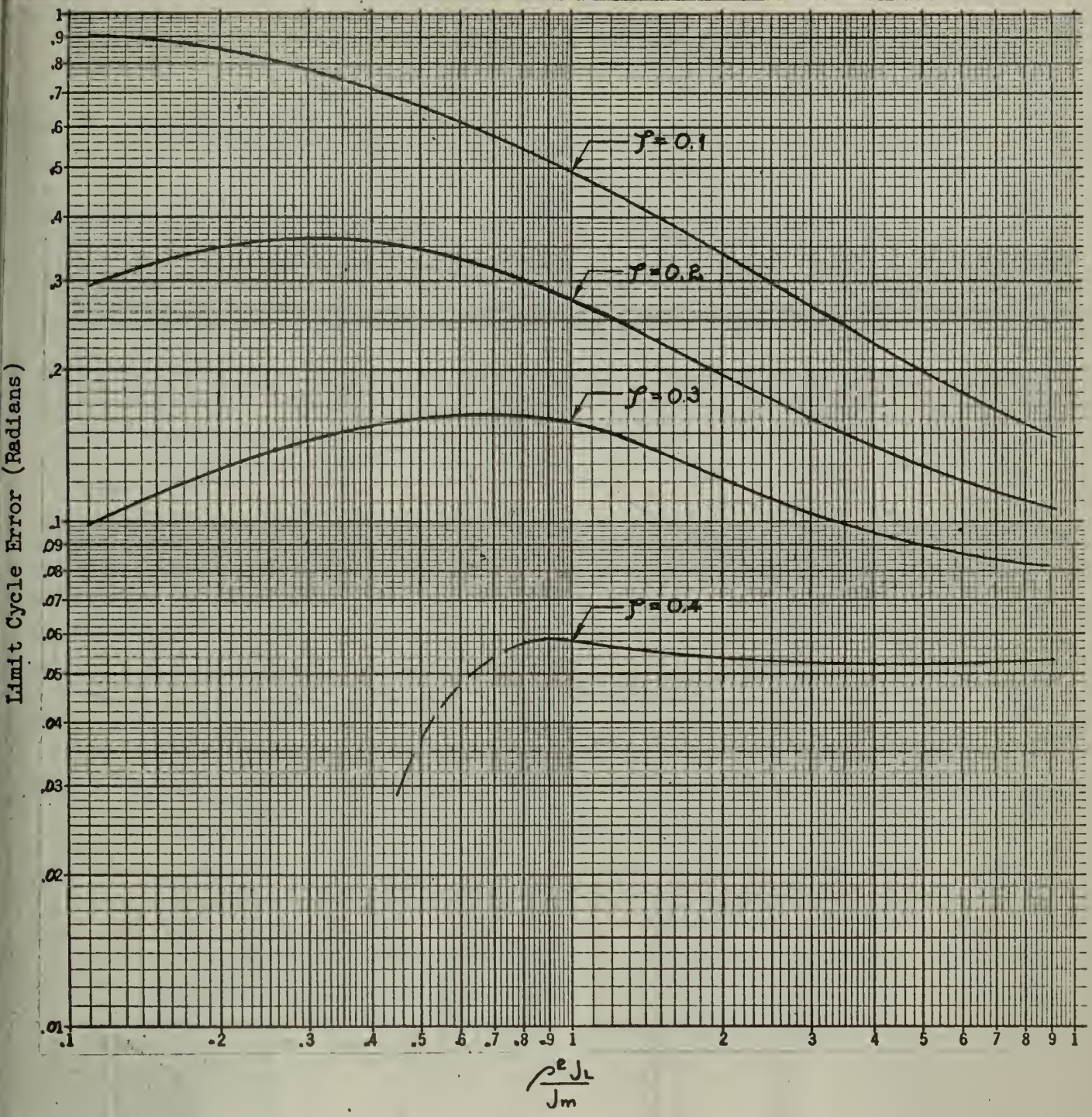

Fig. 5

Maximum Error of Limit Cycle from Unit Step Input

Limit Cycle Error (Radians) $\left(\frac{0.3}{\Delta}\right)$ for $\frac{\rho^2 J_L}{Jm}$ Variable

$$\frac{\rho^2 f_L}{F_T} = \frac{1}{\frac{f_m}{\rho^2 f_L} + 1} = 0.4$$

$$e = 0$$

No limit cycle exists for $\rho \geq 0.5$

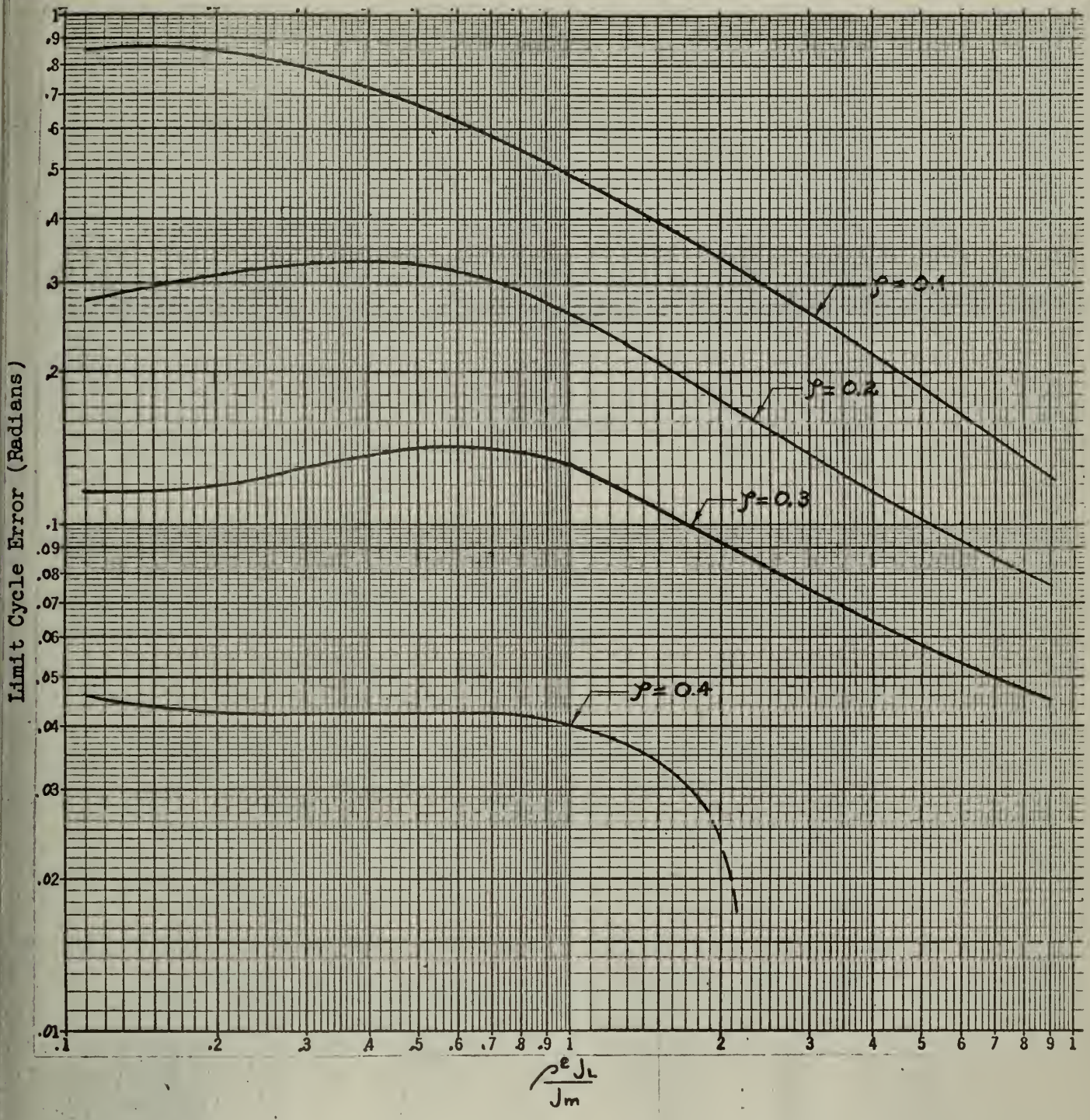

Fig. 6

Maximum Error of Limit Cycle from Unit Step Input

Limit Cycle Error (Radians) $\left(\frac{0.3}{\Delta}\right)$ for $\frac{\rho^2 J_L}{J_m}$ Variable

$$\frac{\rho^2 f_L}{F_T} = \frac{1}{\frac{f_m}{\rho^2 f_L} + 1} = 0.6$$

$$e = 0$$

No limit cycle exists for $\rho \geq 0.5$

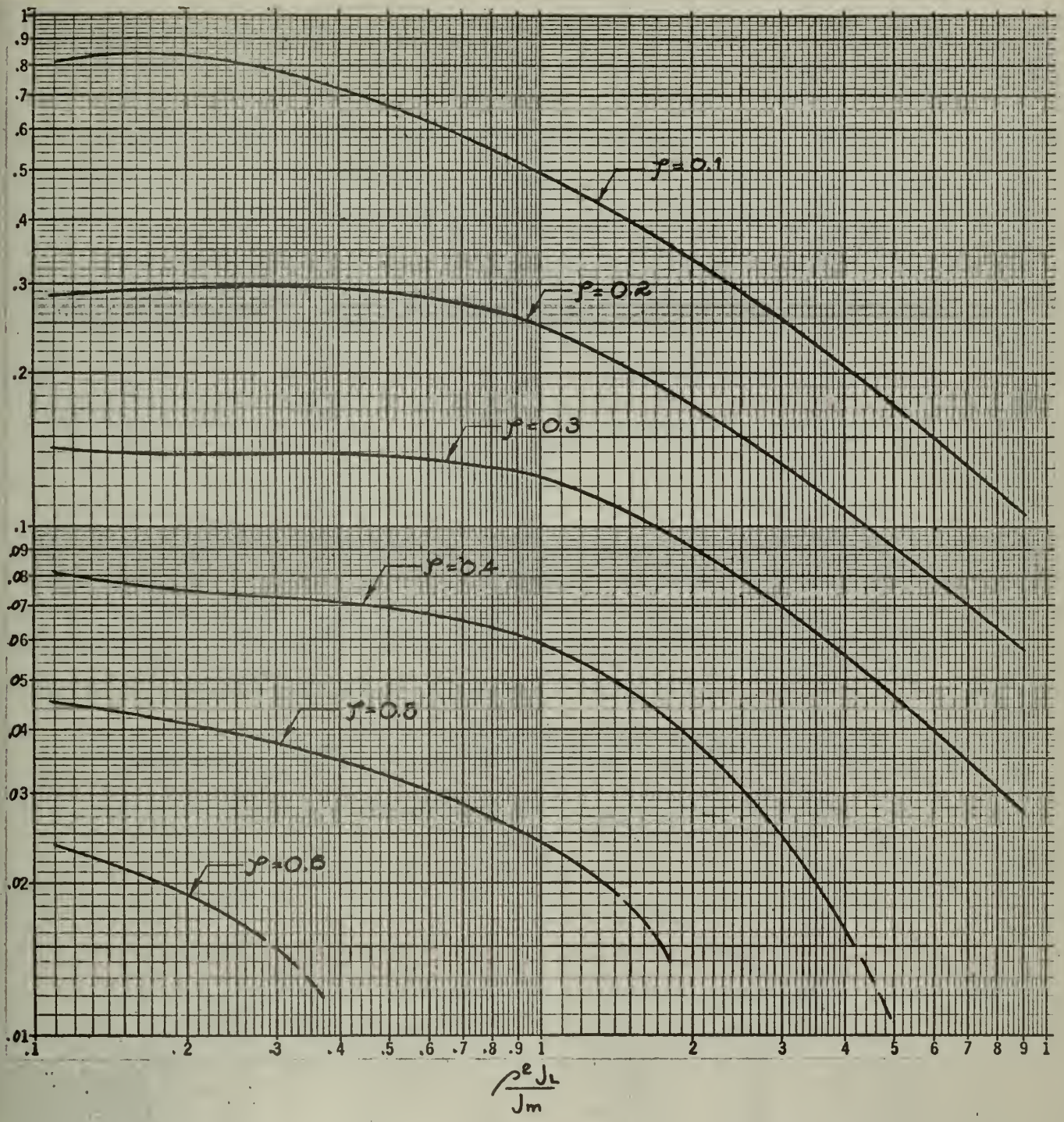

Fig. 7

Maximum Error of Limit Cycle from Unit Step Input

Limit Cycle Error (Radians) $\left(\frac{0.3}{\Delta}\right)$ for $\frac{\rho^2 J_L}{Jm}$ Variable

$$\frac{\rho^2 f_L}{F_T} = \frac{1}{\frac{f_m}{\rho^2 f_L} + 1} = 0.8$$

$$e = 0$$

No limit cycle exists for $\rho \geq 0.8$

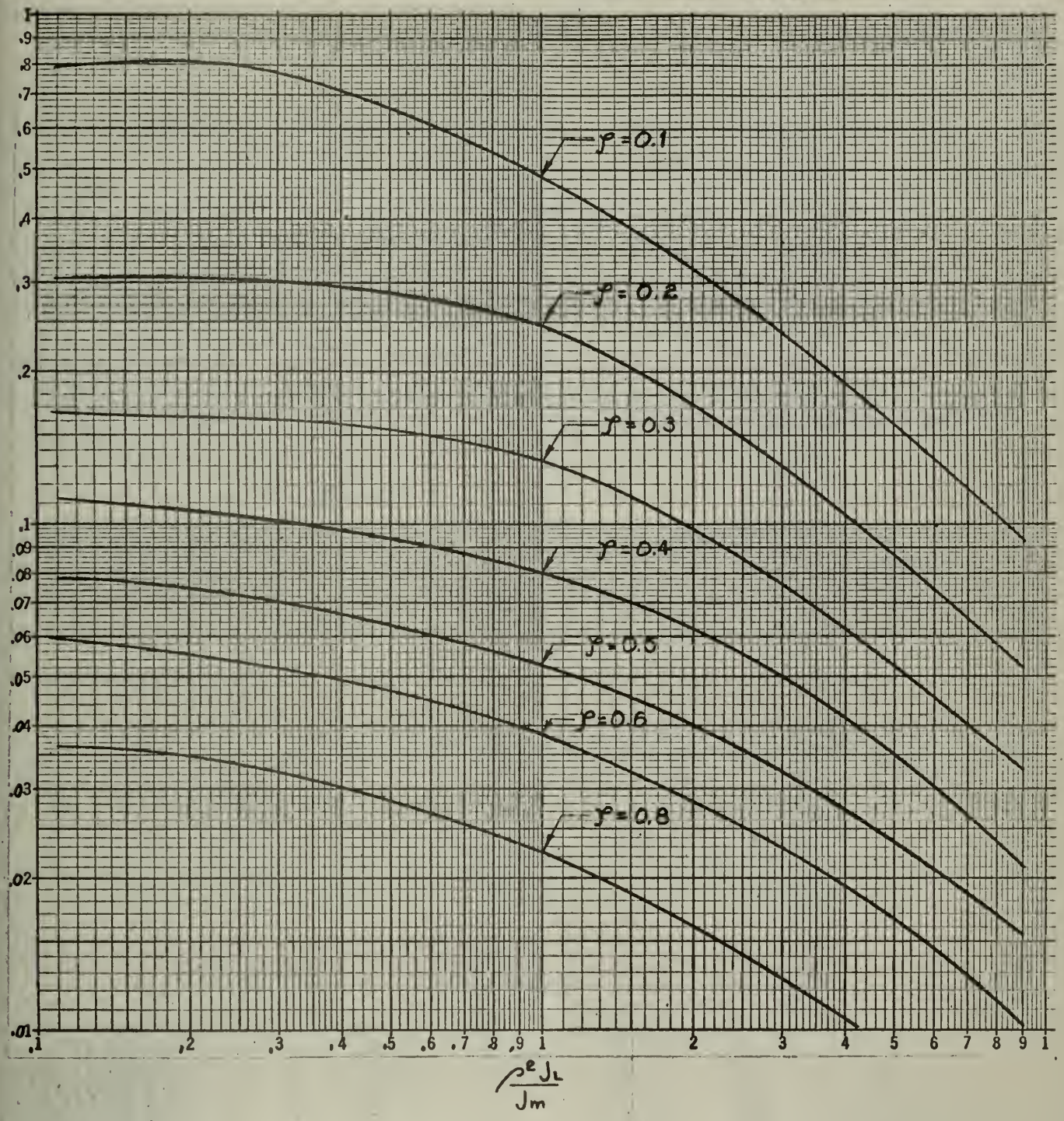

Fig. 8

Maximum Error of Limit Cycle from Unit Step Input

Limit Cycle Error (Radians) $\left(\frac{0.3}{\Delta}\right)$ for $\frac{\rho^2 J_L}{Jm}$ Variable

$$\frac{\rho^2 f_L}{F_T} = \frac{1}{\frac{f_m}{\rho^2 f_L} + 1} = 1.0$$

$$e = 0$$

No limit cycle exists for $\rho \geq 1.0$

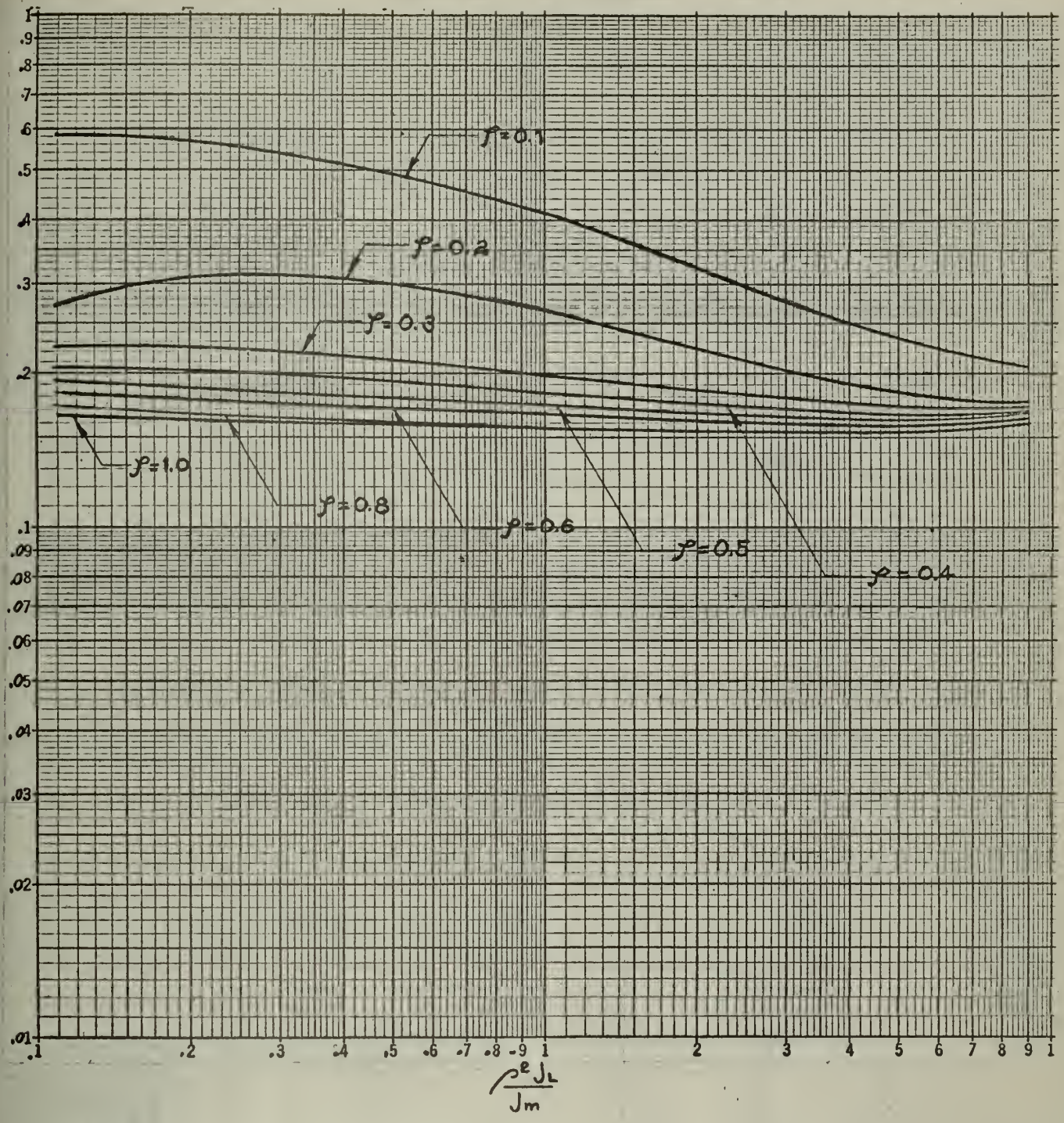

Fig. 9

Maximum Error of Limit Cycle from Unit Step Input

Limit Cycle Error (Radians) $\left(\frac{0.3}{\Delta}\right)$ for $\frac{\rho^2 J_L}{Jm}$ Variable

$$\frac{\rho^2 f_L}{Fr} = \frac{1}{\frac{fm}{\rho^2 f_L} + 1} = 0$$

e = 0.6

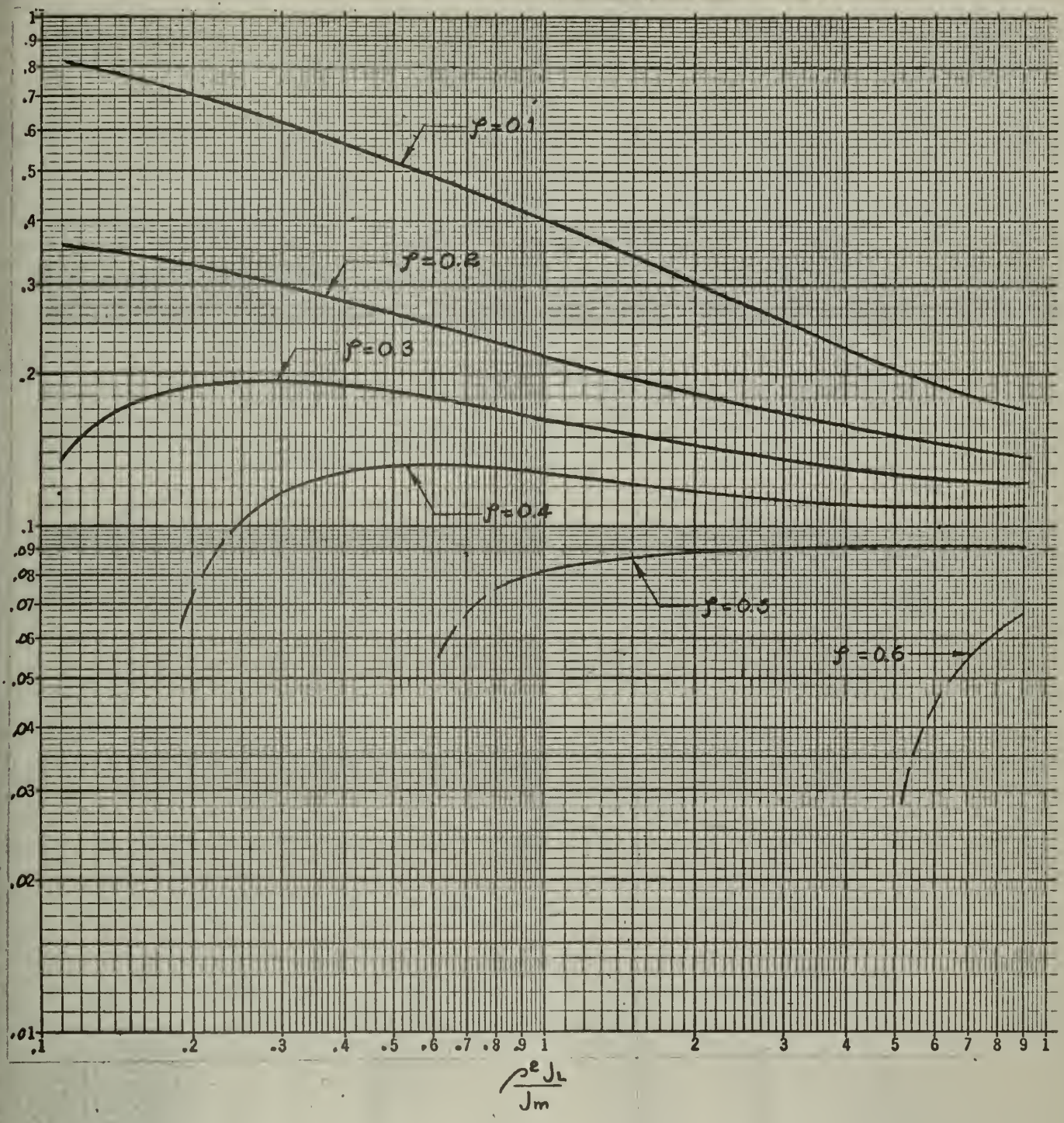

Fig. 10

Maximum Error of Limit Cycle from Unit Step Input

Limit Cycle Error (Radians) $\left(\frac{0.3}{\Delta}\right)$ for $\frac{\rho^2 J_L}{Jm}$ Variable

$$\frac{\rho^2 f_L}{F_T} = \frac{1}{\frac{f_m}{\rho^2 f_L} + 1} = 0.2$$

$$e = 0.6$$

No limit cycle exists for $\rho \geq 0.8$

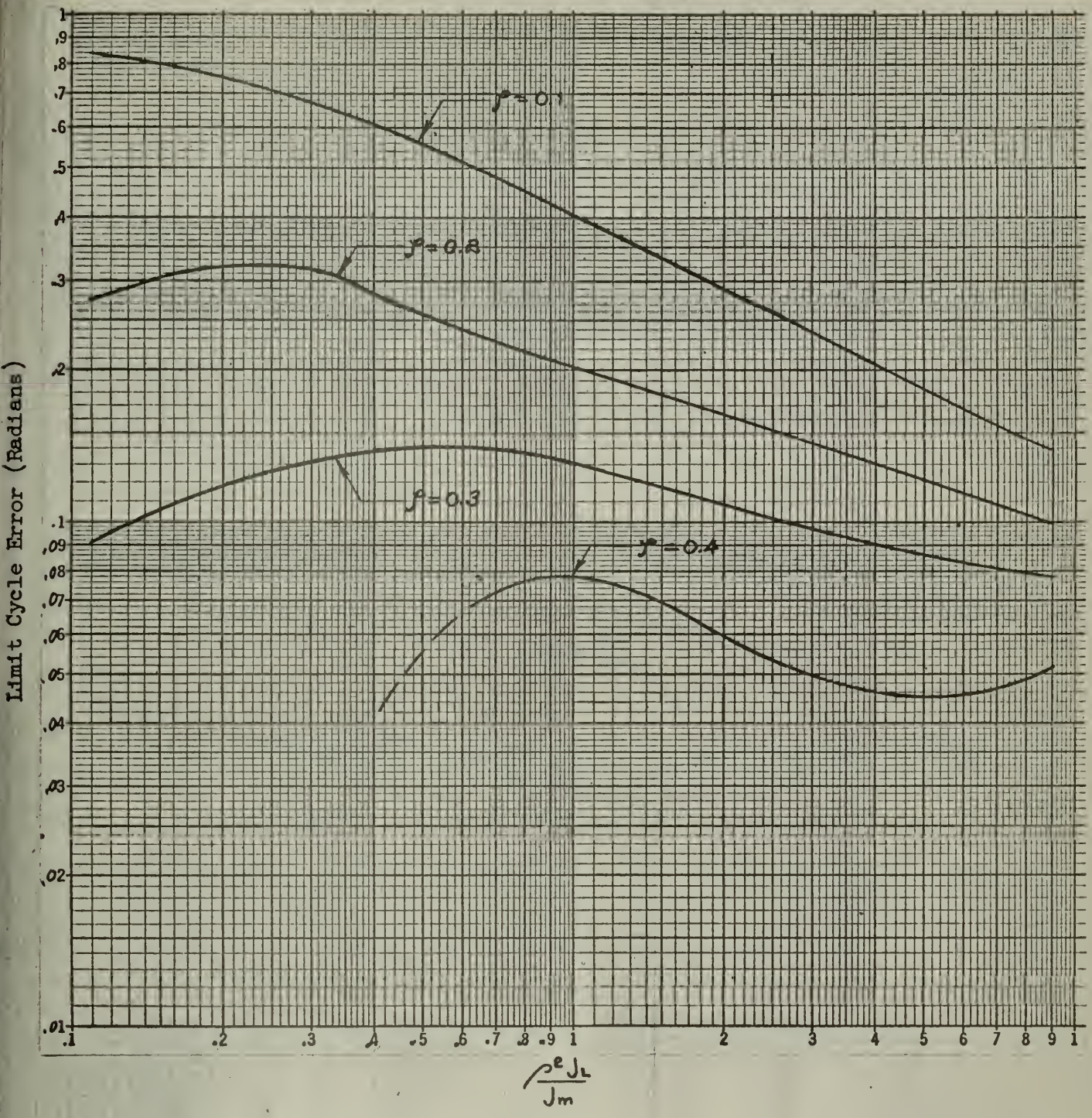

Fig. 11

Maximum Error of Limit Cycle from Unit Step Input

Limit Cycle Error (Radians) $\left(\frac{0.3}{\Delta}\right)$ for $\frac{\rho^2 J_L}{J_m}$ Variable

$$\frac{\rho^2 f_L}{F_T} = \frac{1}{\frac{f_m}{\rho^2 f_L} + 1} = 0.4$$

$$e = 0.6$$

No limit cycle exists for $\rho \geq 0.5$

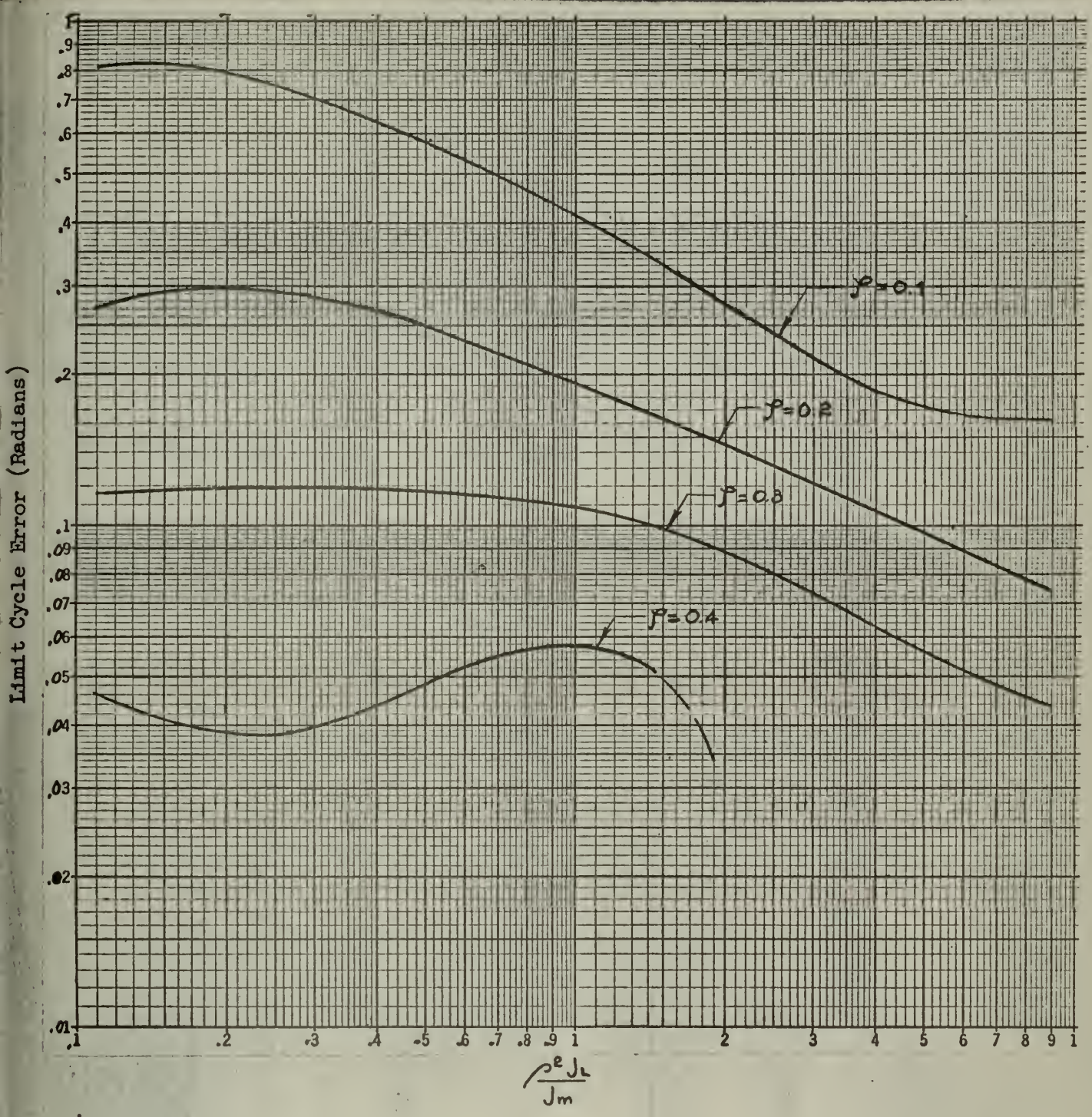

Fig. 12

Maximum Error of Limit Cycle from Unit Step Input

Limit Cycle Error (Radians) $\left(\frac{0.3}{\Delta}\right)$ for $\frac{\rho^2 J_L}{Jm}$ Variable

$$\frac{\rho^2 f_L}{F_T} = \frac{1}{\frac{f_m}{\rho^2 f_L} + 1} = 0.6$$

$$e = 0.6$$

No limit cycle exists for $\zeta \geq 0.5$

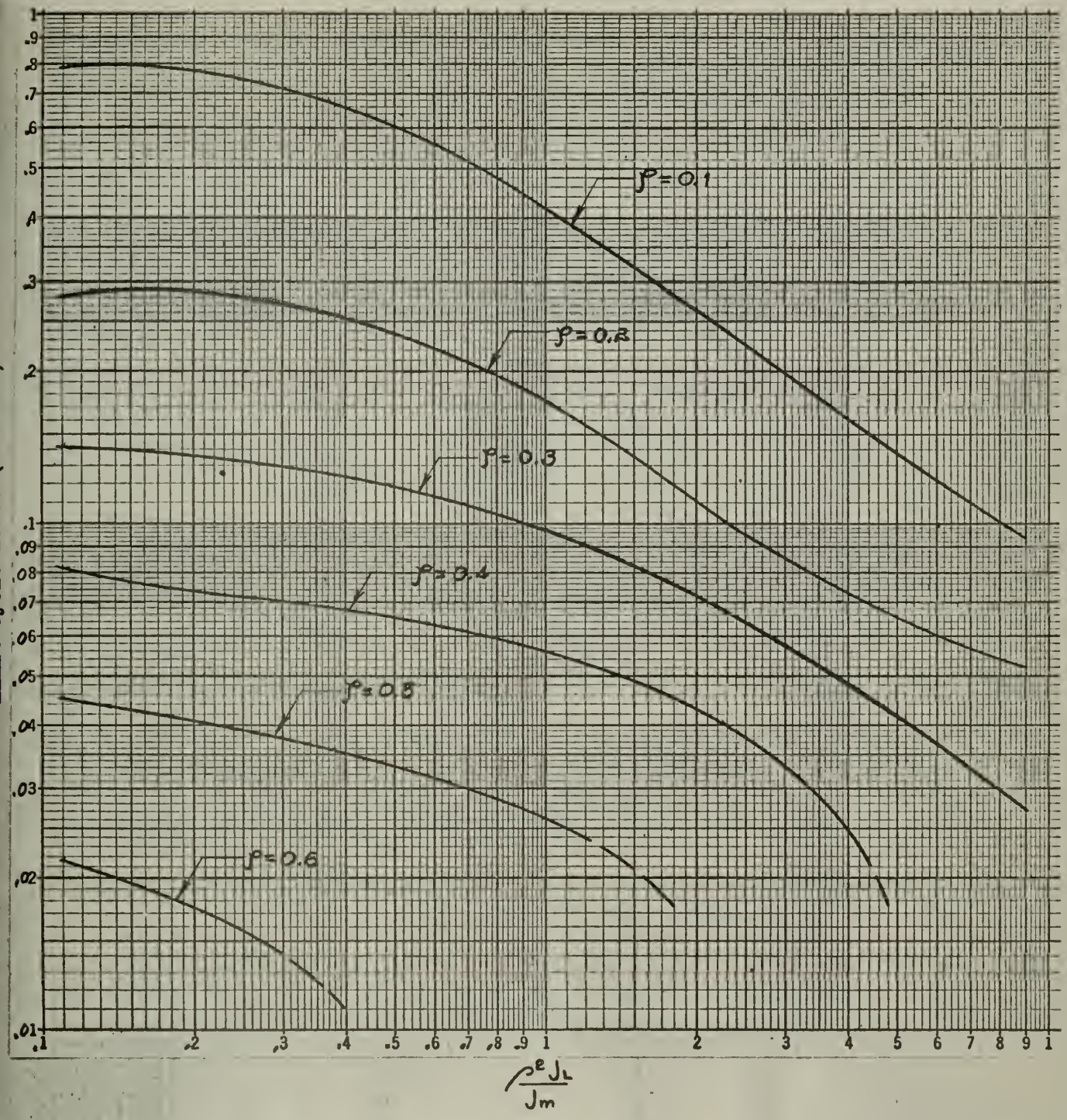

Fig. 13

Maximum Error of Limit Cycle from Unit Step Input

Limit Cycle Error (Radians) $\left(\frac{0.3}{\Delta}\right)$ for $\frac{\rho^2 J_L}{J_m}$ Variable

$$\frac{\rho^2 f_L}{F_T} = \frac{1}{\frac{f_m}{\rho^2 f_L} + 1} = 0.8$$

$$e = 0.6$$

No limit cycle exists for $\rho \geq 0.8$

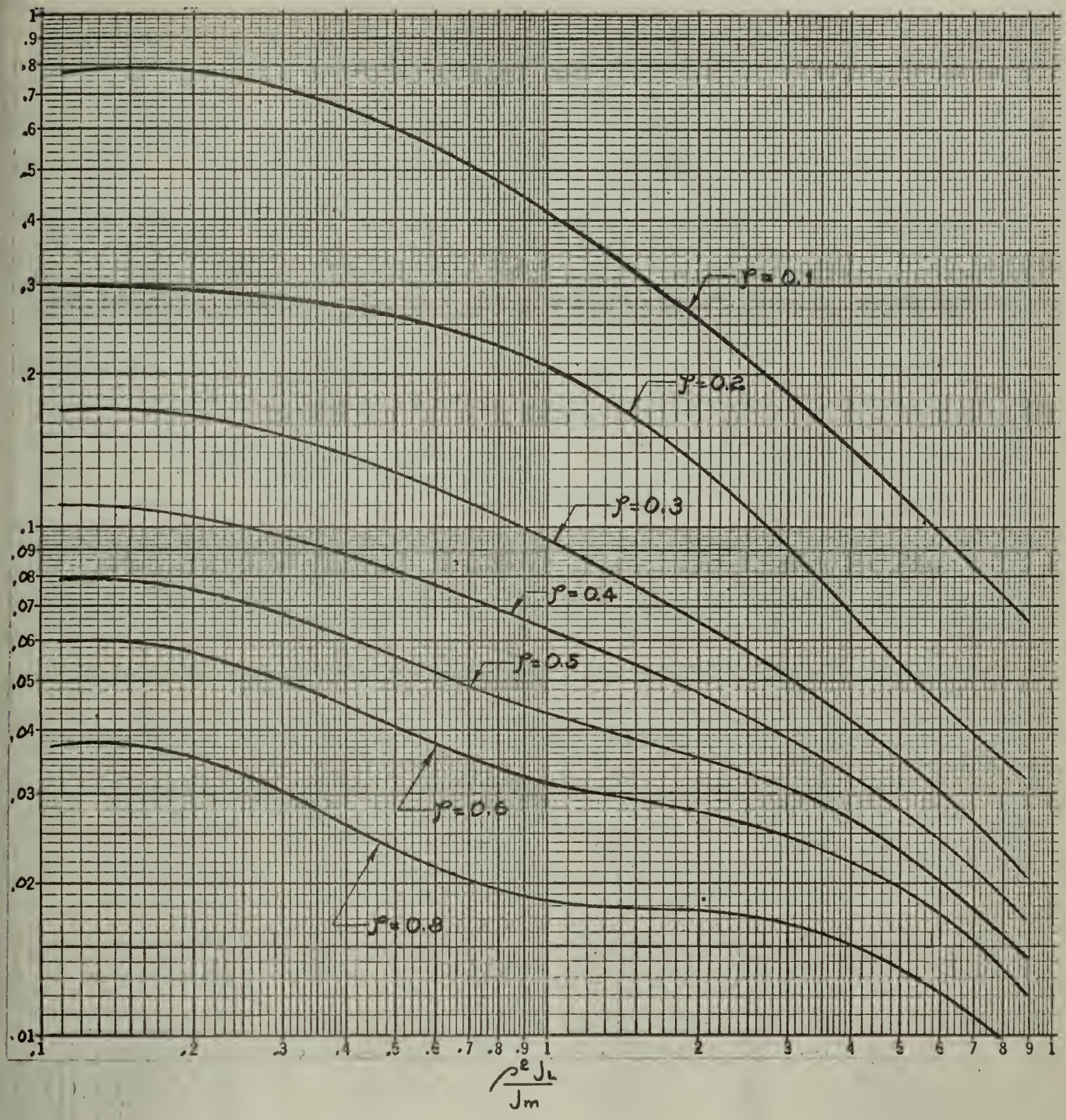

Fig. 14

Maximum Error of Limit Cycle from Unit Step Input

Limit Cycle Error (Radians) $\left(\frac{0.3}{\Delta}\right)$ for $\frac{\rho^2 J_L}{J_m}$ Variable

$$\frac{\rho^2 f_L}{F_T} = \frac{1}{\frac{f_m}{\rho^2 f_L} + 1} = 1.0$$

$$e = 0.6$$

No limit cycle exists for $\rho \geq 1.0$

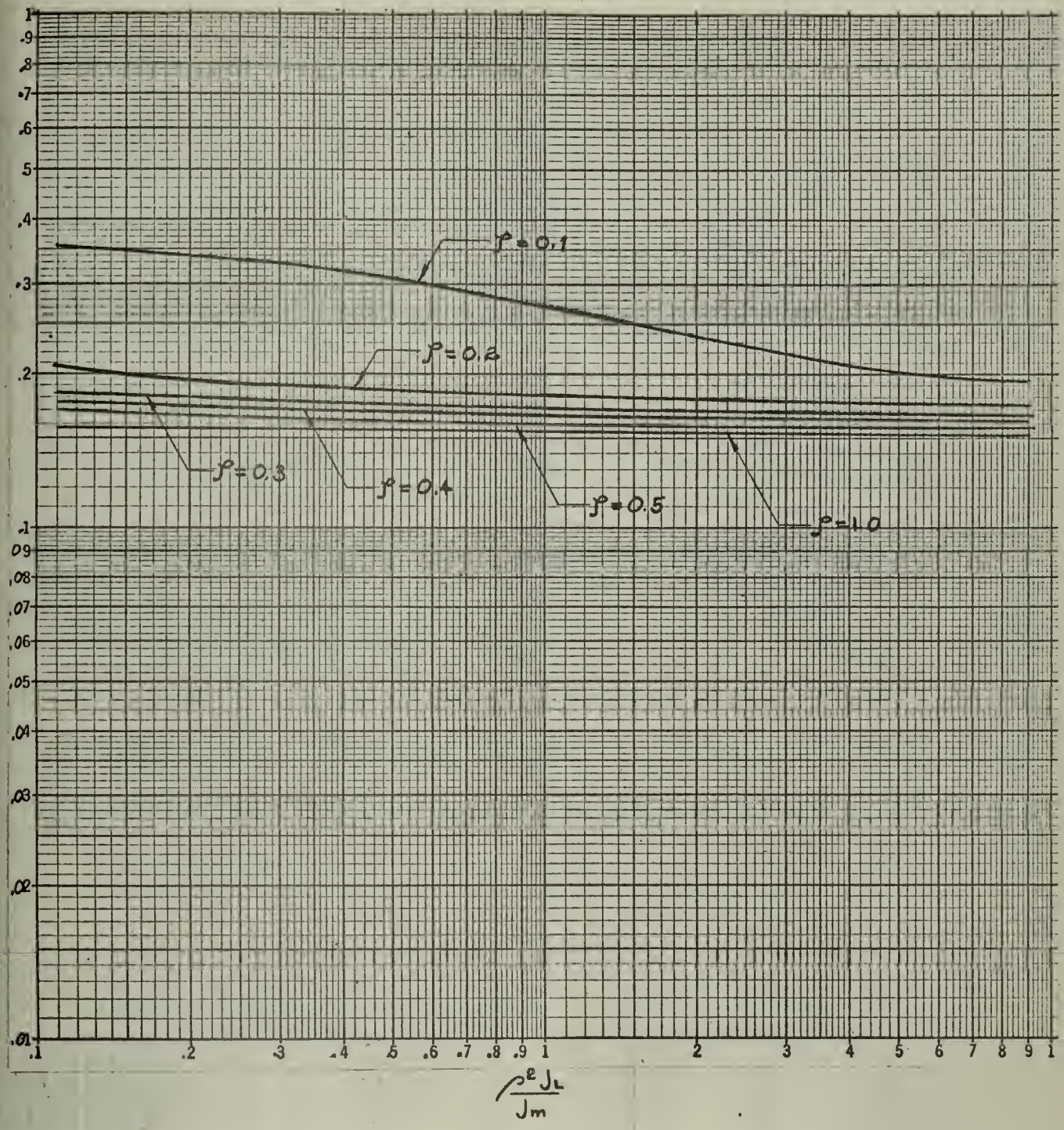

Fig. 15

Maximum Error of Limit Cycle from Unit Step Input

Limit Cycle Error (Radians) $\left(\frac{0.3}{\Delta}\right)$ for $\frac{\rho^2 J_L}{Jm}$ Variable

$$\frac{\rho^2 f_L}{Fr} = \frac{1}{\frac{fm}{\rho^2 f_L} + 1} = 0$$

$$e = 0.8$$

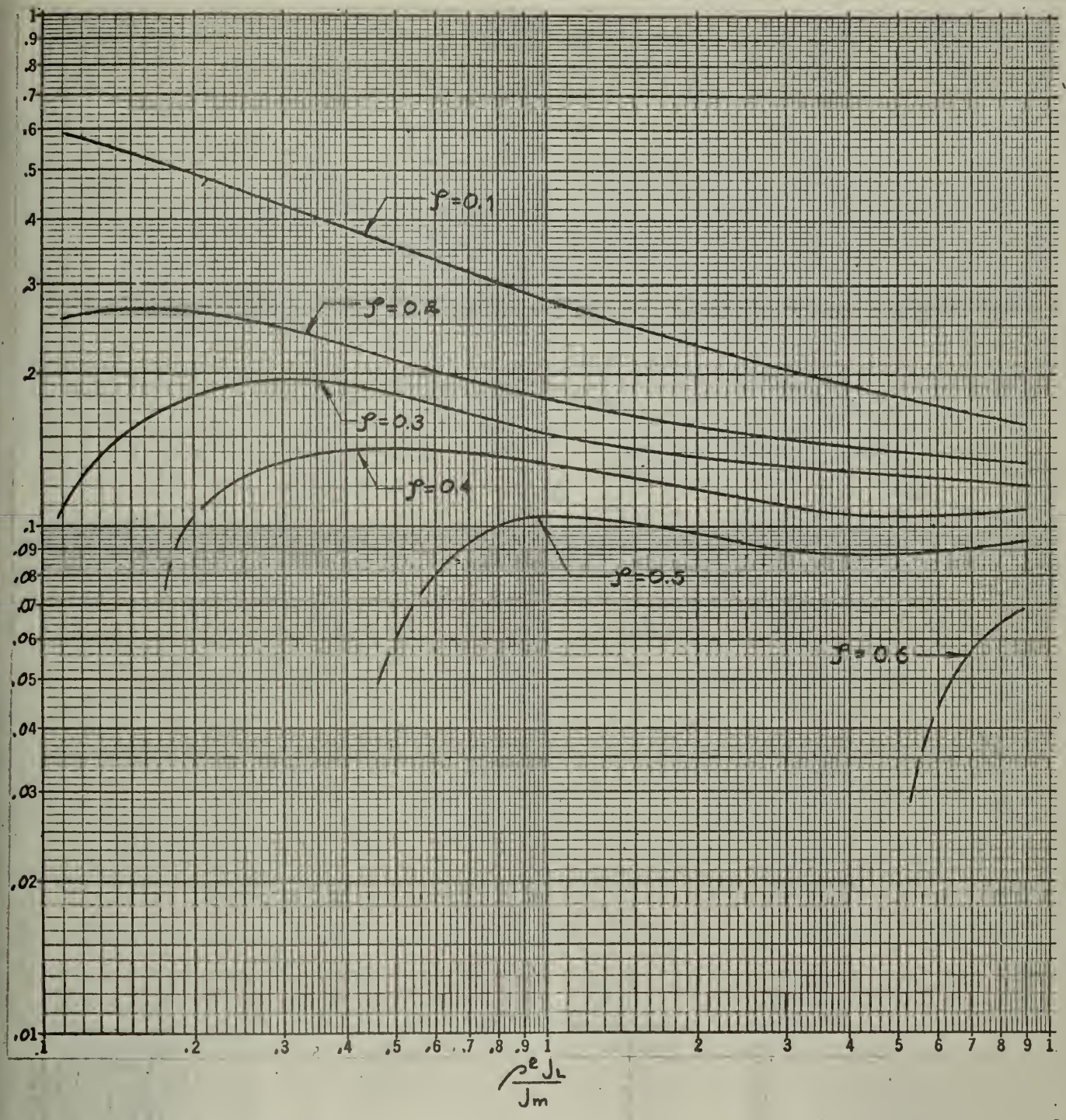

Fig. 16

Maximum Error of Limit Cycle from Unit Step Input

Limit Cycle Error (Radians) $\left(\frac{0.3}{\Delta}\right)$ for $\frac{\rho^2 J_L}{J_m}$ Variable

$$\frac{\rho^2 f_L}{F_T} = \frac{1}{\frac{f_m}{\rho^2 f_L} + 1} = 0.2$$

$$e = 0.8$$

No limit cycle exists for $\rho \geq 0.8$

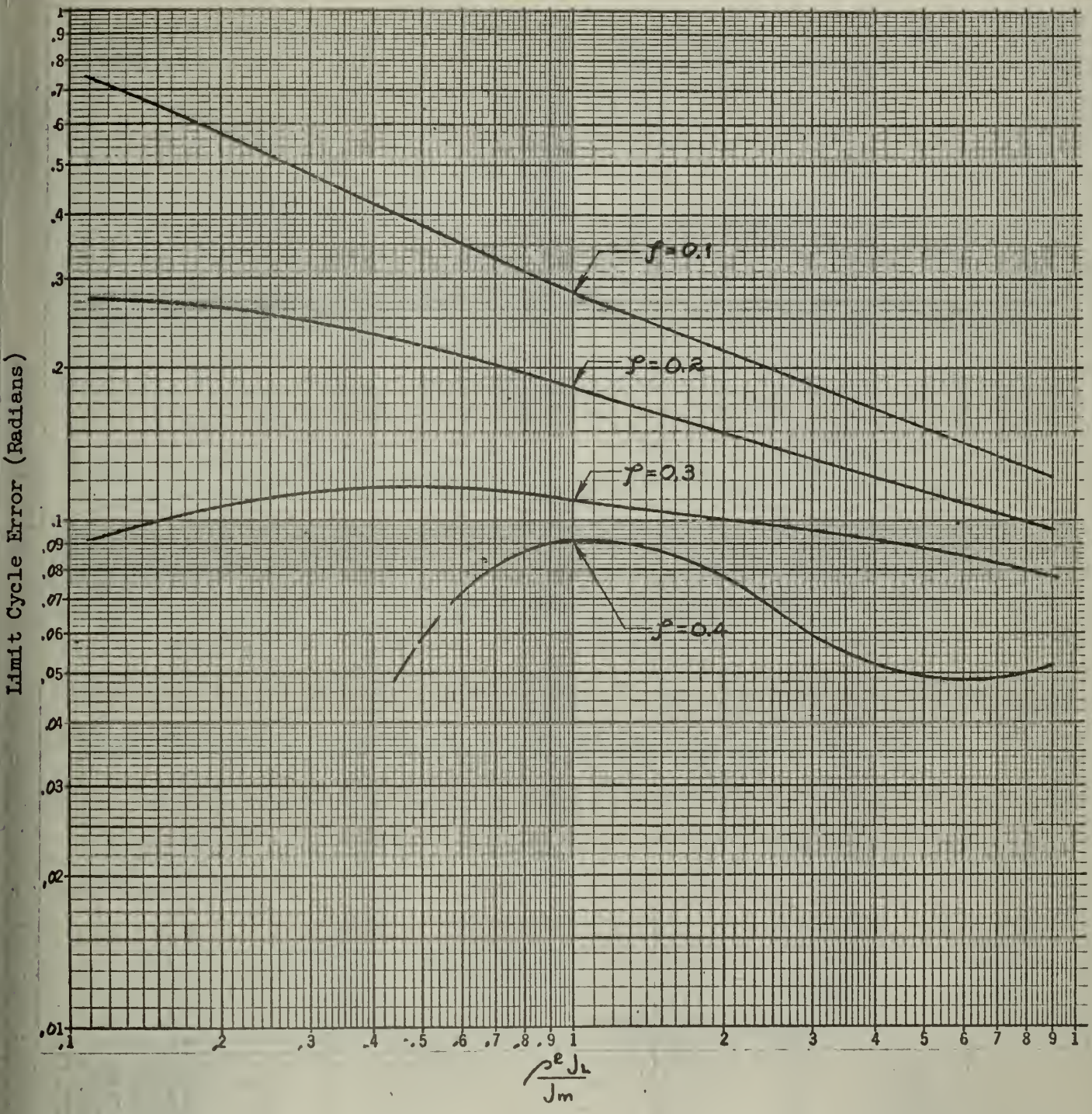

Fig. 17

Maximum Error of Limit Cycle from Unit Step Input

Limit Cycle Error (Radians) $\left(\frac{0.3}{\Delta}\right)$ for $\frac{\rho^2 J_L}{Jm}$ Variable

$$\frac{\rho^2 f_L}{F_T} = \frac{1}{\frac{f_m}{\rho^2 f_L} + 1} = 0.4$$

$$e = 0.8$$

No limit cycle exists for $\rho \geq 0.5$

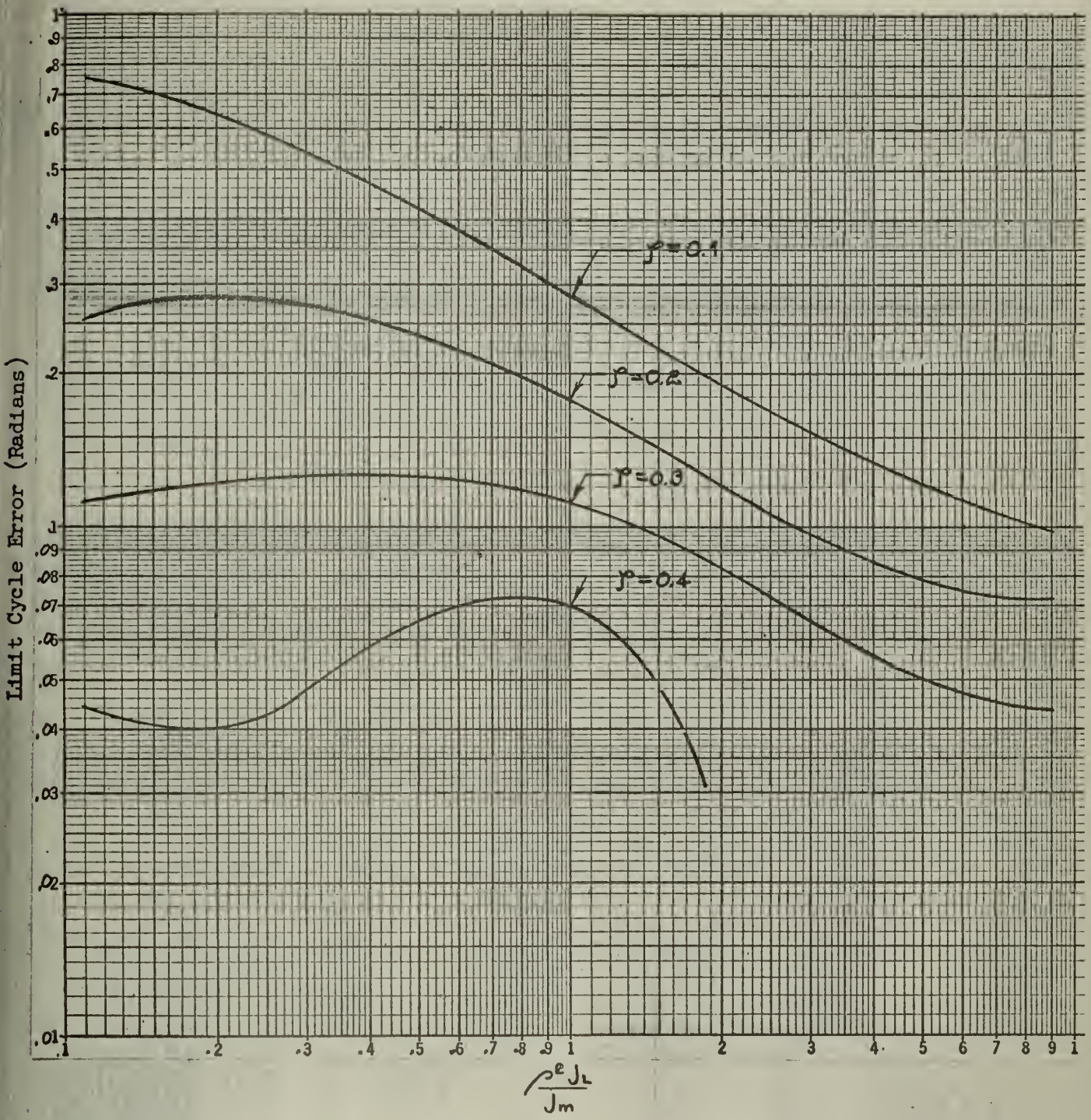

Fig. 18

Maximum Error of Limit Cycle from Unit Step Input

Limit Cycle Error (Radians) $\left(\frac{0.3}{\Delta}\right)$ for $\frac{\rho^2 J_L}{Jm}$ Variable

$$\frac{\rho^2 f_L}{F_T} = \frac{1}{\frac{f_m}{\rho^2 f_L} + 1} = 0.6$$

$$e = 0.8$$

No limit cycle exists for $\rho \geq 0.5$

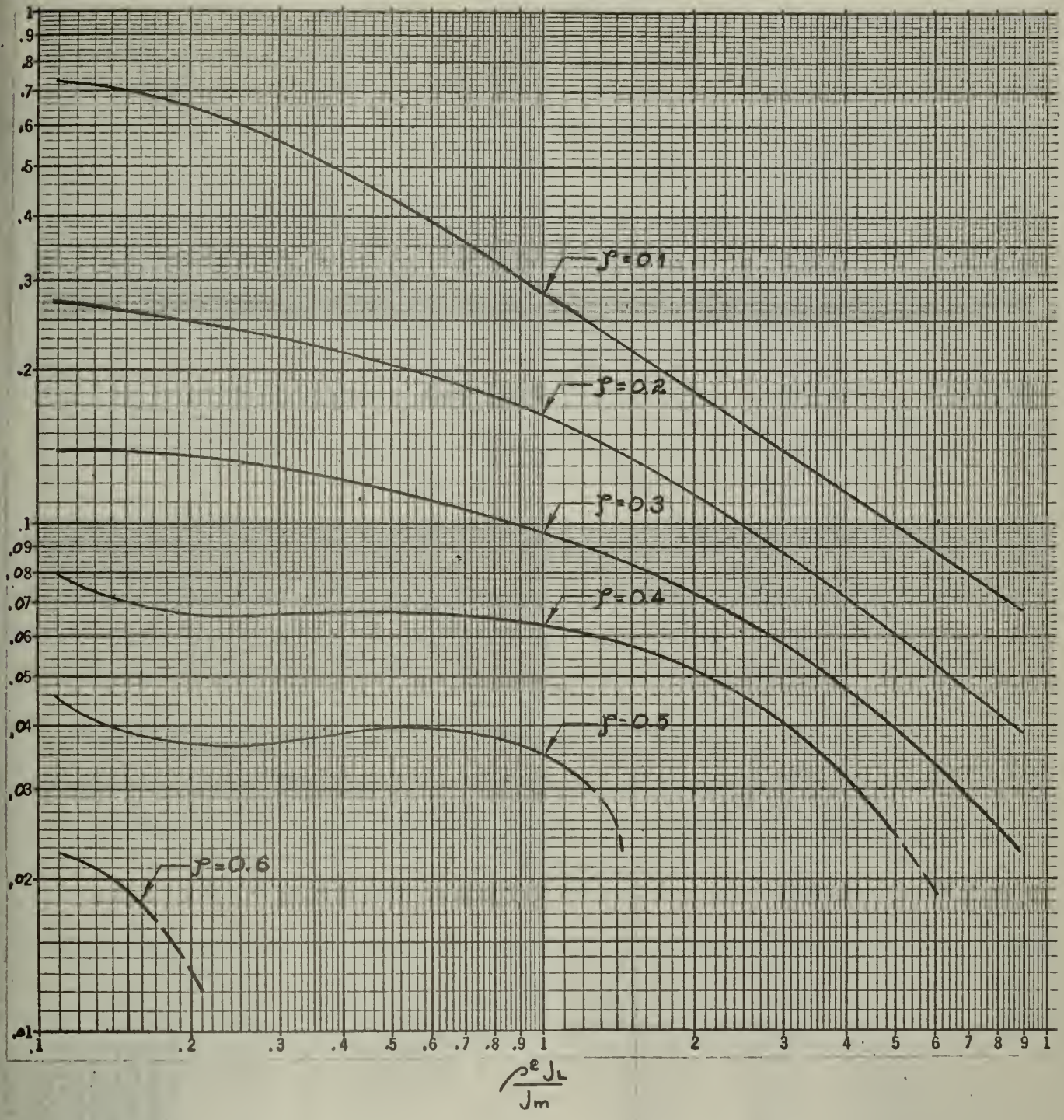

Fig. 19

Maximum Error of Limit Cycle from Unit Step Input

Limit Cycle Error (Radians) $\left(\frac{0.3}{\Delta}\right)$ for $\frac{\rho^2 J_L}{J_m}$ Variable

$$\frac{\rho^2 f_L}{F_T} = \frac{1}{\frac{f_m}{\rho^2 f_L} + 1} = 0.8$$

$$e = 0.8$$

No limit cycle exists for $\rho \geq 0.8$

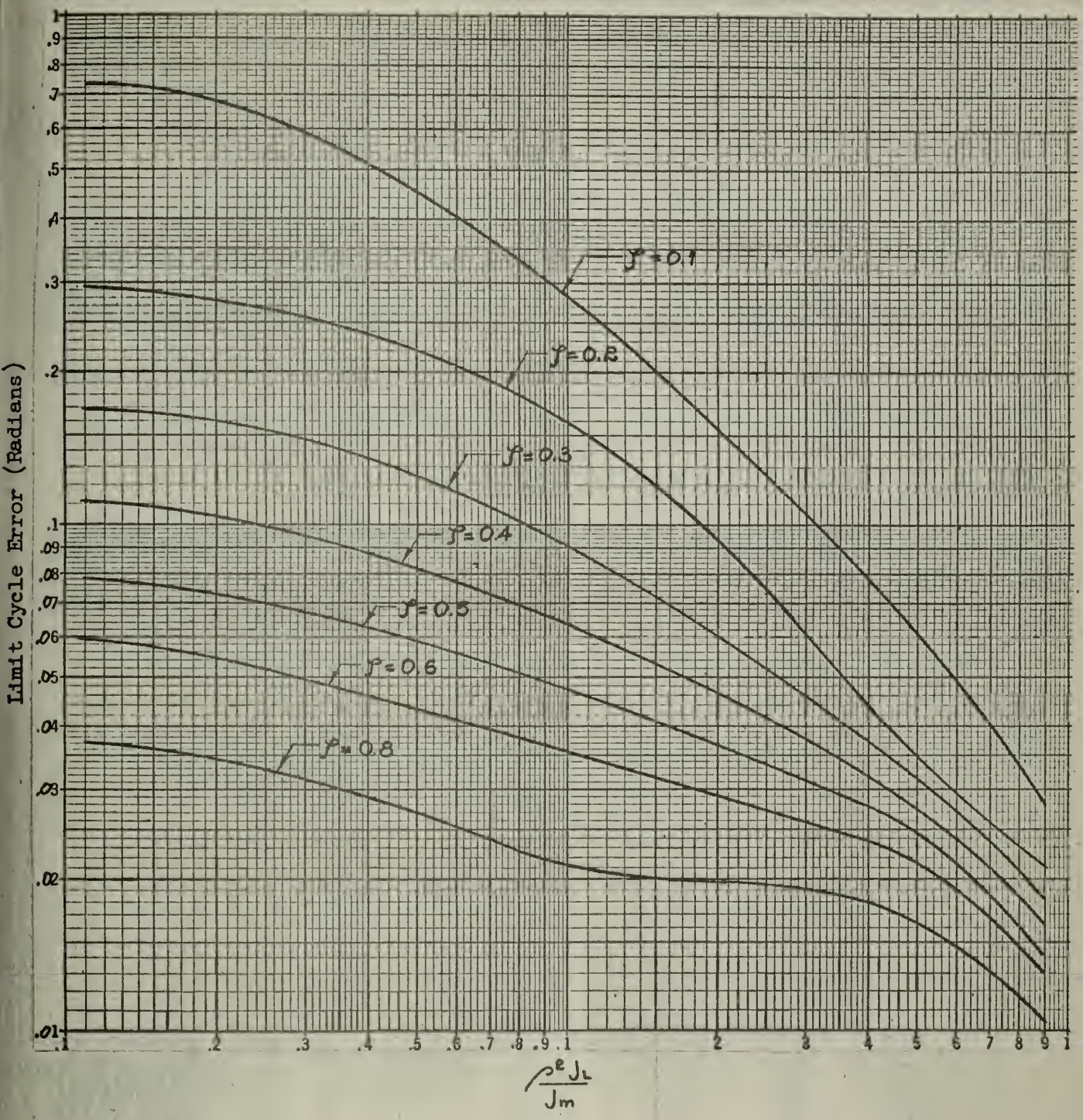

Fig. 20

Maximum Error of Limit Cycle from Unit Step Input

Limit Cycle Error (Radians) $\left(\frac{0.3}{\Delta}\right)$ for $\frac{\rho^2 J_L}{J_m}$ Variable

$$\frac{\rho^2 f_L}{F_T} = \frac{1}{\frac{f_m}{\rho^2 f_L} + 1} = 1.0$$

$$e = 0.8$$

No limit cycle exists for $\zeta \geq 1.0$

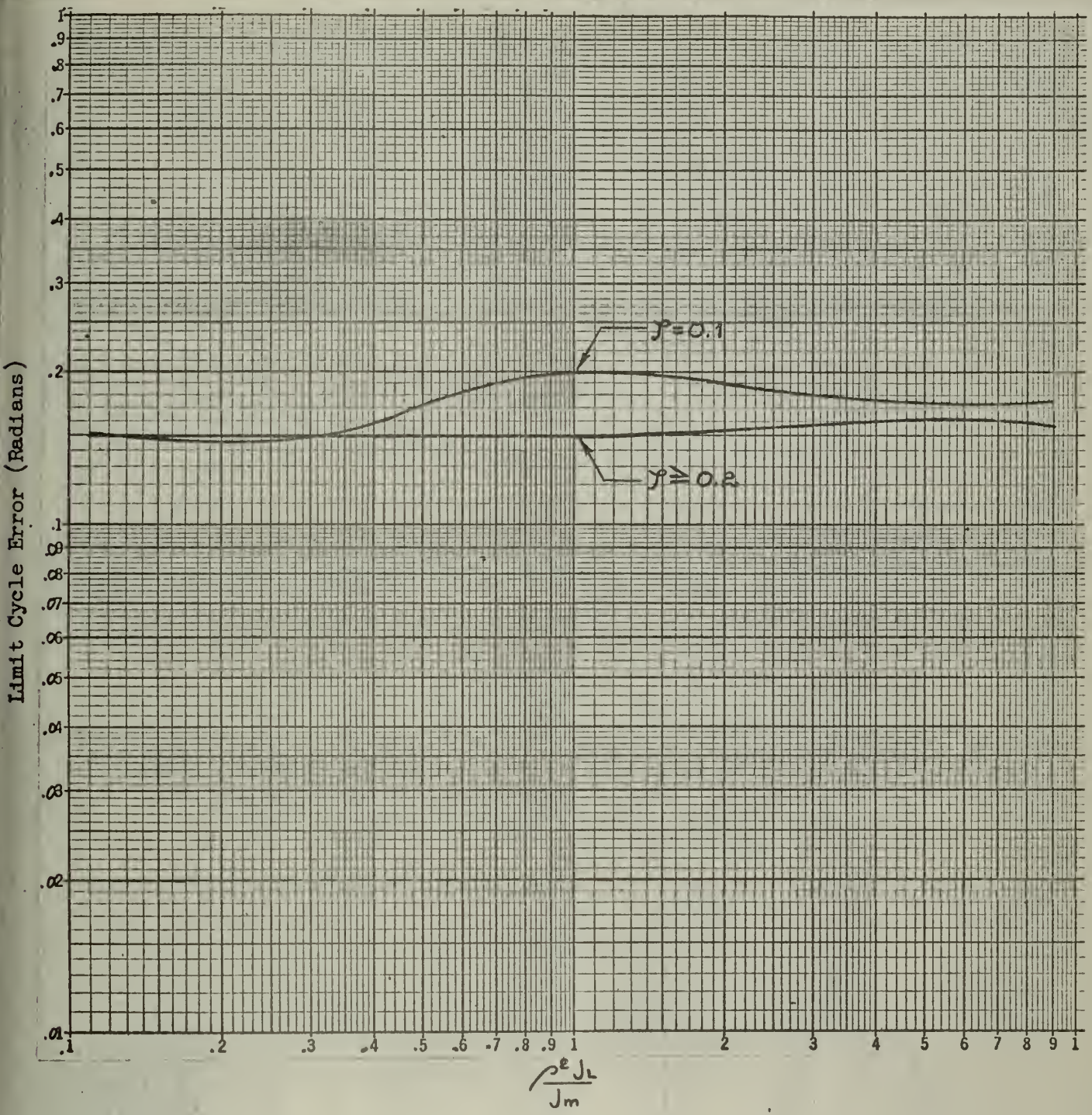

Fig. 21

Maximum Error of Limit Cycle from Unit Step Input

Limit Cycle Error (Radians) $\left(\frac{0.3}{\Delta}\right)$ for $\frac{\rho^2 J_L}{Jm}$ Variable

$$\frac{\rho^2 f_L}{F_T} = \frac{1}{\frac{f_m}{\rho^2 f_L} + 1} = 0$$

$$e = 1.0$$

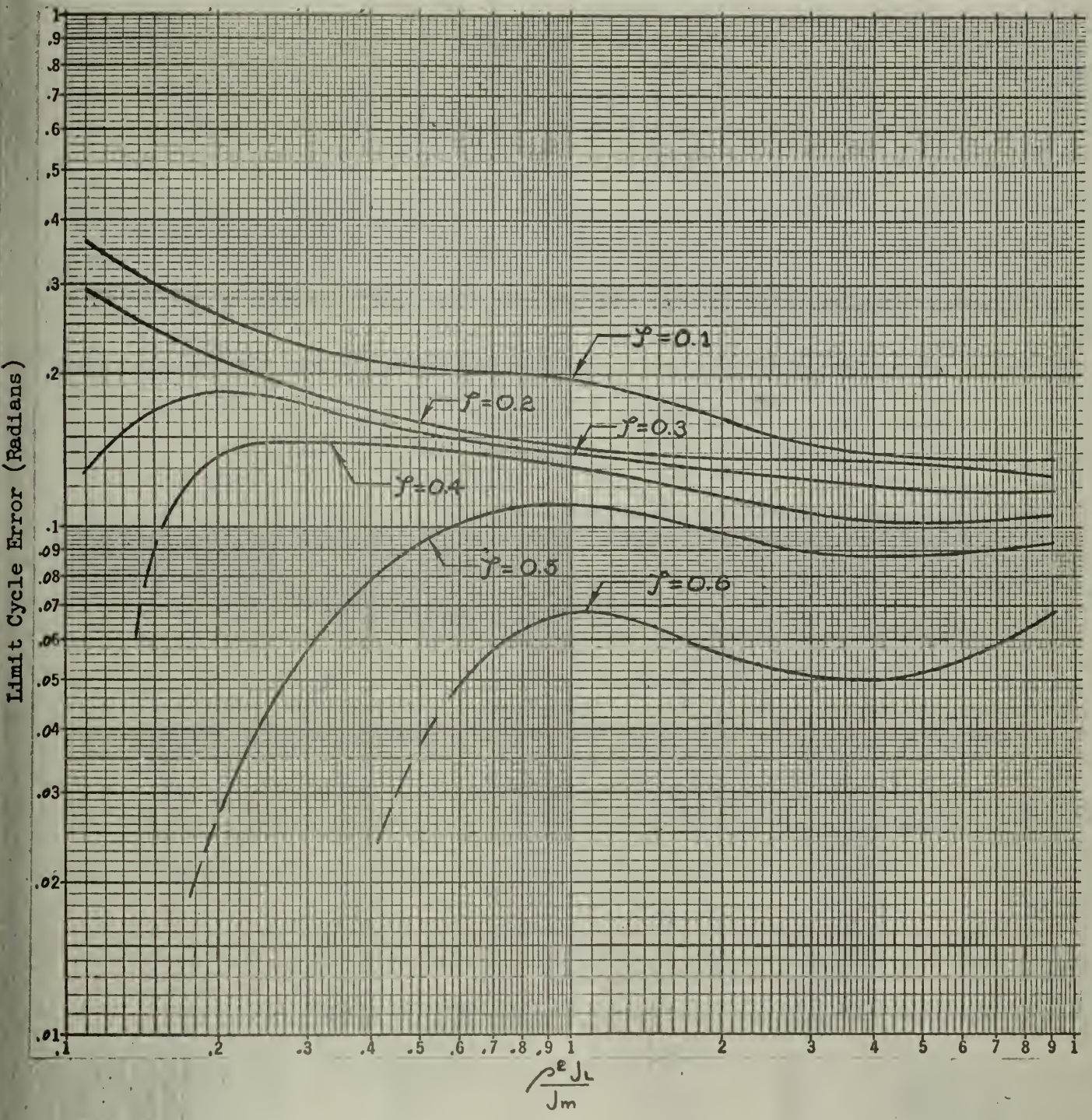

Fig. 22

Maximum Error of Limit Cycle from Unit Step Input

Limit Cycle Error (Radians) $\left(\frac{0.3}{\Delta}\right)$ for $\frac{\rho^2 J_L}{J_m}$ Variable

$$\frac{\rho^2 f_L}{F_T} = \frac{1}{\frac{f_m}{\rho^2 f_L} + 1} = 0.2$$

$$e = 1.0$$

No limit cycle exists for $\rho \geq 0.8$

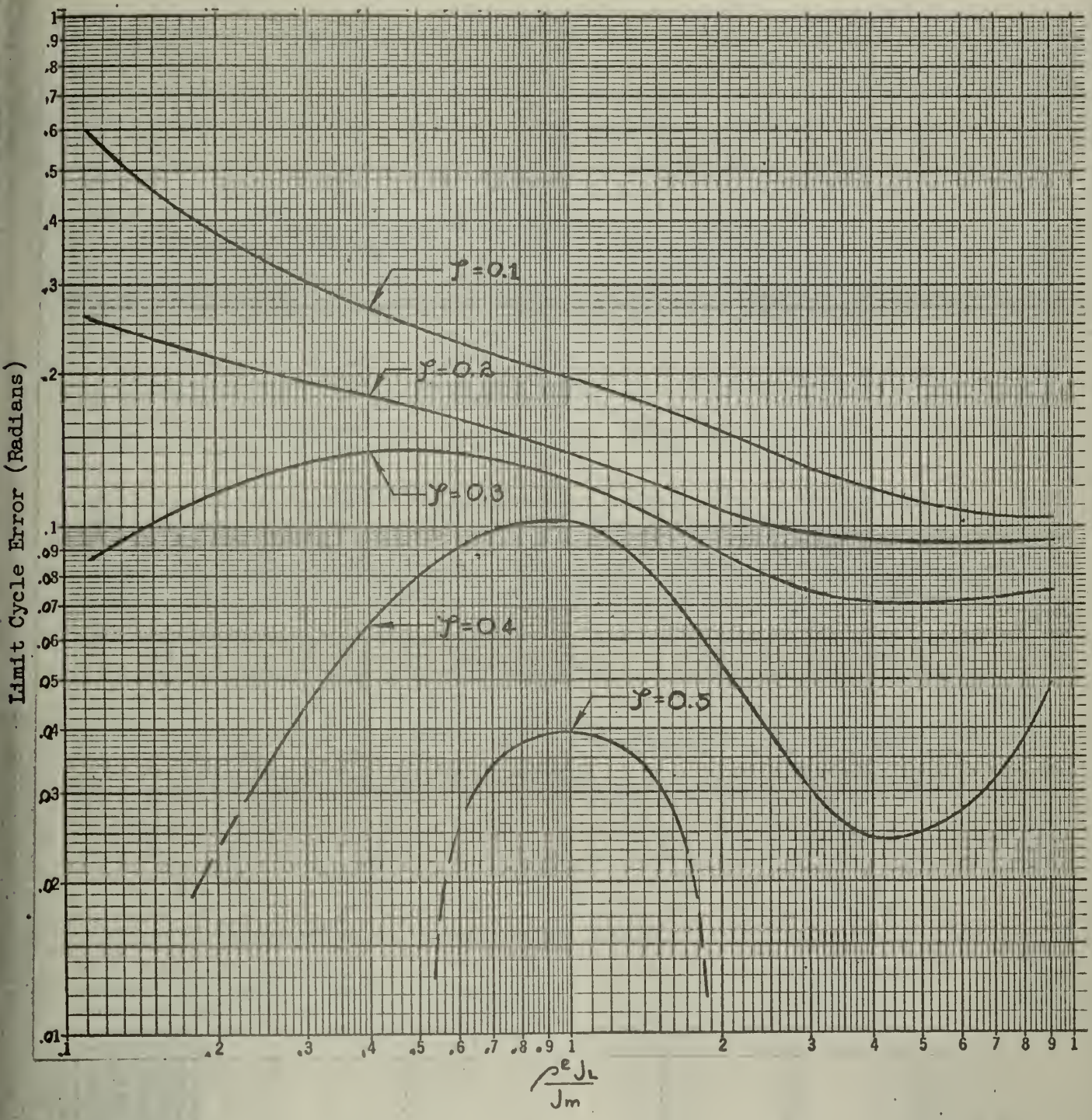

Fig. 23

Maximum Error of Limit Cycle from Unit Step Input

Limit Cycle Error (Radians) $\left(\frac{0.3}{\Delta}\right)$ for $\frac{\rho^2 J_L}{Jm}$ Variable

$$\frac{\rho^2 f_L}{F_T} = \frac{1}{\frac{f_m}{\rho^2 f_L} + 1} = 0.4$$

$$e = 1.0$$

No limit cycle exists for $\zeta \geq 0.6$

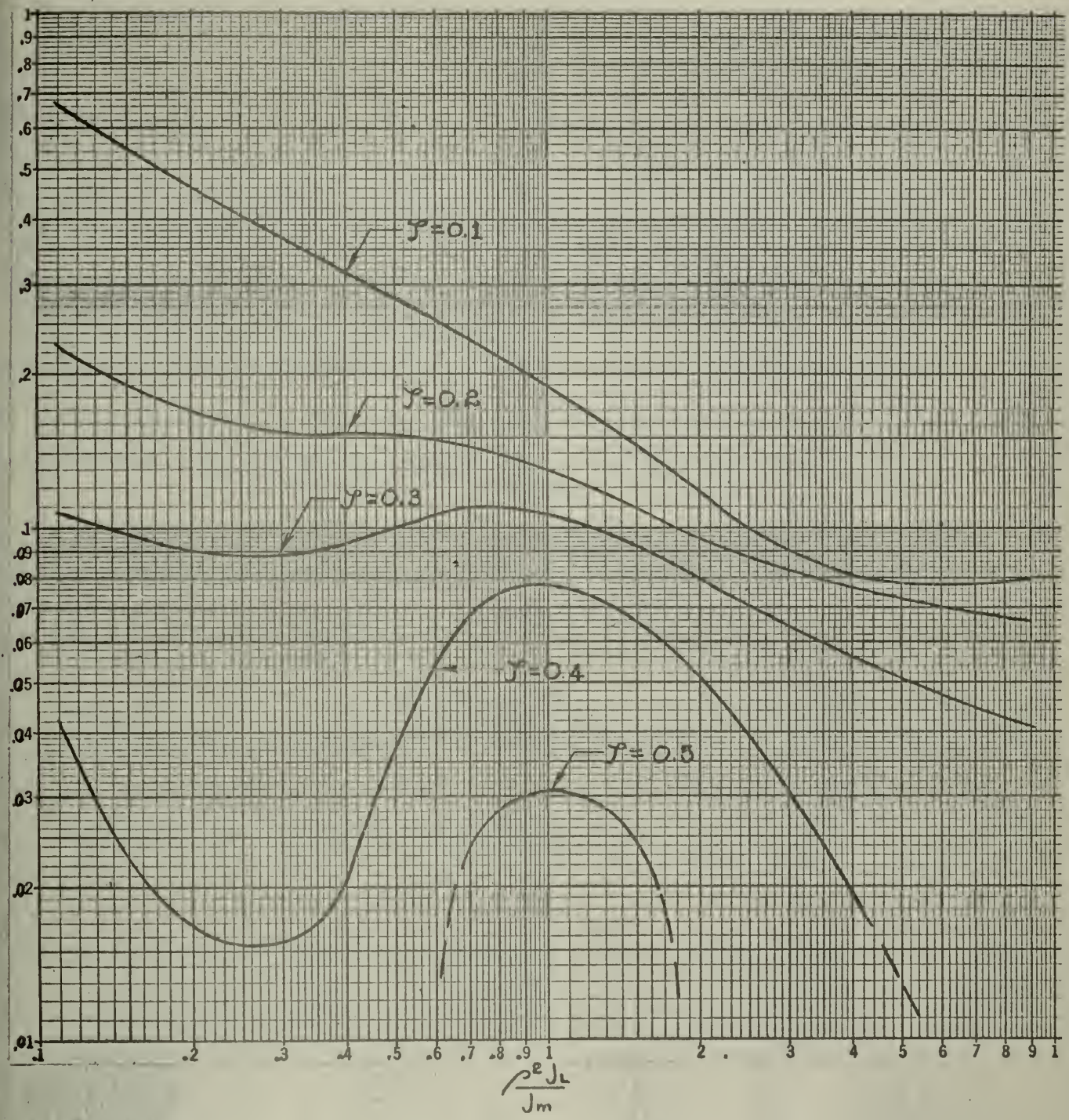

Fig. 24

Maximum Error of Limit Cycle from Unit Step Input

Limit Cycle Error (Radians) $\left(\frac{0.3}{\Delta}\right)$ for $\frac{\rho^2 J_L}{J_m}$ Variable

$$\frac{\rho^2 f_L}{F_r} = \frac{1}{\frac{f_m}{\rho^2 f_L} + 1} = 0.6$$

$$e = 1.0$$

No limit cycle exists for $\mathcal{Y} \geq 0.6$

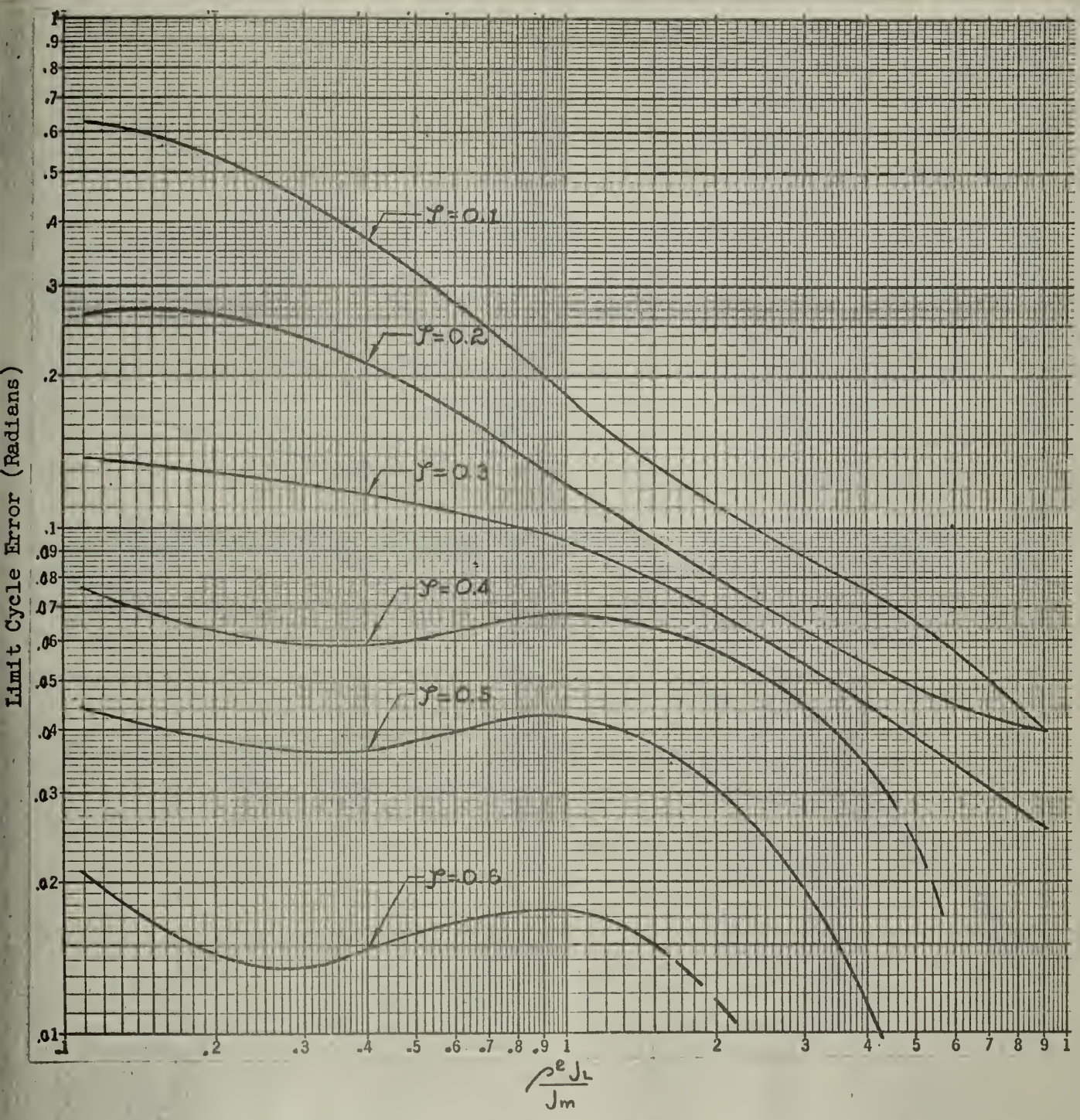

Fig. 25

Maximum Error of Limit Cycle from Unit Step Input

Limit Cycle Error (Radians) $\left(\frac{0.3}{\Delta}\right)$ for $\frac{\rho^2 J_L}{Jm}$ Variable

$$\frac{\rho^2 f_L}{F_T} = \frac{1}{\frac{f_m}{\rho^2 f_L} + 1} = 0.8$$

$$e = 1.0$$

No limit cycle exists for $\zeta \geq 0.8$

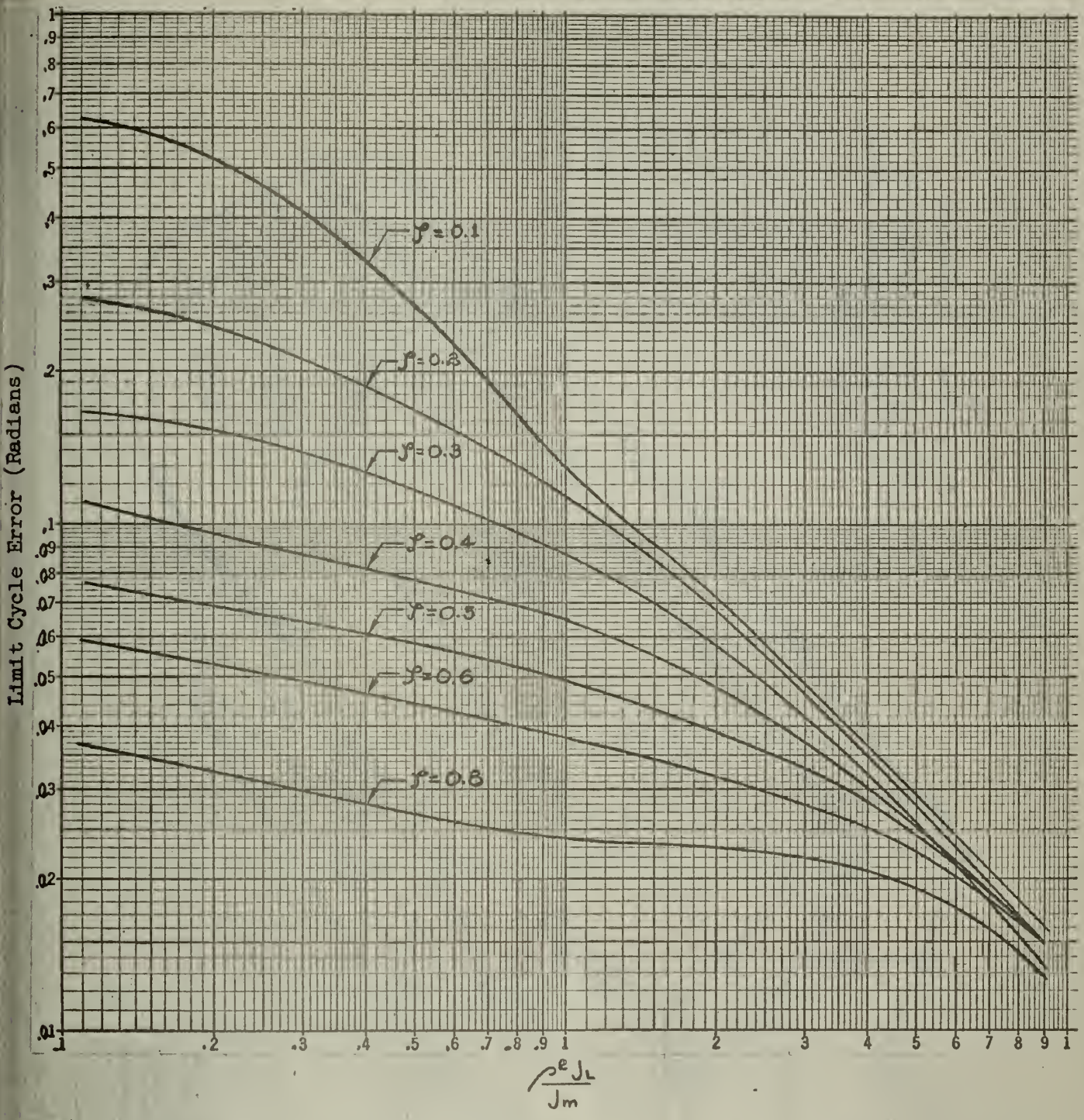

Fig. 26

Maximum Error of Limit Cycle from Unit Step Input

Limit Cycle Error (Radians) $\left(\frac{0.3}{\Delta}\right)$ for $\frac{\rho^2 J_L}{J_m}$ Variable

$$\frac{\rho^2 f_L}{F_T} = \frac{1}{\frac{f_m}{\rho^2 f_L} + 1} = 1.0$$

$$e = 1.0$$

No limit cycle exists for $\rho \geq 1.0$

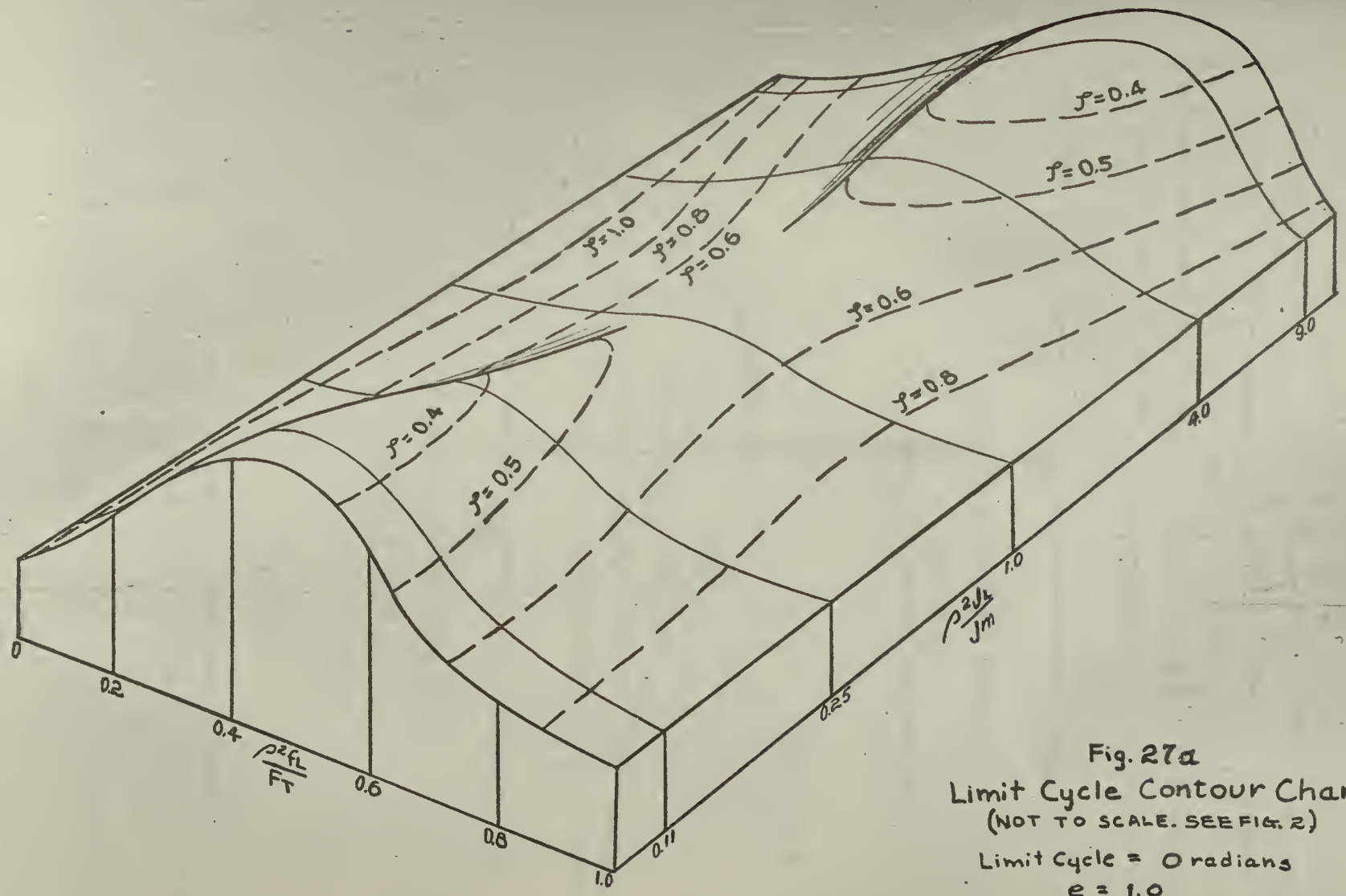

Fig. 27a
Limit Cycle Contour Chart
(NOT TO SCALE. SEE FIG. 2)
Limit Cycle = 0 radians
e = 1.0

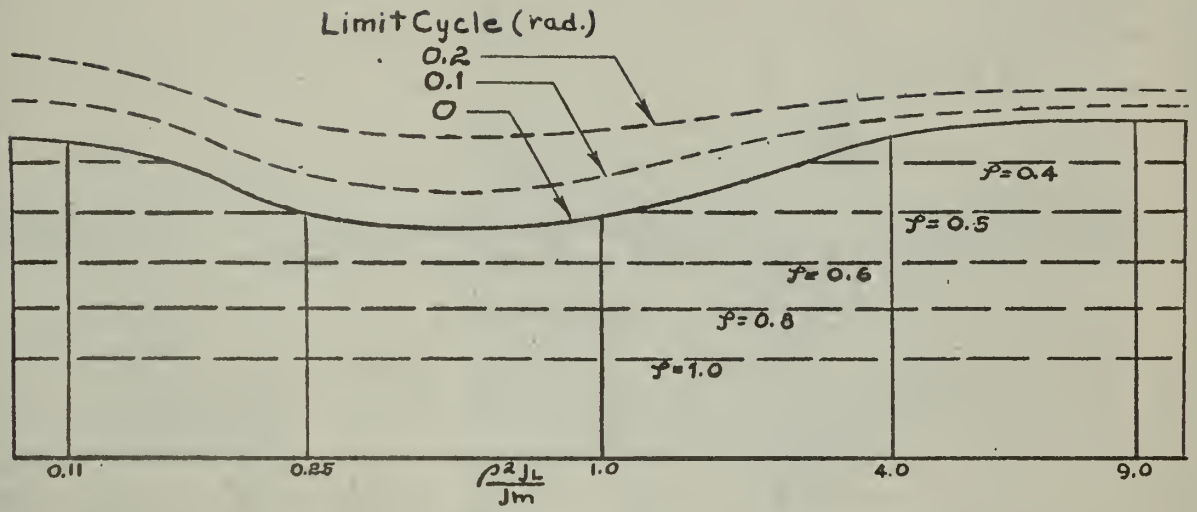

Constant $\frac{\rho^2 f_L}{F_T}$ Profile

$\frac{\rho^2 f_L}{F_T} = 0.6$

(NOT TO SCALE. SEE FIG. 24)

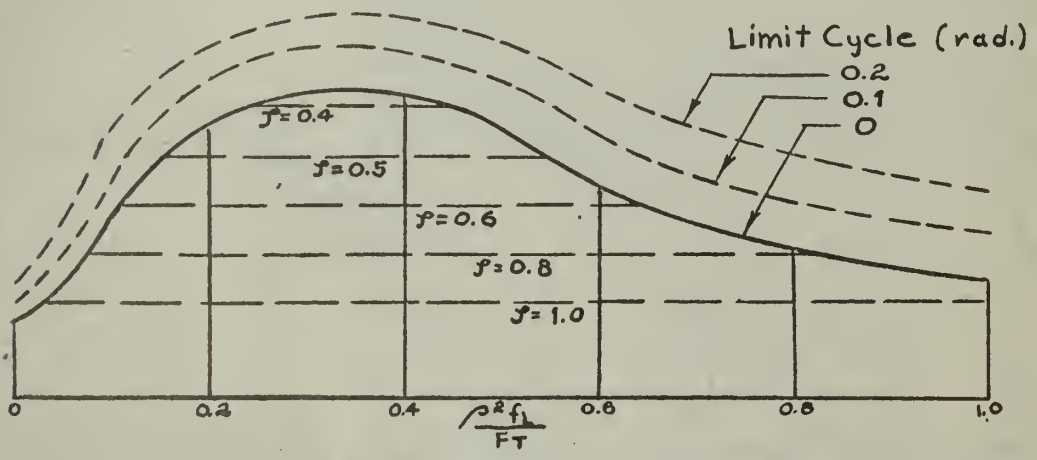

Constant $\frac{\rho^2 J_L}{Jm}$ Profile

$\frac{\rho^2 J_L}{Jm} = 0.11$

Fig. 27b

Limit Cycle Contour Chart
Profile Views

$e = 1.0$

$\Delta = 0.3$

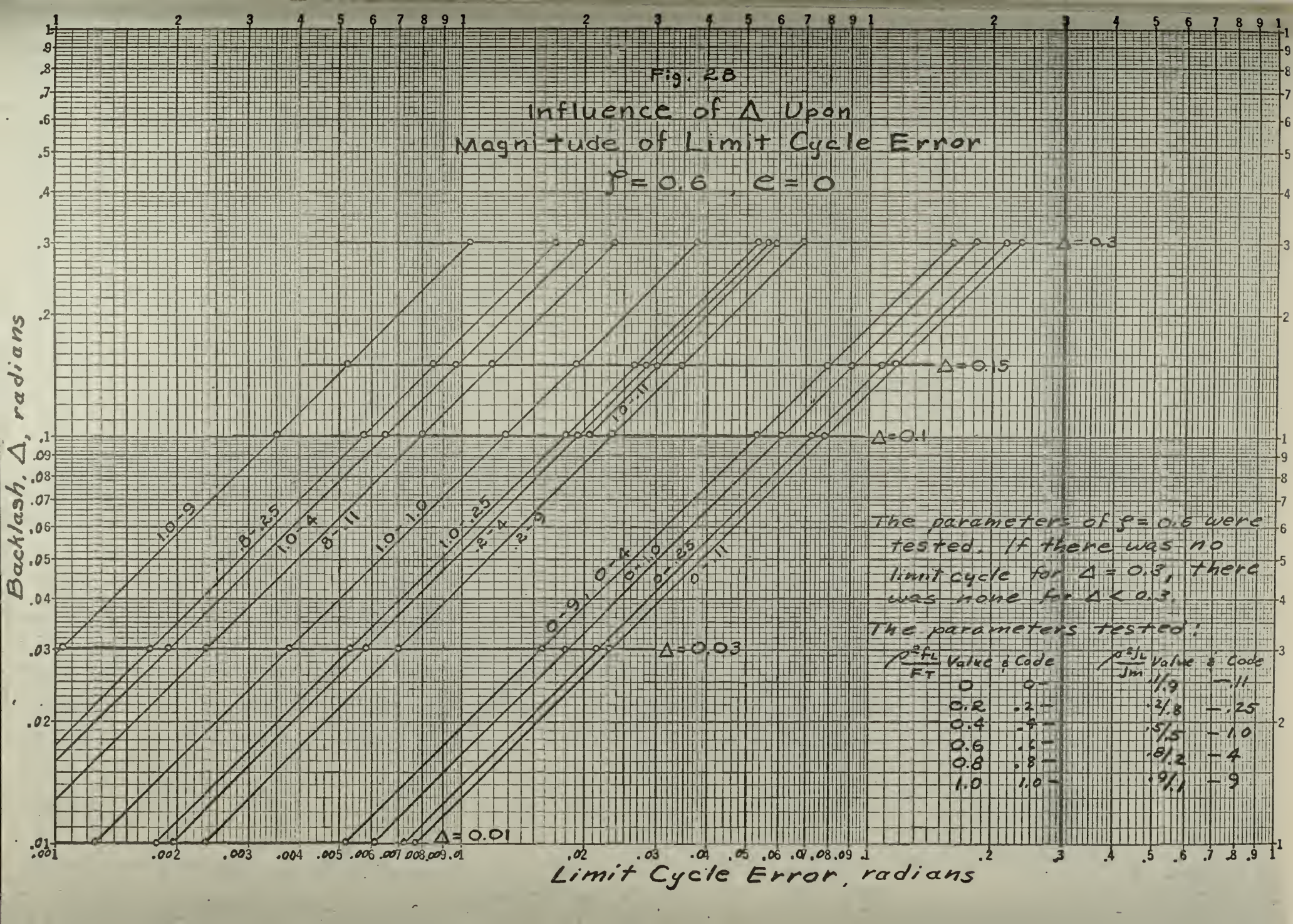
Fig. 28
Influence of Δ Upon
Magnitude of Limit Cycle Error
ρ = 0.6 , e = 0
Backlash, Δ, radians
Limit Cycle Error, radians
Δ = 0.3
Δ = 0.15
Δ = 0.1
Δ = 0.03
Δ = 0.01
1.0-.9
.8-.25
1.0-.4
.8-.11
1.0-1.0
1.0-.25
.2-.4
.2-.9
1.0-.11
0-.9
0-.8
0-1.0
0-.25
0-.11
The parameters of ρ = 0.6 were tested. If there was no limit cycle for Δ = 0.3, there was none for Δ < 0.3.
The parameters tested:
ρ²f_L/F_T Value & Code
0 0-
0.2 .2-
0.4 .4-
0.6 .6-
0.8 .8-
1.0 1.0-
ρ²f_L/Jm Value & Code
.1/.9 -.11
.2/.8 -.25
.5/.5 -1.0
.8/.2 -4
.9/.1 -9

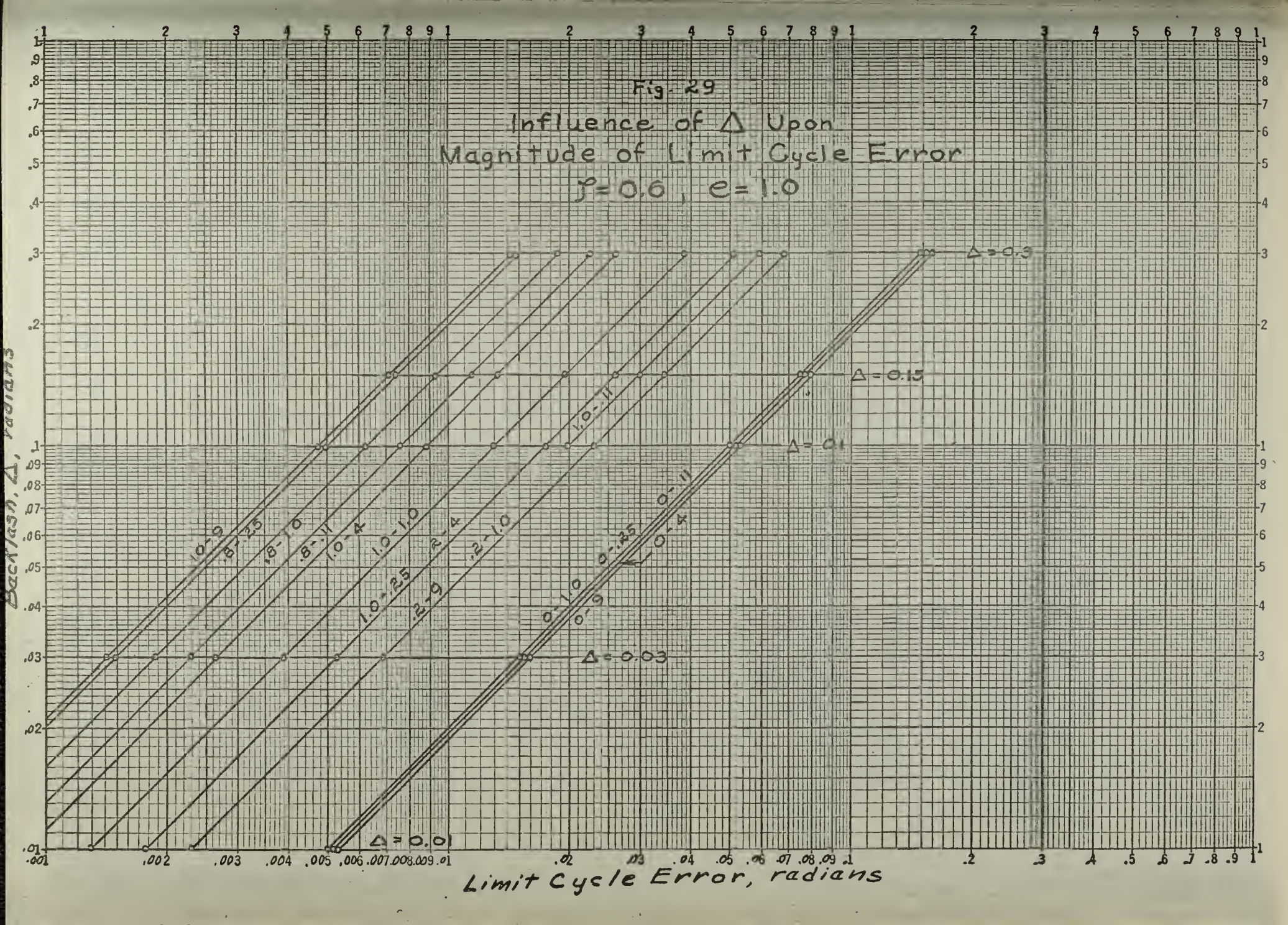
Fig. 29
Influence of Δ Upon
Magnitude of Limit Cycle Error
f=0.6, e=1.0
Δ=0.3
Δ=0.15
Δ=0.1
Δ=0.03
Δ=0.01
.8-.9
.8-.25
.8-1.0
.8-.11
1.0-.4
1.0-1.0
1.0-.11
1.0-.25
.2-.9
.2-.4
.2-1.0
0-.11
0-.35
0-.4
0-1.0
0-.9
Backlash, Δ, radians
Limit Cycle Error, radians

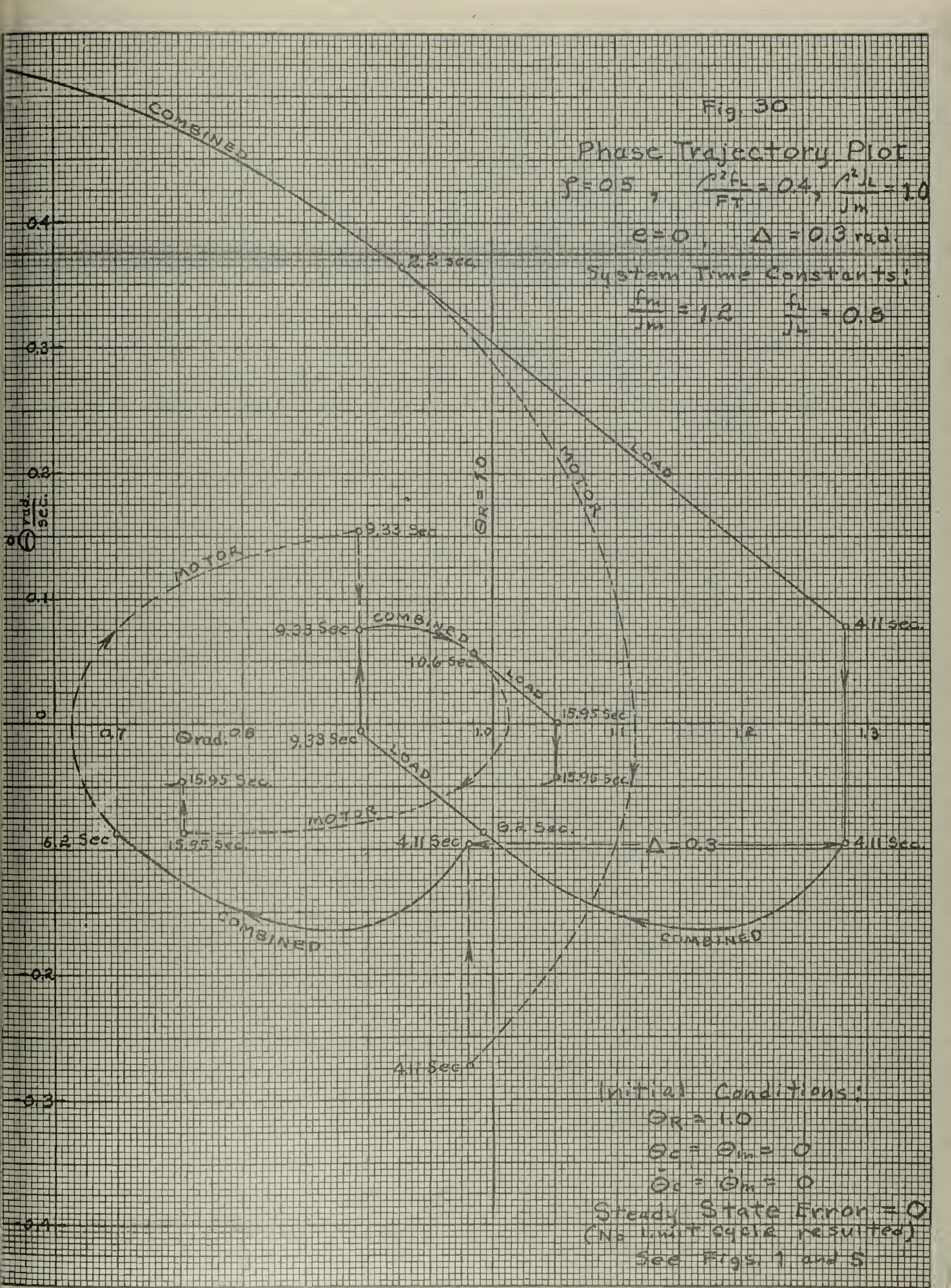
Fig. 30
Phase Trajectory Plot
ρ=0.5, $\frac{\rho^2 f_L}{F_T}=0.4$, $\frac{\rho^2 J_L}{J_m}=1.0$
e=0, Δ = 0.3 rad.
System Time Constants:
$\frac{f_m}{J_m}=1.2$ $\frac{f_L}{J_L}=0.8$
COMBINED
LOAD
MOTOR
12.2 sec.
9.33 Sec
9.38 Sec
10.6 Sec
15.95 Sec
12.96 Sec
6.2 Sec
4.11 Sec
0.8 Sec.
Δ = 0.3
θR = 1.0
θ rad.
θ̇ rad/sec
Initial Conditions:
θR = 1.0
θc = θm = 0
θ̇c = θ̇m = 0
Steady State Error = 0
(No Limit cycle resulted)
See Figs. 1 and 5

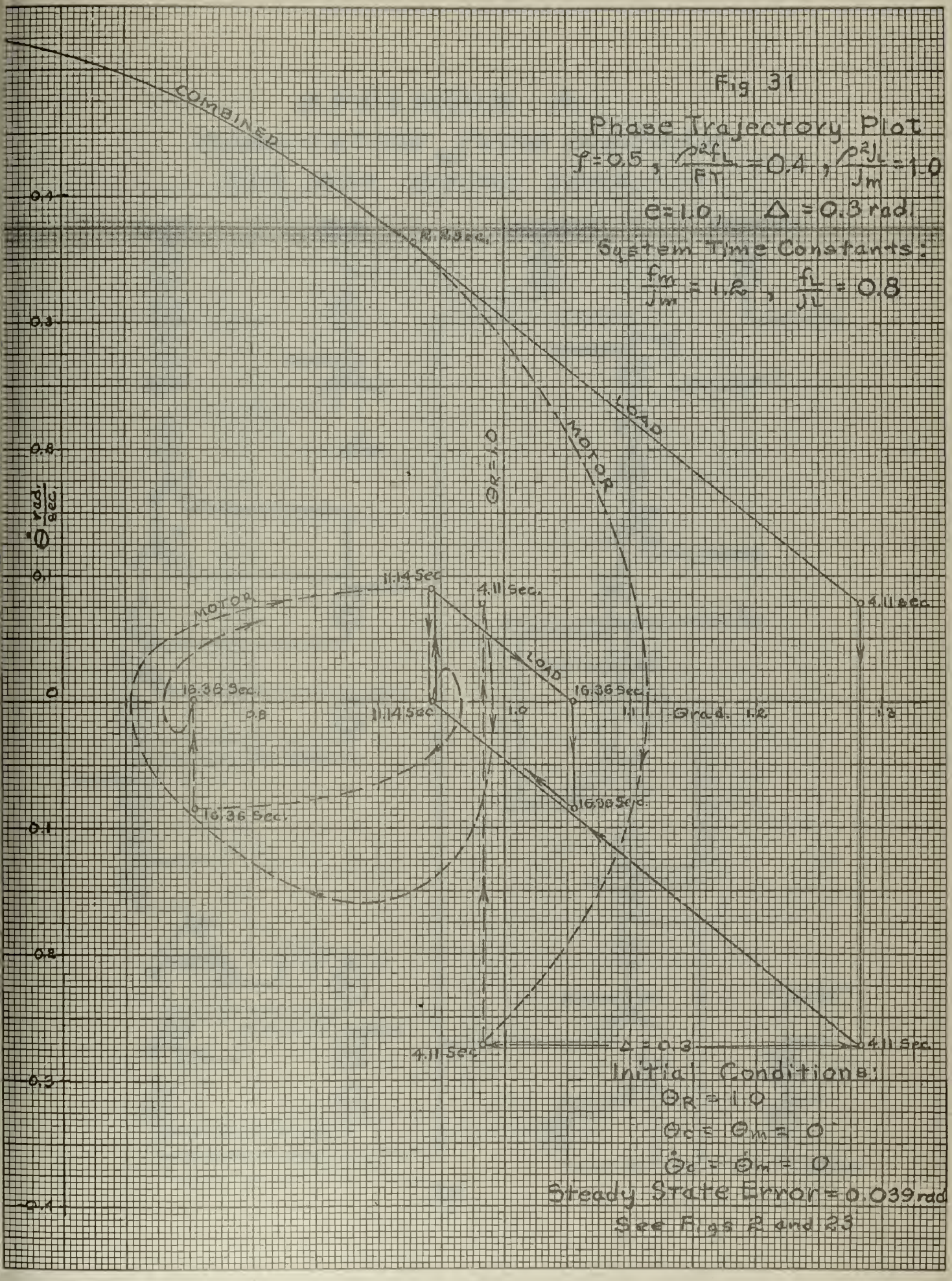
Fig 31
Phase Trajectory Plot
$f=0.5$, $\frac{\rho^2 f_L}{FT}=0.4$, $\frac{\rho^2 J_L}{Jm}=1.0$
$e=1.0$, $\Delta=0.3$ rad.
System Time Constants:
$\frac{fm}{Jm}=1.2$, $\frac{fl}{JL}=0.8$
COMBINED
LOAD
MOTOR
$\Theta_R=0$
$\Delta=0.3$
Grad. 1.2
11.14 Sec
4.11 Sec.
16.36 Sec.
Initial Conditions:
$\Theta_R=1.0$
$\Theta_c=\Theta_m=0$
$\dot{\Theta}_c=\dot{\Theta}_m=0$
Steady State Error = 0.039 rad
See Figs 22 and 23

APPENDIX A

COMPUTATION FLOW DIAGRAM for CDC 1604 DIGITAL COMPUTER

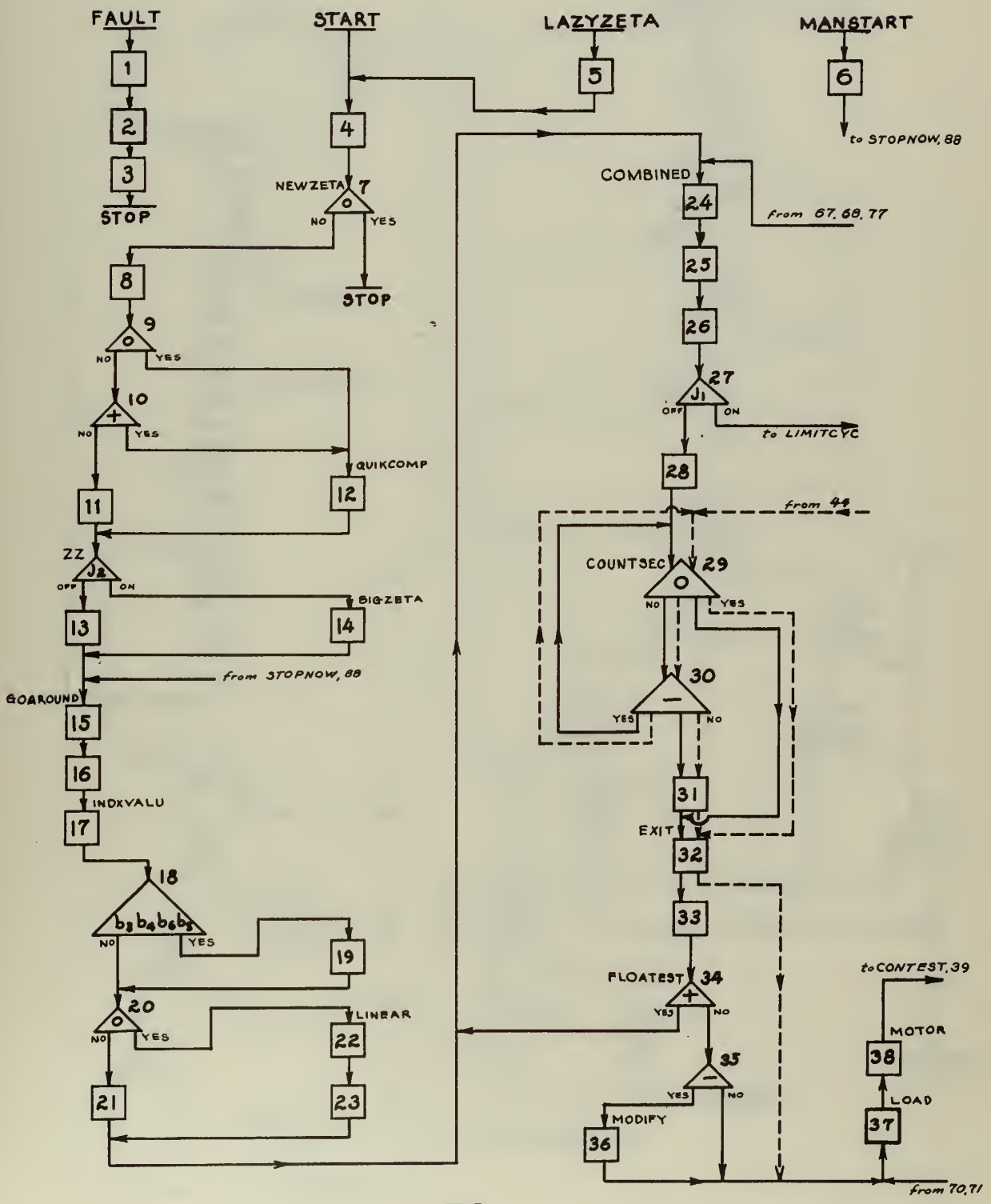

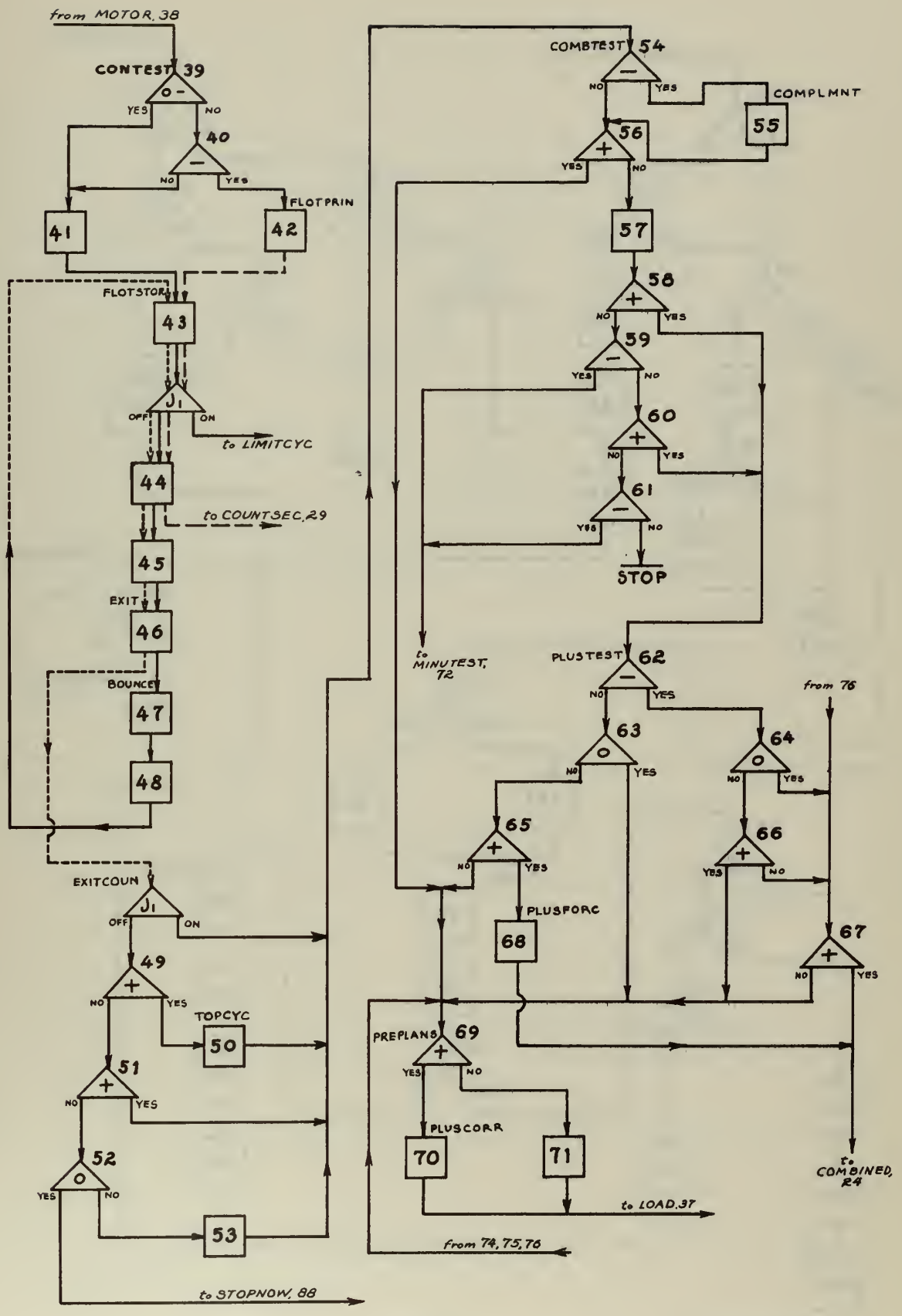
from MOTOR, 38
CONTEST 39
YES
NO
40
NO
YES
FLOTPRIN
41
42
FLOTSTOR
43
J1
OFF
ON
to LIMITCYC
44
to COUNTSEC, 29
45
EXIT
46
BOUNCE
47
48
EXITCOUN
J1
OFF
ON
49
NO
YES
TOPCYC
50
51
NO
YES
52
YES
NO
53
to STOPNOW, 88
COMBTEST 54
NO
YES
COMPLMNT
55
56
YES
NO
57
58
NO
YES
59
YES
NO
60
NO
YES
61
YES
NO
STOP
to MINUTEST, 72
PLUSTEST 62
NO
YES
from 76
63
NO
YES
64
NO
YES
65
NO
YES
66
YES
NO
PLUSFORC
68
67
NO
YES
PREPLANS 69
YES
NO
PLUSCORR
70
71
to COMBINED, 24
to LOAD, 37
from 74, 75, 76

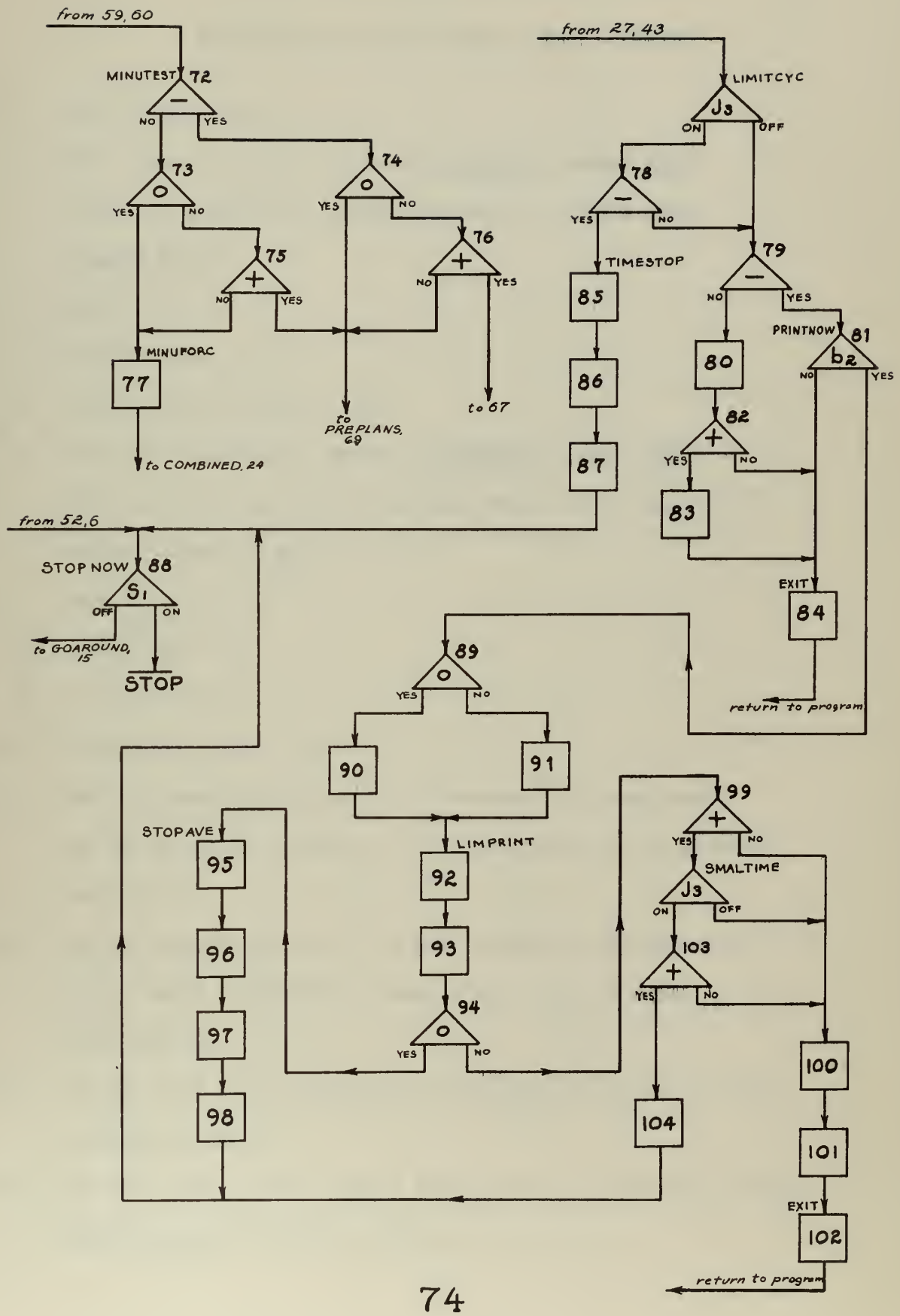
from 59, 60
MINUTEST 72
NO
YES
73
YES
NO
74
YES
NO
75
NO
YES
76
NO
YES
MINUFORC
77
to COMBINED, 24
to PREPLANS, 69
to 67
from 27, 43
LIMITCYC
J3
ON
OFF
78
YES
NO
TIMESTOP
85
86
87
79
NO
YES
PRINTNOW 81
b2
NO
YES
80
82
YES
NO
83
EXIT
84
return to program
from 52, 6
STOP NOW 88
S1
OFF
ON
to GOAROUND, 15
STOP
89
YES
NO
90
91
LIMPRINT
92
93
94
YES
NO
STOPAVE
95
96
97
98
99
YES
NO
SMALTIME
J3
ON
OFF
103
YES
NO
104
100
101
EXIT
102
return to program

EXPLANATION OF FLOW DIAGRAM BLOCK SYMBOLS

1. Clear fault stop.
2. Print last overshoot stored in LIMITBUF (symbol 888). Print out position in phase trajectory of fault stop (symbol 666).
3. End of file.
4. Actuate fault stop.
5. Load zeta from Index 1 (b_1).
6. Print last overshoot stored on LIMITBUF (symbol 888). Print position in phase trajectory where it was manually stopped (symbol 1961).
7. Stop if Zeta = 0.
8. $2\zeta\omega_n = A$
9. Is zeta = 0.1?
10. Is zeta less than 0.1?
11. Set up computation time of 0.01 seconds for problem and set up for print at every 0.1 seconds when zeta is greater than 0.1.
12. Set up computation time of 0.004 seconds for problem and set up for print at every 0.1 seconds when zeta is equal to or less than 0.1.
13. Set up limit cycle print-out routine for 20 overshoots and average the last 8.
14. Set up number of limit cycle print-outs and averaging routine depending upon the size of zeta:

ρ	Overshoots	Start Averaging	Divide by *	Comp. Time
$\geq$ 0.8	6	4	2.0	0.01
0.6	7	5	2.0	0.01
0.5	8	5	3.0	0.01
0.4	10	7	3.0	0.01
0.3	14	10	4.0	0.01
0.2	20	12	8.0	0.01
$\leq$ 0.1	17	12	5.0	0.004

*The last row printed has this number printed on the far left if the problem has a normal solution. This number indicates how many overshoots were averaged. The average value has 1.0 subtracted from it and is printed in the far right of the same last row.

15. Page reject.

16. Clear buffers and set up for new problem.

17. Restitution, e, from Index 3 (b_3).

    Backlash, Δ , from Index 4 (b_4).

    J_m from Index 5 (b_5).

$$\frac{J_T - J_m}{\rho^2} = J_L; \quad \frac{K}{J_m} = C; \quad \frac{J_m}{J_L}$$

    $\frac{f_L}{F_T}$ from Index 6 (b_6).

$$(f_L/F_T)(2\rho\omega_n)(J_T) = f_L; \quad f_L/J_L = B$$

$$\frac{f_L}{f_L/F_T} - \rho^2 f_L = f_m; \quad f_m/J_m = D$$

18. Have all values been cycled through?

19. Set STOPNOW after this run to stop absolutely.

20. Backlash, Δ , = 0?

21. Print consecutive number of this parameter run and all the parameters used:

$2\rho\omega_n = A$ $\quad J_m/J_L$ $\quad f_L/F_T$ $\quad e$ $\quad \Delta$ $\quad \rho$

J_m $\quad J_L$ $\quad J_m+\rho^2 J_L$ $\quad f_m$ $\quad f_L$ $\quad \rho^2$

K $\quad K/J_m = C$ $\quad f_m/J_m = D$ $\quad f_L/J_L = B$ $\quad \omega_n^2$ $\quad \rho$

22. Set program so always acts as combined system.

23. Print consecutive number of this parameter run and selected parameters for linear system:

$2\rho\omega_n = A$ $\quad J_m+\rho^2 J_L$ $\quad K$ $\quad \omega_n^2$ $\quad \rho$ $\quad \rho^2$

24. Solve the second order equation by Runge-Kutta-Gill numerical integration every 0.01 seconds problem time when zeta is greater than 0.1, otherwise every 0.004 seconds. Initial conditions are $\Theta_R = 1.0$, $\dot{\Theta}_c = \Theta_c = 0$ and $\ddot{\Theta}_c = 1.0$ or the previously computed point. Next point is computed by four iterations of:

$$\ddot{\Theta}_c = \omega_n^2(\Theta_R - \Theta_c) - 2\rho\omega_n\dot{\Theta}_c$$

25. Set EXIT from print routine.

26. Load time, $\dot{\Theta}_c$ and Θ_c in print buffer.

27. Go to LIMITCYC to print only the overshoot. Otherwise print the phase trajectory points for each 0.1 seconds up to a maximum of 12 cycles.

28. Store 0 for $\dot{\Theta}_m$ and Θ_m

29. Is problem time 0.1 sec.?

30. Is problem time greater than 0.1 sec.?

31. Print the number of point computed, time, $\dot{\Theta}_c$ and Θ_c.

32. EXIT (automatically set for desired jump-out.)

33. Store time, $\ddot{\Theta}_c$, $\dot{\Theta}_c$ and Θ_c for motor and load initial conditions.

34. Is slope $N_L = N_S$?

$$\frac{(\Theta_R - \Theta_c)\omega_n^2}{\dot{\Theta}_c} - 2\rho\omega_n + \frac{f_L}{J_L} = \text{positive value?}$$

35. Is $\dot{\Theta}_c$ negative?

36. Store $\frac{\Theta_c - \Delta}{\rho}$ in Θ_m

37. Solve $\ddot{\Theta}_c = -\left(f_L/J_L\right)\left(\dot{\Theta}_c\right)$ for $\dot{\Theta}_c$ and Θ_c by Runge-Kutta-Gill.

38. Solve $\ddot{\Theta}_m = -\left(f_m/J_m\right)\left(\dot{\Theta}_m\right) + \left(K/J_m\right)\left(\Theta_R - \Theta_c\right)$ for $\dot{\Theta}_m$ and Θ_m by Runge-Kutta-Gill

39. $\Theta_L - \rho\,\Theta_m \leq 0$?

40. $\Theta_L - \rho\,\Theta_m - \Delta$ = negative?

41. Set EXIT from print routine.

42. Set EXIT from print routine.

43. Load time, $\dot{\Theta}_c$ and Θ_c.

44. Load $\dot{\Theta}_m$ and Θ_m.

45. Print number of point computed and stored values.

46. EXIT (automatically set for desired jump-out).

47. Solve

$$\dot{\Theta}_c' = \frac{J_m}{J_m + \rho^2 J_L}\left[\rho\dot{\Theta}_m(1+e) + \dot{\Theta}_c\left(\rho^2\frac{J_L}{J_m} - e\right)\right]$$

$$\dot{\Theta}_m' = \frac{\dot{\Theta}' - e(\rho\dot{\Theta}_m + \dot{\Theta}_c)}{\rho}$$

$$\ddot{\Theta}_m' = -\frac{f_m}{J_m}\dot{\Theta}_m' + \frac{K}{J_m}(\Theta_R - \Theta_c)$$

48. Set EXIT from print routine.

49. Is $\dot{\Theta}_c$ positive?

50. Set up to count one phase trajectory when $\dot{\Theta}_c$ is negative.

51. Is $\Theta_c > 1.0$?

52. Have 12 cycles of phase trajectory been completed?

53. Arrange for no counting until $\dot{\Theta}_c$ is positive again.

54. Is $\rho\dot{\Theta}_m - \dot{\Theta}_c$ negative?

55. Set up $-(\rho\dot{\Theta}_m - \dot{\Theta}_c)$.

56. Is $\rho\dot{\Theta}_m - \dot{\Theta}_c$ greater than preselected ϵ ?

57. Set up combined system.

58. Is $\dot{\Theta}_c$ positive?

59. Is $\dot{\Theta}_c$ negative?

60. Is $\Theta_c - 1$ positive?

61. Is $\Theta_c - 1$ negative?

62. Is $\Theta_c - 1$ negative?

63. $\Theta_c - \rho\Theta_m = 0$?

64. $\Theta_c - \rho\Theta_m = 0$?

65. Is $\Theta_c - \rho\Theta_m$ positive?

66. Is $\Theta_c - \rho\Theta_m$ positive?

67. Is Slope $N_L = N_S$?

$$\frac{(1-\Theta_c)\,\omega_n^2}{\dot{\Theta}_c} - 2\rho\omega_n + \frac{f_L}{J_L} = \text{positive value?}$$

68. Modify FLOATEST to keep system combined. Takes off modification when $\dot{\Theta}_c$ is negative.

69. Is $\Theta_c - \rho\Theta_m$ positive?

70. Store $\frac{\Theta_L - \Delta}{\rho}$ in Θ_m.

71. Store $\frac{\Theta_c}{\rho}$ in Θ_m.

72. Is $\Theta_c - 1$ negative?

73. $\Theta_c - \rho\Theta_m = 0$?

74. $\Theta_c - \rho\Theta_m = 0$?

75. Is $\Theta_c - \rho\Theta_m$ positive?

76. Is $\Theta_c - \rho\Theta_m$ positive?

77. Modify FLOATEST to keep system combined. Takes off modification when $\dot{\Theta}_c$ is positive.

78. Have 1 1/2 minutes of real time elapsed since the last print-out?

79. Is $\Theta_c < 1.0$?

80. Set up to print when in the fourth quadrant.

81. Check if in the fourth quadrant.

82. Is the new Θ_c greater than the previous Θ_c ?

83. Store the new time, $\dot{\Theta}_c$ and Θ_c.

84. EXIT (automatically set for desired jump-out).

85. Print the last overshoot stored in LIMITBUF (symbol 888)

86. Stop real time clock.

87. Print position in phase trajectory where it was stopped by the real time clock (symbol 999).

88. Return to beginning to start new problem if new parameters remain to be evaluated. Unconditional stop if all parameters have been evaluated.

89. Has the required number of overshoots been evaluated prior to starting the averaging routine?

90. Add the Θ_c just evaluated to the previous sum for averaging.

91. Add one to the count prior to averaging.

92. Clear time clock.

93. Print time, $\dot{\Theta}_c$ and Θ_c.

94. Required number of total print-outs?

95. Clear buffers.

96. Obtain the average of Θ_c.

97. Subtract 1.0.

98. Print the average of Θ_c - 1.0 and how many overshoots were utilized to obtain the average.

99. Is Θ_c less than 1.005 radians?

100. Clear buffers.

101. Start real time clock.

102. EXIT (automatically set to desired jump-out).

103. Has 30 seconds of real time elapsed since the last print-out?

104. Print the position in the phase trajectory where it was stopped by the real time clock and Θ_c being less than 1.005 radians (symbol 1005).

Jump Switches:

J_1 - For LIMITCYC, allows the maximum overshoot print-out only. With J_1 down, a phase trajectory is printed for a maximum of 12 cycles.

J_2 - Set the number of print-outs depending on zeta. Change the number of overshoot values used to obtain the average value.

J_3 - Use the real time clock for an automatic recycle to a new parameter when have:

a. 1 1/2 minutes maximum after the last print-out.

b. 30 seconds maximum and Θ_c is 1.005 radians or less.

Stop Switches:

S_1 - Stops at the end of this parameter run or stops at the end of the manual print-out.

APPENDIX B

COMPUTER PROGRAM

```
                                        ORG     00007
00007   74 0 00070      FAULT           EXF   0 00070
        75 0 40701                      SLJ   0 FAULPRIN
                                        ORG     40000
40000   74 0 00100      START           EXF   0 00100
        75 0 40004                      SLJ   0 NEWZETA-1
40001   12 1 40623      LAZYZETA        LDA   1 ZETAINDX
        20 0 40425                      STA   0 ZETA
40002   50 1 00000                      ENI   1 0
        75 0 40000                      SLJ   0 START
40003   75 0 40674      MANSTART        SLJ   0 MANUAL
        50 0 00000                      ENI   0 0
40004   12 0 40565                      LDA   0 NEWSTOP
        20 0 40563                      STA   0 STOPNOW
40005   12 0 40425      NEWZETA         LDA   0 ZETA
        22 0 40564                      AJP   0 STOPINDX
40006   32 0 40665                      FMU   0 TWO
        32 0 40426                      FMU   0 OMEGAN
40007   20 0 40404                      STA   0 A
        12 0 40624                      LDA   0 ZETAINDX+1
40010   31 0 40425                      FSB   0 ZETA
        22 0 40433                      AJP   0 QUIKCOMP
40011   22 2 40433                      AJP   2 QUIKCOMP
        12 0 40402                      LDA   0 POINT01
40012   20 0 40154                      STA   0 TABLES+1
        20 0 40173                      STA   0 TABLEL+1
40013   20 0 40207                      STA   0 TABLEM+1
        12 0 40631                      LDA   0 COUNT10
40014   20 0 40400                      STA   0 TENTHSEC
        50 0 00000                      ENI   0 0
40015   75 2 40437      ZZ              SLJ   2 BIGZETA
        50 0 00000                      ENI   0 0
40016   12 0 40652                      LDA   0 STOP20
        20 0 40616                      STA   0 STOPZETA
40017   12 0 40662                      LDA   0 COUNT12
        20 0 40617                      STA   0 COUNTZET
40020   12 0 40672                      LDA   0 EIGHT
        20 0 40620                      STA   0 DIVIDE
40021   10 0 00010                      ENA   0 10
        61 0 40562                      SAL   0 STOPRINT
40022   75 4 71000      GOAROUND        SLJ   4 DECOF
        50 0 00000                      ENI   0 0
40023   02 0 40427                        02  0 FORZEROS
        04 0 00000                        04  0 0
40024   12 0 40664                      LDA   0 ONE
        20 0 40156                      STA   0 UDOT
40025   10 0 00000                      ENA   0 0
        20 0 00000                      STA   0 0
40026   20 0 40162                      STA   0 THETA
        20 0 40161                      STA   0 THETADOT
40027   20 0 40157                      STA   0 U
        20 0 40155                      STA   0 T
40030   20 0 40377                      STA   0 INDEX
        20 0 40615                      STA   0 INDEXAVE
40031   20 0 40351                      STA   0 PRINTBUF+3
        20 0 40352                      STA   0 PRINTBUF+4
40032   20 0 40353                      STA   0 PRINTBUF+5
        20 0 40614                      STA   0 LIMINDEX
40033   20 0 40607                      STA   0 LIMITBUF+2
        20 0 40610                      STA   0 LIMITBUF+3
40034   20 0 40611                      STA   0 LIMITBUF+4
        20 0 40612                      STA   0 LIMITBUF+5
40035   20 0 40613                      STA   0 LIMITBUF+6
        12 0 40621                      LDA   0 PRINTSET
40036   20 0 40326                      STA   0 OK2PRINT+1
        20 0 40335                      STA   0 BOUNPRIN+4
40037   12 0 40622                      LDA   0 NEWLIMPT
        20 0 40544                      STA   0 LIMPRINT+1
40040   12 0 40253                      LDA   0 FLOTDATA
        20 0 40071                      STA   0 FLOATEST
40041   12 0 40254                      LDA   0 FLOTDATA+1
        20 0 40072                      STA   0 FLOATEST+1
40042   75 0 40452      NEWINPUT        SLJ   0 INDXVALU
        50 0 00000                      ENI   0 00000
```

```
40043   12 0 40410              LDA  0 DELTA
        22 0 40500              AJP  0 LINEAR
40044   12 0 40513              LDA  0 NOSINK
        20 0 40071              STA  0 FLOATEST
40045   75 4 71000              SLJ  4 DECOF
        50 0 00000              ENI  0 0
40046   01 0 40404                01 0 A
        06 0 00001                06 0 1
40047   72 0 40046              RAO  0 7-1
        75 4 71000              SLJ  4 DECOF
40050   01 0 40412                01 0 MOINERT
        06 0 00000                06 0 0
40051   72 0 40510              RAO  0 LINEAR+10
        75 4 71000              SLJ  4 DECOF
40052   01 0 40420                01 0 KMOTCONS
        06 0 00000                06 0 0
40053   10 0 00000  COMBINED    ENA  0 0
        20 0 40160              STA  0 QX
40054   20 0 40163              STA  0 QY
        75 4 60200              SLJ  4 RUNGE
40055   00 0 40153                 0 0 TABLES
        00 0 40164                 0 0 DERIVES
40056   75 4 60201              SLJ  4 RUNGE+1
        50 0 00000              ENI  0 0
40057   75 0 40310              SLJ  0 COMBPRIN
        50 0 00000              ENI  0 0
40060   12 0 40155              LDA  0 T
        20 0 40174              STA  0 TL
40061   20 0 40210              STA  0 TM
        12 0 40156              LDA  0 UDOT
40062   20 0 40175              STA  0 VDOT
        33 0 40411              FDV  0 RHO
40063   20 0 40211              STA  0 WDOT
        12 0 40157              LDA  0 U
40064   20 0 40176              STA  0 V
        20 0 40200              STA  0 THETADL
40065   33 0 40411              FDV  0 RHO
        20 0 40212              STA  0 W
40066   20 0 40214              STA  0 THETADM
        12 0 40162              LDA  0 THETA
40067   20 0 40201              STA  0 THETAL
        33 0 40411              FDV  0 RHO
40070   20 0 40215              STA  0 THETAM
        50 0 00000              ENI  0 0
40071   13 0 40162  FLOATEST    LAC  0 THETA
        30 0 40664              FAD  0 ONE
40072   32 0 40424              FMU  0 OMEGANSQ
        33 0 40161              FDV  0 THETADOT
40073   31 0 40404              FSB  0 A
        30 0 40423              FAD  0 B
40074   22 2 40053              AJP  2 COMBINED
        12 0 40161              LDA  0 THETADOT
40075   22 3 40270              AJP  3 MODIFY
        50 0 00000              ENI  0 0
40076   10 0 00000  LOAD        ENA  0 0
        20 0 40177              STA  0 QL
40077   20 0 40202              STA  0 QLL
        20 0 40213              STA  0 QM
40100   20 0 40216              STA  0 QMM
        75 4 60200              SLJ  4 RUNGE
40101   00 0 40172                 0 0 TABLEL
        00 0 40203                 0 0 DERIVL
40102   75 4 60201              SLJ  4 RUNGE+1
        50 0 00000              ENI  0 0
40103   75 4 60200  MOTOR       SLJ  4 RUNGE
        50 0 00000              ENI  0 0
40104   00 0 40206                 0 0 TABLEM
        00 0 40217                 0 0 DERIVM
40105   75 4 60201              SLJ  4 RUNGE+1
        50 0 00000              ENI  0 0
40106   13 0 40215  CONTEST     LAC  0 THETAM
        32 0 40411              FMU  0 RHO
40107   30 0 40201              FAD  0 THETAL
        22 0 40112              AJP  0 BOUNCE
```

```
40110   22 3 40112            AJP  3 BOUNCE
        31 0 40410            FSB  0 DELTA
40111   22 3 40317            AJP  3 FLOTPRIN
        50 0 00000            ENI  0 0
40112   75 0 40331  BOUNCE    SLJ  0 BOUNPRIN
        50 0 00000            ENI  0 0
40113   12 0 40200            LDA  0 THETADL
        20 0 40212            STA  0 W
40114   12 0 40417            LDA  0 RHOSQ
        33 0 40405            FDV  0 INERTRAT
40115   31 0 40407            FSB  0 RESTITUT
        32 0 40200            FMU  0 THETADL
40116   20 0 40200            STA  0 THETADL
        12 0 40664            LDA  0 ONE
40117   30 0 40407            FAD  0 RESTITUT
        32 0 40411            FMU  0 RHO
40120   32 0 40214            FMU  0 THETADM
        30 0 40200            FAD  0 THETADL
40121   33 0 40414            FDV  0 TOTINERT
        32 0 40412            FMU  0 MOINERT
40122   20 0 40200            STA  0 THETADL
        20 0 40176            STA  0 V
40123   13 0 40176            LAC  0 V
        32 0 40423            FMU  0 B
40124   20 0 40175            STA  0 VDOT
        13 0 40214            LAC  0 THETADM
40125   32 0 40411            FMU  0 RHO
        30 0 40212            FAD  0 W
40126   32 0 40407            FMU  0 RESTITUT
        30 0 40200            FAD  0 THETADL
40127   33 0 40411            FDV  0 RHO
        20 0 40214            STA  0 THETADM
40130   20 0 40212            STA  0 W
        13 0 40212            LAC  0 W
40131   32 0 40422            FMU  0 D
        20 0 40211            STA  0 WDOT
40132   13 0 40201            LAC  0 THETAL
        30 0 40664            FAD  0 ONE
40133   32 0 40421            FMU  0 C
        30 0 40211            FAD  0 WDOT
40134   20 0 40211            STA  0 WDOT
        75 0 40332            SLJ  0 BOUNPRIN+1
40135   50 0 00000  COMBTEST  ENI  0 0
        12 0 40214            LDA  0 THETADM
40136   32 0 40411            FMU  0 RHO
        31 0 40200            FSB  0 THETADL
40137   22 3 40276            AJP  3 COMPLMNT
        50 0 00000            ENI  0 00000
40140   65 0 40403            THS  0 DIFFERNT
        75 0 40301            SLJ  0 PREPLANS
40141   12 0 40200            LDA  0 THETADL
        20 0 40161            STA  0 THETADOT
40142   20 0 40157            STA  0 U
        13 0 40157            LAC  0 U
40143   32 0 40404            FMU  0 A
        20 0 40156            STA  0 UDOT
40144   12 0 40201            LDA  0 THETAL
        20 0 40162            STA  0 THETA
40145   13 0 40162            LAC  0 THETA
        30 0 40664            FAD  0 ONE
40146   32 0 40424            FMU  0 OMEGANSQ
        30 0 40156            FAD  0 UDOT
40147   20 0 40156            STA  0 UDOT
        12 0 40174            LDA  0 TL
40150   20 0 40155            STA  0 T
        12 0 40200            LDA  0 THETADL
40151   22 2 40225            AJP  2 PLUSTEST
        22 3 40255            AJP  3 MINUTEST
40152   75 0 40273            SLJ  0 TESTZERO
        50 0 00000            ENI  0 0
40153   00 0 00000  TABLES    OCT    2
        00 0 00002
40154   17 7 15075            DEC    .01
        34 1 21727
```

```
40155   00 0 00000   T          DEC     0
        00 0 00000
40156   20 0 14000   UDOT       DEC     1.0
        00 0 00000
40157   00 0 00000   U          DEC     0
        00 0 00000
40160   00 0 00000   QX         DEC     0
        00 0 00000
40161   00 0 00000   THETADOT   DEC     0
        00 0 00000
40162   00 0 00000   THETA      DEC     0
        00 0 00000
40163   00 0 00000   QY         DEC     0
        00 0 00000
40164   13 0 40157   DERIVES    LAC   0 U
        32 0 40404              FMU   0 A
40165   20 0 40156              STA   0 UDOT
        13 0 40162              LAC   0 THETA
40166   30 0 40664              FAD   0 ONE
        32 0 40424              FMU   0 OMEGANSQ
40167   30 0 40156              FAD   0 UDOT
        20 0 40156              STA   0 UDOT
40170   12 0 40157              LDA   0 U
        20 0 40161              STA   0 THETADOT
40171   75 0 60202              SLJ   0 RUNGE+2
        50 0 00000              ENI   0 0
40172   00 0 00000   TABLEL      OCT     2
        00 0 00002
40173   17 7 15075                 DEC     .01
        34 1 21727
40174   00 0 00000   TL         DEC     0
        00 0 00000
40175   00 0 00000   VDOT       DEC     0
        00 0 00000
40176   00 0 00000   V          DEC     0
        00 0 00000
40177   00 0 00000   QL         DEC     0
        00 0 00000
40200   00 0 00000   THETADL    DEC     0
        00 0 00000
40201   00 0 00000   THETAL     DEC     0
        00 0 00000
40202   00 0 00000   QLL        DEC     0
        00 0 00000
40203   13 0 40176   DERIVL     LAC   0 V
        32 0 40423              FMU   0 B
40204   20 0 40175              STA   0 VDOT
        12 0 40176              LDA   0 V
40205   20 0 40200              STA   0 THETADL
        75 0 60202              SLJ   0 RUNGE+2
40206   00 0 00000   TABLEM      OCT     2
        00 0 00002
40207   17 7 15075                 DEC     .01
        34 1 21727
40210   00 0 00000   TM         DEC     0
        00 0 00000
40211   00 0 00000   WDOT       DEC     0
        00 0 00000
40212   00 0 00000   W          DEC     0
        00 0 00000
40213   00 0 00000   QM         DEC     0
        00 0 00000
40214   00 0 00000   THETADM    DEC     0
        00 0 00000
40215   00 0 00000   THETAM     DEC     0
        00 0 00000
40216   00 0 00000   QMM        DEC     0
        00 0 00000
40217   13 0 40201   DERIVM     LAC   0 THETAL
        32 0 40421              FMU   0 C
40220   20 0 40211              STA   0 WDOT
        13 0 40212              LAC   0 W
40221   32 0 40422              FMU   0 D
        30 0 40421              FAD   0 C
```

```
40222   30  0  40211          FAD   0 WDOT
        20  0  40211          STA   0 WDOT
40223   12  0  40212          LDA   0 W
        20  0  40214          STA   0 THETADM
40224   75  0  60202          SLJ   0 RUNGE+2
        50  0  00000          ENI   0 0
40225   12  0  40201 PLUSTEST LDA   0 THETAL
        31  0  40664          FSB   0 ONE
40226   22  3  40232          AJP   3 PLUSTEST+5
        13  0  40215          LAC   0 THETAM
40227   32  0  40411          FMU   0 RHO
        30  0  40201          FAD   0 THETAL
40230   22  0  40301          AJP   0 PREPLANS
        22  2  40241          AJP   2 PLUSFORC
40231   75  0  40301          SLJ   0 PREPLANS
        50  0  00000          ENI   0 0
40232   13  0  40215          LAC   0 THETAM
        32  0  40411          FMU   0 RHO
40233   30  0  40201          FAD   0 THETAL
        22  0  40235          AJP   0 PLUSTEST+10
40234   22  2  40301          AJP   2 PREPLANS
        50  0  00000          ENI   0 0
40235   13  0  40162          LAC   0 THETA
        30  0  40664          FAD   0 ONE
40236   32  0  40424          FMU   0 OMEGANSQ
        33  0  40161          FDV   0 THETADOT
40237   31  0  40404          FSB   0 A
        30  0  40423          FAD   0 B
40240   22  2  40053          AJP   2 COMBINED
        75  0  40301          SLJ   0 PREPLANS
40241   12  0  40244 PLUSFORC LDA   0 NUMB
        20  0  40071          STA   0 FLOATEST
40242   12  0  40245          LDA   0 NUMB+1
        20  0  40072          STA   0 FLOATEST+1
40243   75  0  40053          SLJ   0 COMBINED
        50  0  00000          ENI   0 0
40244   12  0  40161 NUMB     LDA   0 THETADOT
        22  2  40053          AJP   2 COMBINED
40245   75  0  40250          SLJ   0 RESTORET
        50  0  00000          ENI   0 0
40246   12  0  40161 DUMB     LDA   0 THETADOT
        22  3  40053          AJP   3 COMBINED
40247   75  0  40250          SLJ   0 RESTORET
        50  0  00000          ENI   0 0
40250   12  0  40253 RESTORET LDA   0 FLOTDATA
        20  0  40071          STA   0 FLOATEST
40251   12  0  40254          LDA   0 FLOTDATA+1
        20  0  40072          STA   0 FLOATEST+1
40252   75  0  40053          SLJ   0 COMBINED
        50  0  00000          ENI   0 0
40253   13  0  40162 FLOTDATA LAC   0 THETA
        30  0  40664          FAD   0 ONE
40254   32  0  40424          FMU   0 OMEGANSQ
        33  0  40161          FDV   0 THETADOT
40255   12  0  40201 MINUTEST LDA   0 THETAL
        31  0  40664          FSB   0 ONE
40256   22  2  40262          AJP   2 MINUTEST+5
        13  0  40215          LAC   0 THETAM
40257   32  0  40411          FMU   0 RHO
        30  0  40201          FAD   0 THETAL
40260   22  0  40265          AJP   0 MINUFORC
        22  2  40301          AJP   2 PREPLANS
40261   75  0  40265          SLJ   0 MINUFORC
        50  0  00000          ENI   0 0
40262   13  0  40215          LAC   0 THETAM
        32  0  40411          FMU   0 RHO
40263   30  0  40201          FAD   0 THETAL
        22  0  40301          AJP   0 PREPLANS
40264   22  2  40235          AJP   2 PLUSTEST+10
        75  0  40301          SLJ   0 PREPLANS
40265   12  0  40246 MINUFORC LDA   0 DUMB
        20  0  40071          STA   0 FLOATEST
40266   12  0  40247          LDA   0 DUMB+1
        20  0  40072          STA   0 FLOATEST+1
```

```
40267   75 0 40053          SLJ  0 COMBINED
        50 0 00000          ENI  0 0
40270   12 0 40162 MODIFY   LDA  0 THETA
        31 0 40410          FSB  0 DELTA
40271   33 0 40411          FDV  0 RHO
        20 0 40215          STA  0 THETAM
40272   75 0 40076          SLJ  0 LOAD
        50 0 00000          ENI  0 0
40273   12 0 40201 TESTZERO LDA  0 THETAL
        31 0 40664          FSB  0 ONE
40274   22 2 40225          AJP  2 PLUSTEST
        22 3 40255          AJP  3 MINUTEST
40275   76 0 00000          SLS  0 0
        50 0 00000          ENI  0 0
40276   20 0 40300 COMPLMNT STA  0 COMPLMNT+2
        13 0 40300          LAC  0 COMPLMNT+2
40277   75 0 40140          SLJ  0 COMBTEST+3
        50 0 00000          ENI  0 0
40300   00 0 00000          BSS    1
        00 0 00000
40301   13 0 40215 PREPLANS LAC  0 THETAM
        32 0 40411          FMU  0 RHO
40302   30 0 40201          FAD  0 THETAL
        22 2 40305          AJP  2 PLUSCORR
40303   12 0 40201          LDA  0 THETAL
        33 0 40411          FDV  0 RHO
40304   20 0 40215          STA  0 THETAM
        75 0 40076          SLJ  0 LOAD
40305   12 0 40201 PLUSCORR LDA  0 THETAL
        31 0 40410          FSB  0 DELTA
40306   33 0 40411          FDV  0 RHO
        20 0 40215          STA  0 THETAM
40307   75 0 40076          SLJ  0 LOAD
        50 0 00000          ENI  0 0
40310   12 0 40354 COMBPRIN LDA  0 COMBEXIT
        20 0 40360          STA  0 EXIT
40311   12 0 40155          LDA  0 T
        20 0 40346          STA  0 PRINTBUF
40312   12 0 40157          LDA  0 U
        20 0 40347          STA  0 PRINTBUF+1
40313   12 0 40162          LDA  0 THETA
        20 0 40350          STA  0 PRINTBUF+2
40314   75 1 40522          SLJ  1 LIMITCYC
        10 0 00000          ENA  0 0
40315   20 0 40351          STA  0 PRINTBUF+3
        20 0 40352          STA  0 PRINTBUF+4
40316   75 0 40321          SLJ  0 COUNTSEC
        50 0 00000          ENI  0 0
40317   12 0 40355 FLOTPRIN LDA  0 FLOTEXIT
        20 0 40360          STA  0 EXIT
40320   75 4 40337          SLJ  4 FLOTSTOR
        50 0 00000          ENI  0 0
40321   72 0 40377 COUNTSEC RAO  0 INDEX
        12 0 40377          LDA  0 INDEX
40322   15 0 40400          SUB  0 TENTHSEC
        22 0 40325          AJP  0 OK2PRINT
40323   22 2 40322          AJP  2 COUNTSEC+1
        14 0 40400          ADD  0 TENTHSEC
40324   20 0 40377          STA  0 INDEX
        75 0 40360          SLJ  0 EXIT
40325   75 4 71000 OK2PRINT SLJ  4 DECOF
        50 0 00000          ENI  0 0
40326   00 0 40346            00 0 PRINTBUF
        06 0 00001            06 0 1
40327   72 0 40326          RAO  0 /-1
        10 0 00000          ENA  0 0
40330   20 0 40377          STA  0 INDEX
        75 0 40360          SLJ  0 EXIT
40331   12 0 40356 BOUNPRIN LDA  0 BOUNEXIT
        75 0 40333          SLJ  0 BOUNPRIN+2
40332   12 0 40357          LDA  0 BOUNEXIT+1
        50 0 00000          ENI  0 0
40333   20 0 40360          STA  0 EXIT
        75 4 40337          SLJ  4 FLOTSTOR
```

```
40334   75 4 71000              SLJ  4 DECOF
        50 0 00000              ENI  0 0
40335   00 0 40346                00 0 PRINTBUF
        06 0 00001                06 0 1
40336   75 0 40360              SLJ  0 EXIT
        50 0 00000              ENI  0 0
40337   75 0 00000  FLOTSTOR    SLJ  0 0
        12 0 40174              LDA  0 TL
40340   20 0 40346              STA  0 PRINTBUF
        12 0 40176              LDA  0 V
40341   20 0 40347              STA  0 PRINTBUF+1
        12 0 40201              LDA  0 THETAL
40342   20 0 40350              STA  0 PRINTBUF+2
        75 1 40522              SLJ  1 LIMITCYC
40343   12 0 40212              LDA  0 W
        20 0 40351              STA  0 PRINTBUF+3
40344   12 0 40215              LDA  0 THETAM
        20 0 40352              STA  0 PRINTBUF+4
40345   75 0 40337              SLJ  0 FLOTSTOR
        50 0 00000              ENI  0 0
40346   00 0 00000  PRINTBUF    BSS    6
        00 0 00000
40354   75 0 40060  COMBEXIT    SLJ  0 COMBINED+5
        50 0 00000              ENI  0 0
40355   75 0 40076  FLOTEXIT    SLJ  0 LOAD
        50 0 00000              ENI  0 0
40356   75 0 40113  BOUNEXIT    SLJ  0 BOUNCE+1
        50 0 00000              ENI  0 0
40357   75 0 40361              SLJ  0 EXITCOUN
        50 0 00000              ENI  0 0
40360   00 0 00000  EXIT        BSS    1
        00 0 00000
40361   75 1 40135  EXITCOUN    SLJ  1 COMBTEST
        72 0 40377              RAO  0 INDEX
40362   72 0 40335              RAO  0 BOUNPRIN+4
        12 0 40347              LDA  0 PRINTBUF+1
40363   22 2 40372              AJP  2 TOPCYC
        12 0 40350              LDA  0 PRINTBUF+2
40364   31 0 40664              FSB  0 ONE
        22 2 40135              AJP  2 COMBTEST
40365   72 0 40615              RAO  0 INDEXAVE
        12 0 40615              LDA  0 INDEXAVE
40366   15 0 40662              SUB  0 COUNT12
        22 0 40563              AJP  0 STOPNOW
40367   14 0 40662              ADD  0 COUNT12
        20 0 40615              STA  0 INDEXAVE
40370   12 0 40375              LDA  0 NEGAJUMP
        20 0 40364              STA  0 EXITCOUN+3
40371   75 0 40135              SLJ  0 COMBTEST
        50 0 00000              ENI  0 00000
40372   12 0 40350  TOPCYC      LDA  0 PRINTBUF+2
        31 0 40664              FSB  0 ONE
40373   22 3 40135              AJP  3 COMBTEST
        12 0 40376              LDA  0 NEWLOWER
40374   20 0 40364              STA  0 EXITCOUN+3
        75 0 40135              SLJ  0 COMBTEST
40375   75 0 40135  NEGAJUMP    SLJ  0 COMBTEST
        50 0 00000              ENI  0 0
40376   31 0 40664  NEWLOWER    FSB  0 ONE
        22 2 40135              AJP  2 COMBTEST
40377   00 0 00000  INDEX       OCT    0
        00 0 00000
40400   00 0 00000  TENTHSEC    OCT    12
        00 0 00012
40401   17 7 04061  POINT004    DEC    0.004
        11 5 64570
40402   17 7 15075  POINT01     DEC    0.01
        34 1 21727
40403   17 3 74000  DIFFERNT    OCT    1737400000000000
        00 0 00000
40404   20 0 06314  A           DEC    .8
        63 1 46314
40405   20 0 14000  INERTRAT    DEC    1.0
        00 0 00000
```

```
40406   00 0 00000   FLFTPRIN BSS     1
        00 0 00000
40407   00 0 00000   RESTITUT DEC     0
        00 0 00000
40410   17 7 64631   DELTA    DEC     .3
        46 3 14631
40411   20 0 14000   RHO      DEC     1.0
        00 0 00000
40412   20 0 04000   MOINERT  DEC     .5
        00 0 00000
40413   00 0 00000   JLOADVAL BSS     1
        00 0 00000
40414   20 0 14000   TOTINERT DEC     1.0
        00 0 00000
40415   00 0 00000   FMOTOR   BSS     1
        00 0 00000
40416   00 0 00000   FLOAD    BSS     1
        00 0 00000
40417   20 0 14000   RHOSQ    DEC     1.0
        00 0 00000
40420   20 0 14000   KMOTCONS DEC     1.0
        00 0 00000
40421   20 0 24000   C        DEC     2.0
        00 0 00000
40422   17 7 66314   D        DEC     .4
        63 1 46314
40423   17 7 15075   B        DEC     .01
        34 1 21727
40424   20 0 14000   OMEGANSQ DEC     1.0
        00 0 00000
40425   00 0 00000   ZETA     BSS     1
        00 0 00000
40426   20 0 14000   OMEGAN   DEC     1.0
        00 0 00000
40427   00 0 00000   FORZEROS BSS     4
        00 0 00000

                     RUNGE    EQU     60200
                     DECOF    EQU     71000
40433   12 0 40401   QUIKCOMP LDA  0  POINT004
        20 0 40154            STA  0  TABLES+1
40434   20 0 40173            STA  0  TABLEL+1
        20 0 40207            STA  0  TABLEM+1
40435   12 0 40654            LDA  0  STOP25
        20 0 40400            STA  0  TENTHSEC
40436   75 0 40015            SLJ  0  ZZ
        50 0 00000            ENI  0  0
40437   50 1 00000   BIGZETA   ENI  1  0
        50 0 00000            ENI  0  0
40440   12 0 40425            LDA  0  ZETA
        31 1 40636            FSB  1  POINT8
40441   22 2 40444            AJP  2  ZETAPLUS
        22 0 40444            AJP  0  ZETAPLUS
40442   54 1 00006            ISK  1  6
        75 0 40440            SLJ  0  /-2
40443   50 1 00006            ENI  1  6
        50 0 00000            ENI  0  0
40444   12 1 40645   ZETAPLUS LDA  1  STOP6
        20 0 40616            STA  0  STOPZETA
40445   12 1 40655            LDA  1  COUNT4
        20 0 40617            STA  0  COUNTZET
40446   12 1 40665            LDA  1  TWO
        20 0 40620            STA  0  DIVIDE
40447   12 1 40645            LDA  1  STOP6
        15 1 40655            SUB  1  COUNT4
40450   61 0 40562            SAL  0  STOPRINT
        50 1 00000            ENI  1  0
40451   75 0 40022            SLJ  0  GOAROUND
        50 0 00000            ENI  0  0
40452   12 3 40706   INDXVALU LDA  3  RESTVALU
        20 0 40407            STA  0  RESTITUT
40453   12 4 40726            LDA  4  DELTAVAL
        20 0 40410            STA  0  DELTA
40454   12 5 40747            LDA  5  JMOTVALU
        20 0 40412            STA  0  MOINERT
```

```
40455   12 0 40414          LDA  0 TOTINERT
        31 0 40412          FSB  0 MOINERT
40456   33 0 40417          FDV  0 RHOSQ
        20 0 40413          STA  0 JLOADVAL
40457   12 0 40420          LDA  0 KMOTCONS
        33 0 40412          FDV  0 MOINERT
40460   20 0 40421          STA  0 C
        12 0 40412          LDA  0 MOINERT
40461   33 0 40413          FDV  0 JLOADVAL
        20 0 40405          STA  0 INERTRAT
40462   12 6 40774          LDA  6 FLFTRATO
        20 0 40406          STA  0 FLFTPRIN
40463   32 0 40404          FMU  0 A
        32 0 40414          FMU  0 TOTINERT
40464   20 0 40416          STA  0 FLOAD
        33 0 40413          FDV  0 JLOADVAL
40465   20 0 40423          STA  0 B
        12 0 40416          LDA  0 FLOAD
40466   32 0 40417          FMU  0 RHOSQ
        20 0 40415          STA  0 FMOTOR
40467   12 0 40404          LDA  0 A
        32 0 40414          FMU  0 TOTINERT
40470   31 0 40415          FSB  0 FMOTOR
        20 0 40415          STA  0 FMOTOR
40471   33 0 40412          FDV  0 MOINERT
        20 0 40422          STA  0 D
40472   54 3 00001          ISK  3 1
        75 0 40043          SLJ  0 NEWINPUT+1
40473   54 4 00000          ISK  4 0
        75 0 40043          SLJ  0 NEWINPUT+1
40474   54 6 00005          ISK  6 5
        75 0 40043          SLJ  0 NEWINPUT+1
40475   54 5 00004          ISK  5 4
        75 0 40043          SLJ  0 NEWINPUT+1
40476   12 0 40564          LDA  0 STOPINDX
        20 0 40563          STA  0 STOPNOW
40477   75 0 40043          SLJ  0 NEWINPUT+1
        50 0 00000          ENI  0 0
40500   12 0 40512  LINEAR  LDA  0 NOFLOAT
        20 0 40071          STA  0 FLOATEST
40501   12 0 40404          LDA  0 A
        20 0 40514          STA  0 PRINDELT
40502   12 0 40414          LDA  0 TOTINERT
        20 0 40515          STA  0 PRINDELT+1
40503   12 0 40420          LDA  0 KMOTCONS
        20 0 40516          STA  0 PRINDELT+2
40504   12 0 40424          LDA  0 OMEGANSQ
        20 0 40517          STA  0 PRINDELT+3
40505   12 0 40411          LDA  0 RHO
        20 0 40520          STA  0 PRINDELT+4
40506   12 0 40417          LDA  0 RHOSQ
        20 0 40521          STA  0 PRINDELT+5
40507   72 0 40510          RAO  0 /+1
        75 4 71000          SLJ  4 DECOF
40510   01 0 40514            01 0 PRINDELT
        06 0 00000            06 0 0
40511   72 0 40046          RAO  0 NEWINPUT+4
        75 0 40053          SLJ  0 COMBINED
40512   75 0 40053  NOFLOAT  SLJ  0 COMBINED
        50 0 00000          ENI  0 0
40513   13 0 40162  NOSINK   LAC  0 THETA
        30 0 40664          FAD  0 ONE
40514   00 0 00000  PRINDELT BSS    6
        00 0 00000
40522   75 3 40523  LIMITCYC SLJ  3 /+1
        75 0 40525           SLJ  0 /+3
40523   50 0 00000           ENI  0 0
        12 0 00000           LDA  0 0
40524   65 0 40603           THS  0 TIME90SC
        75 0 40566           SLJ  0 TIMESTOP
40525   12 0 40350           LDA  0 PRINTBUF+2
        31 0 40664           FSB  0 ONE
40526   22 3 40534           AJP  3 PRINTNOW
        50 2 77775           ENI  2 77775
```

```
40527   12 0 40607            LDA  0 LIMITBUF+2
        31 0 40350            FSB  0 PRINTBUF+2
40530   22 2 40360            AJP  2 EXIT
        12 0 40346            LDA  0 PRINTBUF
40531   20 0 40605            STA  0 LIMITBUF
        12 0 40347            LDA  0 PRINTBUF+1
40532   20 0 40606            STA  0 LIMITBUF+1
        12 0 40350            LDA  0 PRINTBUF+2
40533   20 0 40607            STA  0 LIMITBUF+2
        75 0 40360            SLJ  0 EXIT
40534   54 2 77775 PRINTNOW   ISK  2 77775
        75 0 40360            SLJ  0 EXIT
40535   12 0 40615            LDA  0 INDEXAVE
        15 0 40617            SUB  0 COUNTZET
40536   22 0 40541            AJP  0 /+3
        14 0 40617            ADD  0 COUNTZET
40537   20 0 40615            STA  0 INDEXAVE
        72 0 40615            RAO  0 INDEXAVE
40540   75 0 40543            SLJ  0 LIMPRINT
        50 0 00000            ENI  0 0
40541   12 0 40607            LDA  0 LIMITBUF+2
        30 0 40613            FAD  0 LIMITBUF+6
40542   20 0 40613            STA  0 LIMITBUF+6
        50 0 00000            ENI  0 0
40543   74 0 02000 LIMPRINT   EXF  0 02000
        75 4 71000            SLJ  4 DECOF
40544   01 0 40605             01  0 LIMITBUF
        06 0 00001             06  0 1
40545   72 0 40544            RAO  0 /-1
        72 0 40614            RAO  0 LIMINDEX
40546   12 0 40614            LDA  0 LIMINDEX
        15 0 40616            SUB  0 STOPZETA
40547   22 0 40555            AJP  0 STOPAVE
        14 0 40616            ADD  0 STOPZETA
40550   20 0 40614            STA  0 LIMINDEX
        12 0 40604            LDA  0 TOOSMALL
40551   31 0 40607            FSB  0 LIMITBUF+2
        22 2 40573            AJP  2 SMALTIME
40552   10 0 00000            ENA  0 0
        20 0 40607            STA  0 LIMITBUF+2
40553   20 0 00000            STA  0 0
        74 0 01000            EXF  0 01000
40554   75 0 40360            SLJ  0 EXIT
        50 0 00000            ENI  0 0
40555   10 0 00000 STOPAVE    ENA  0 0
        20 0 40605            STA  0 LIMITBUF
40556   20 0 40606            STA  0 LIMITBUF+1
        20 0 40607            STA  0 LIMITBUF+2
40557   12 0 40613            LDA  0 LIMITBUF+6
        33 0 40620            FDV  0 DIVIDE
40560   31 0 40664            FSB  0 ONE
        20 0 40610            STA  0 LIMITBUF+3
40561   75 4 71000            SLJ  4 DECOF
        50 0 00000            ENI  0 0
40562   01 0 40605 STOPRINT    01  0 LIMITBUF
        06 0 00000             06  0 0
40563   76 1 40022 STOPNOW    SLS  1 GOAROUND
        50 0 00000            ENI  0 0
40564   76 0 40000 STOPINDX   SLS  0 START
        50 0 00000            ENI  0 0
40565   76 1 40022 NEWSTOP    SLS  1 GOAROUND
        50 0 00000            ENI  0 0
40566   50 2 00000 TIMESTOP   ENI  2 0
        75 4 71000            SLJ  4 DECOF
40567   01 0 40605             01  0 LIMITBUF
        04 0 01570             04  0 1570
40570   74 0 02000            EXF  0 02000
        75 4 71000            SLJ  4 DECOF
40571   01 0 40346             01  0 PRINTBUF
        04 0 01747             04  0 1747
40572   75 0 40563            SLJ  0 STOPNOW
        50 0 00000            ENI  0 0
40573   75 3 40574 SMALTIME   SLJ  3 /+1
        75 0 40552            SLJ  0 LIMPRINT+7
```

```
40574   50 0 00000                      ENI   0 0
        12 0 00000                      LDA   0 0
40575   65 0 40602                      THS   0 TIME30SC
        75 0 40577                      SLJ   0 /+2
40576   75 0 40552                      SLJ   0 LIMPRINT+7
        50 0 00000                      ENI   0 0
40577   75 4 71000                      SLJ   4 DECOF
        50 0 00000                      ENI   0 0
40600   01 0 40346                      01    0 PRINTBUF
        04 0 01755                      04    0 1755
40601   75 0 40563                      SLJ   0 STOPNOW
        50 0 00000                      ENI   0 0
40602   00 0 00000  TIME30SC OCT        3410
        00 0 03410
40603   00 0 00000  TIME90SC OCT        12430
        00 0 12430
40604   20 0 14012  TOOSMALL DEC        1.005
        17 2 70243
40605   00 0 00000  LIMITBUF BSS        7
        00 0 00000
40614   00 0 00000  LIMINDEX BSS        1
        00 0 00000
40615   00 0 00000  INDEXAVE BSS        1
        00 0 00000
40616   00 0 00000  STOPZETA BSS        1
        00 0 00000
40617   00 0 00000  COUNTZET BSS        1
        00 0 00000
40620   00 0 00000  DIVIDE   BSS        1
        00 0 00000
40621   00 0 40346  PRINTSET  00  0 PRINTBUF
        06 0 00001                06  0 1
40622   01 0 40605  NEWLIMPT   01  0 LIMITBUF
        06 0 00001                06  0 1
40623   17 7 36314  ZETAINDX DEC        0.05
        63 1 46314
40624   17 7 46314               DEC        0.1
        63 1 46314
40625   17 7 56314               DEC        0.2
        63 1 46314
40626   17 7 64631               DEC        0.3
        46 3 14631
40627   17 7 66314               DEC        0.4
        63 1 46314
40630   20 0 04000               DEC        0.5
        00 0 00000
40631   20 0 04631               DEC        0.6
        46 3 14631
40632   20 0 05463               DEC        0.7
        14 6 31463
40633   20 0 06314               DEC        0.8
        63 1 46314
40634   20 0 07146               DEC        0.9
        31 4 63146
40635   20 0 14000               DEC        1.0
        00 0 00000
40636   20 0 06314  POINT8    DEC        .8
        63 1 46314
40637   20 0 04631  POINT6    DEC        .6
        46 3 14631
40640   20 0 04000  POINT5    DEC        .5
        00 0 00000
40641   17 7 66314  POINT4    DEC        .4
        63 1 46314
40642   17 7 64631  POINT3    DEC        .3
        46 3 14631
40643   17 7 56314  POINT2    DEC        0.2
        63 1 46314
40644   17 7 46314  POINT1    DEC        0.1
        63 1 46314
40645   00 0 00000  STOP6     OCT        6
        00 0 00006
40646   00 0 00000  STOP7     OCT        7
        00 0 00007
```

```
40647   00 0 00000   STOP8     OCT    10
        00 0 00010
40650   00 0 00000   STOP10    OCT    12
        00 0 00012
40651   00 0 00000   STOP14    OCT    16
        00 0 00016
40652   00 0 00000   STOP20    OCT    24
        00 0 00024
40653   00 0 00000   STOP17    OCT    21
        00 0 00021
40654   00 0 00000   STOP25    OCT    31
        00 0 00031
40655   00 0 00000   COUNT4    OCT    4
        00 0 00004
40656   00 0 00000   COUNT5    OCT    5
        00 0 00005
40657   00 0 00000             OCT    5
        00 0 00005
40660   00 0 00000   COUNT7    OCT    7
        00 0 00007
40661   00 0 00000   COUNT10   OCT    12
        00 0 00012
40662   00 0 00000   COUNT12   OCT    14
        00 0 00014
40663   00 0 00000             OCT    14
        00 0 00014
40664   20 0 14000   ONE       DEC    1.0
        00 0 00000
40665   20 0 24000   TWO       DEC    2.0
        00 0 00000
40666   20 0 24000             DEC    2.0
        00 0 00000
40667   20 0 26000   THREE     DEC    3.0
        00 0 00000
40670   20 0 26000             DEC    3.0
        00 0 00000
40671   20 0 34000   FOUR      DEC    4.0
        00 0 00000
40672   20 0 44000   EIGHT     DEC    8.0
        00 0 00000
40673   20 0 35000   FIVE      DEC    5.0
        00 0 00000
40674   50 1 00000   MANUAL    ENI    1 0
        75 4 71000             SLJ    4 DECOF
40675   01 0 40605              01    0 LIMITBUF
        04 0 01570              04    0 1570
40676   50 2 00000             ENI    2 0
        75 4 71000             SLJ    4 DECOF
40677   01 0 40346              01    0 PRINTBUF
        04 0 03651              04    0 3651
40700   75 0 40563             SLJ    0 STOPNOW
        50 0 00000             ENI    0 0
40701   50 1 00000   FAULPRIN  ENI    1 0
        75 4 71000             SLJ    4 DECOF
40702   01 0 40605              01    0 LIMITBUF
        04 0 01570              04    0 1570
40703   50 2 00000             ENI    2 0
        75 4 71000             SLJ    4 DECOF
40704   01 0 40346              01    0 PRINTBUF
        04 0 01232              04    0 1232
40705   74 0 42003             EXF    0 42003
        76 0 40000             SLS    0 START
40706   20 0 14000   RESTVALU  DEC      1.0
        00 0 00000
40707   00 0 00000             DEC    0
        00 0 00000
40710   20 0 04631             DEC    0.6
        46 3 14631
40711   20 0 06314             DEC    0.8
        63 1 46314
40712   00 0 00000             BSS    14
        00 0 00000
40726   17 7 64631   DELTAVAL  DEC    .3
        46 3 14631
```

```
40727   17 7 46314          DEC     .1
        63 1 46314
40730   17 7 27534          DEC     .03
        12 1 72702
40731   17 7 15075          DEC     0.01
        34 1 21727
40732   17 7 05075          DEC     0.005
        34 1 21727
40733   00 0 00000          BSS     14
        00 0 00000
40747   17 7 46314  JMOTVALU DEC    .1
        63 1 46314
40750   17 7 56314          DEC     .2
        63 1 46314
40751   20 0 04000          DEC     .5
        00 0 00000
40752   20 0 06314          DEC     .8
        63 1 46314
40753   20 0 07146          DEC     .9
        31 4 63146
40754   00 0 00000          BSS     20
        00 0 00000
40774   00 0 00000  FLFTRATO DEC    0
        00 0 00000
40775   17 7 56314          DEC     .2
        63 1 46314
40776   17 7 66314          DEC     .4
        63 1 46314
40777   20 0 04631          DEC     .6
        46 3 14631
41000   20 0 06314          DEC     .8
        63 1 46314
41001   20 0 14000          DEC     1.0
        00 0 00000
41002   17 7 35075          DEC     0.04
        34 1 21727
41003   17 7 46314          DEC     0.1
        63 1 46314
41004   20 0 07146          DEC     0.9
        31 4 63146
41005   00 0 00000          BSS     20
        00 0 00000
                            END
```

Solution 3 number	$2S\omega_n$ 99999999		$\frac{J_m}{J_L}$ 99999999		$\frac{f_L}{J_L}$ 79999999		e 99999999		Δ 29999999		ρ 99999999
	J_m 49999999		$\frac{J_m}{J_L}$ 49999999		$J_m + \rho^2 J_L$ 99999999		f_m 20000000		f_L 79999999		ρ^2 99999999
	K 99999999		$\frac{K}{J_m}$ 19999999	1	$\frac{f_m}{J_m}$ 40000000		$\frac{f_L}{J_L}$ 15999999	1	ω_n^2 99999999		ζ 49999999
point 1	10000000		95004083-	1	48334152-	2					
number 2	19999999		18006400		18669244-	1					
3	t 29999999		$\dot{\theta}_c$ 25531729		θ_c 40519239-	1					
4	40000000		32098164		69412993-	1					
5	50000000		37734520		10440547						
6	59999999		42475713		14458358						
7	69999999		46361850		18907183						
8	79999999		49437347		23703703						
9	89999999		51750106		28769225						
10	99999999		53350719		34029984						
11	10999999	1	54291737		39417381						
12	11999999	1	54626982		44868139						
13	12999999	1	54410913		50324400						
14	14000000	1	53698048		55733762						
15	15000000	1	52542443		61049253						
16	16000000	1	50997217		66229265						
17	17000000	1	49114140		71237437						
18	18000000	1	46943268		76042502						
19	19000000	1	44532629		80618101						
20	20000000	1	41927962		84942563						
21	21000000	1	39172497		88998670						
22	22000000	1	36306785		92773391						
23	23000000	1	33368563		96257613						
24	24000000	1	30392671		99445851						
25	25000000	1	27410989		10233595	1					
26	26000000	1	24452419		10492882	1					
27	27000000	1	21542892		10722807	1					
28	28000000	1	18705407		10923980	1					
29	29000000	1	15989086		11097264	1	$\dot{\theta}_m$ 15926240		θ_m 11097173	1	
30	30000000	1	13625000		11245019	1	12991268		11241908	1	
31	31000000	1	11610459		11370928	1	99052498-	1	11356496	1	
32	32000000	1	98937811-	1	11478221	1	67134562-	1	11439661	1	
33	33000000	1	84309241-	1	11569649	1	34535657-	1	11490539	1	
34	34000000	1	71843596-	1	11647559	1	15682165-	2	11508610	1	
35	35000000	1	61221074-	1	11713950	1	-31509827-	1	11493639	1	
36	36000000	1	52169158-	1	11770525	1	-64486655-	1	11445624	1	
37	37000000	1	44455624-	1	11818734	1	-97189429-	1	11364757	1	
38	38000000	1	37882584-	1	11859816	1	-12947823		11251384	1	
39	39000000	1	32281408-	1	11894823	1	-16124091		11105976	1	
40	40000000	1	27508401-	1	11924654	1	-19238868		10929107	1	
41	41000000	1	23441113-	1	11950075	1	-22285244		10721427	1	
42	42000000	1	19975199-	1	11971737	1	-25257956		10483648	1	
43	43000000	1	17021742-	1	11990196	1	-28153122		10216527	1	
44	44000000	1	14504971-	1	12005926	1	-30968015		99208537		
45	45000000	1	12360321-	1	12019330	1	-33700866		95974404		
46	46000000	1	10532771-	1	12030752	1	-36350703		92471132		
contact 1	46600000	1	95686438-	2	12036778	1	-37900604		90243442		
number 1	46600000	1	-37900604		12036778	1	95686438-	2	90243442		
47	47000000	1	-35550956		11889925	1	-60605683-	2	90374327		
48	48000000	1	-30294526		11561398	1	-39333994-	1	90140801		
49	49000000	1	-25815292		11281446	1	-65385515-	1	89611697		
50	50000000	1	-21998341		11042886	1	-85373205-	1	88853284		
51	51000000	1	-18745749		10839599	1	-10028037		87921151		
52	52000000	1	-15974074		10666370	1	-11094153		86861815		
53	53000000	1	-13612208		10518753	1	-11806455		85714102		

APPENDIX C

PHASE TRAJECTORY PRINT OUT
(Numbers indicated in tenths followed by power of 10)

Solution number	1	$2S\omega_n$	79999999		J_m/J_L	11111111		F_L/F_T	39999999		C	99999999	Δ 29999999	ρ 99999999
		J_m	99999999-	1	J_L	89999999		$J_m+\rho^2 J_L$	99999999		f_m	47999999	F_L 31999999	ρ^2 99999999
		K	99999999		K/J_m	99999999	1	f_m/J_m	47999999	1	F_L/J_L	35555555	ω_n^2 99999999	ζ 39999999
number of maximum	1	t	33800000	1	$\dot{\Theta}_c$	52456182-	1	Θ_c	13396964	1				
	2		11230000	2		38509278-	1		11053498	1				
	3		21289999	2		12863485-	1		10697107	1				
	4		32499999	2		79971808-	2		10583527	1				
	5		44279999	2		65238396-	2		10542905	1				
	6		56369999	2		59130680-	2		10524201	1				
	7		68649998	2		55271237-	2		10511522	1				
	8		81049998	2		53208045-	2		10504778	1				
	9		93519998	2		51991503-	2		10500457	1				
	10		10602999	3		51279129-	2		10498432	1				
	3	number of maximums averaged										50122288- 1	average positive error in Limit Cycle	

APPENDIX D 1

TYPICAL PRINT OUT ILLUSTRATING LIMIT CYCLE
(Numbers indicated in tenths followed by power of 10)

	2	$2\zeta\omega_n$ 79999999		J_m/J_L 11111111		f_L/F_T 59999999		e 99999999		Δ 29999999		ρ 99999999	
		J_m 99999999-	1	J_L 89999999		$J_m+\rho^2 J_L$ 99999999		f_m 32000000		f_L 47999999		ρ^2 99999999	
		K 99999999		K/J_m 99999999	1	f_m/J_m 32000000	1	f_L/J_L 53333333		ω_n^2 99999999		ζ 39999999	
number of maximum	1	t 35400000	1	$\dot{\theta}_c$ 17098208-	1	θ_c 13104190	1						
	2	11580000	2	17034145-	1	10721242	1						
	3	23279999	2	18292628-	2	10323347	1						
	4	38859999	2	35712402-	3	10200613	1						
	5	58729999	2	72447348-	4	10138780	1						
	6	83939998	2	11243587-	4	10098946	1						
	7	11619999	3	10685365-	5	10071240	1						
	8	15810000	3	47854719-	7	10051391	1						
	9	21077001	3	29068282-	8	10037079	1						
	1005	215160011794	3	-167815371770 -	2	9999968862854							

1005 indicates θ_c max. less than 1 005 and 30 sec. of real time has elapsed since the last maximum was recorded (low velocity).

The time velocity, and position of the last computed point is printed.

APPENDIX D 2

TYPICAL PRINT OUT ILLUSTRATING NO LIMIT CYCLE
(Numbers indicated in tenths followed by power of 10)